Sensitivity Analysis Report - Part I
DRSPALL Version 1.00

Report for
Conceptual Model Peer Review
convening
July 7-11, 2003

Authors:
David Lord, SNL
David Rudeen, GRAM, Inc.

August 2003

Table of Contents

List of Figures

List of Tables

Glossary of Acronyms

Acronym	*Definition*
CCA	Compliance Certification Application (1996)
DDZ	Drilling-damaged zone
DOE	U.S. Department of Energy
DRSPALL	Computer code that implements the new conceptual model for spallings
LHS	Latin Hypercube Sampling
PA	Performance Assessment
PAVT	Performance Assessment Verification Test (1997)
SNL	Sandia National Laboratories
TSPA	Total System Performance Assessment
WIPP	Waste Isolation Pilot Plant

1 TEST OBJECTIVE

This report documents the DRSPALL sensitivity study executed in support of the WIPP Spallings Model Conceptual Model Peer Review convened July 7-9, 2003, in Albuquerque, NM. This is Part I of a sensitivity study series that addresses the panel's requests to (i) capture the oral presentation "DRSPALL Sensitivity Study," given on July 9, 2003, in report format, and (ii) build a DRSPALL "response surface" based on sensitivities to key variables elucidated by Part I. The DRSPALL response surface for the peer review panel will be presented in the forthcoming Part II of this report. Most of the figures that appear in this report come directly from the oral presentation, "DRSPALL Sensitivity Study," presented by David Lord and David Rudeen at the peer review meeting on July 9, 2003.

The objectives of this analysis (Part I) are twofold:

1. To test the DRSPALL code stability over the entire parameter space possible in the WIPP Performance Assessment
2. To identify uncertain parameters that have the most impact on code output

Successful completion of this sensitivity analysis will provide reassurance that the model will behave appropriately and stably when run in the broad parameter space encountered in the WIPP total system performance assessment (TSPA). Moreover, this analysis will allow close inspection for proper implementation of the conceptual model by illustrating the relationships between key inputs such as pressure and tensile strength and outputs such as tensile failure radius and total spall release.

2 PROBLEM SETUP

This analysis focuses on the relationship between uncertain input parameters and code output, addressing what is referred to as subjective uncertainty in the Waste Isolation Pilot Plant Performance Assessment (WIPP PA) context. Uncertainties related to time of intrusion, number of previous intrusions, etc., are not addressed here. Rather, these will be handled when the code is integrated into the TSPA.

2.1 Parameter Sampling

Latin Hypercube Sampling (LHS) (Helton and Davis, 2002) was used to generate the sampled input parameters sets. LHS is a Monte Carlo technique that is frequently used in uncertainty and sensitivity analyses of complex models. The technique was chosen here due to : (a) conceptual simplicity and ease of implementation, (b) robust sampling over the range over the full range of variability of each sampled variable, and (c) it is the current standard for sampling uncertain parameters used in WIPP PA.

DRSPALL requires more than 40 input parameters in order to execute, with a complete list given in appendix DEFAULTS. Within this list, fifteen parameters were deemed sufficiently uncertain and potentially important to code output that they were sampled in the sensitivity analysis described here. Two parameter samplings were run, with the only difference being that the repository gas pressure range was varied from 8-15 MPa in the first sampling, and 12-15 MPa in the second sampling. Table 2-1 shows the parameter names, ranges, and distribution type used for the first sampling. Note that the second sampling is identical except for constraining the pressure range to 12-15 MPa. The reason for running the second sampling was that most of the spall failure and thus interesting model behavior occurs only at pressures above 12 MPa, and the second sampling allowed for more output resolution in the parameter space that leads to spalling. The rationale for the endpoints of the sampled parameters is presented in the Parameter Justification Report for DRSPALL (Hansen et al., 2003). The distributions take two forms, either uniform or loguniform. In the event that the endpoints range over more than one order of magnitude, the distribution is loguniform. Relative to a uniform distribution, loguniform biases the sampling toward the low end of the range, deemed a conservative assumption in all four cases because low values of waste permeability, tensile strength, wellbore wall roughness, and drilling damaged zone (DDZ) permeability are understood to lead to higher or more likely spallings releases.

Table 2-1. Summary of sampled DRSPALL input variables, including range and distribution.

Variable Name	*Units*	*Distribution*	*Low*	*High*
Repository Gas Pressure	Pa	UNIFORM	8.00E+06	1.49E+07
Porosity of Waste	-	UNIFORM	3.50E-01	6.60E-01
Permeability of Waste	m^2	LOGUNIFORM	1.70E-14	1.70E-12
Poisson's Ratio of Waste	-	UNIFORM	3.50E-01	4.30E-01
Tensile Strength of Waste	Pa	LOGUNIFORM	1.20E+05	1.70E+05
Initial Mud Density	kg/m3	UNIFORM	1.14E+03	1.38E+03
Initial Mud Viscosity	Pa*s	UNIFORM	5.00E-03	3.00E-02
Max Solids Vol Fraction in Mud	-	UNIFORM	5.90E-01	6.40E-01
Solids Viscosity Exponent	-	UNIFORM	-1.80E+00	-1.20E+00
Drill Penetration Rate	m/s	UNIFORM	2.96E-03	5.93E-03
Mud Pump Rate	m3/s	UNIFORM	1.61E-02	2.42E-02
DDZ Permeability	m^2	LOGUNIFORM	1.00E-15	1.00E-13
Wall Roughness	m	LOGUNIFORM	5.00E-05	3.10E-03
Particle Shape Factor	-	UNIFORM	1.00E-01	1.00E+00
Particle Diameter	m	UNIFORM	1.00E-03	1.00E-02

2.2 Code flow for sensitivity study

The sensitivity study requires that a series of codes are run in order to create the input files, execute DRSPALL, and view the output. Input files area created by pre-processors, while output data are read and displayed by post-processors. The general code flow is shown in Figures 2-1 and 2-2.

The first step requires running MATSET to create a generic input file for DRSPALL. The input file to MATSET specifies all material names and default property values. The output from MATSET is a binary file that is read directly by LHS.

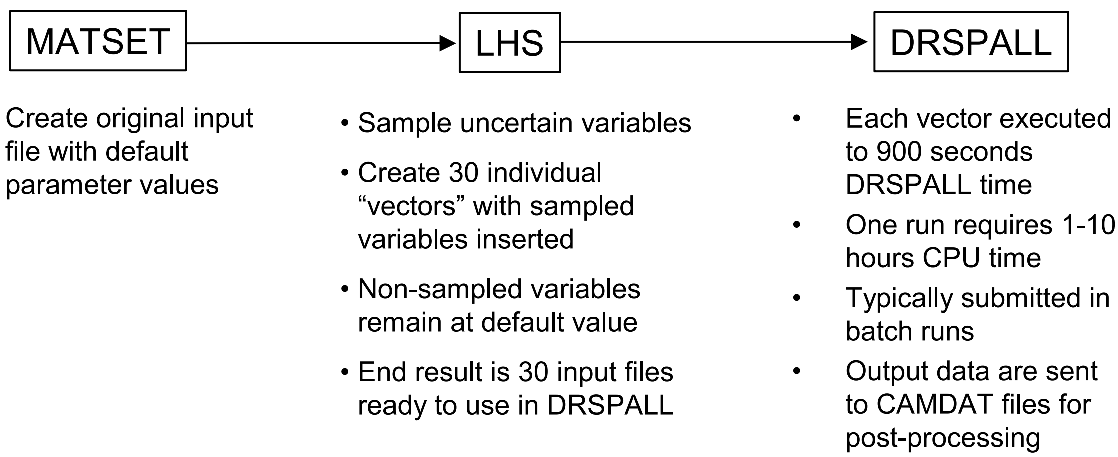

Figure 2-1. Code flow diagram for DRSPALL pre-processors.

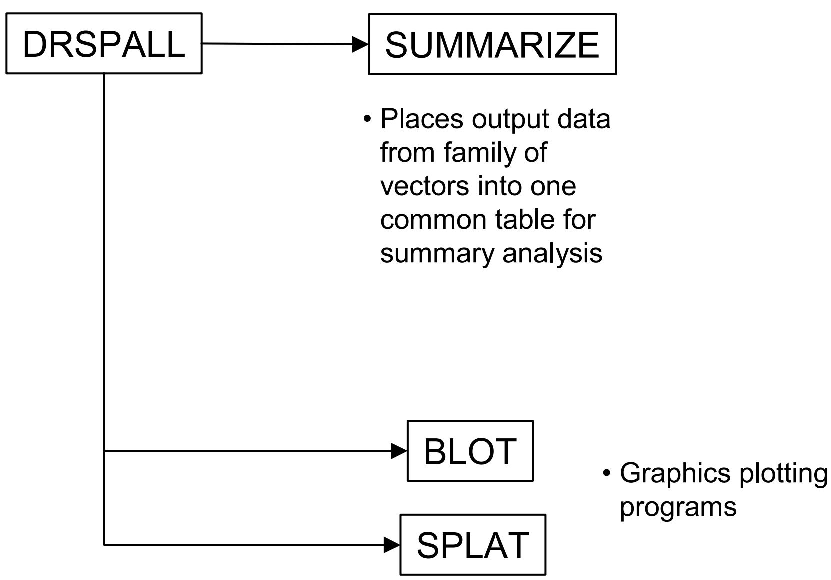

Figure 2-2. Code flow diagram for DRSPALL post-processors.

The second step requires running LHS to create 30 individual output vectors containing unique sets of input variables. The input to LHS includes the binary template created by MATSET and the input file LHS1_DRSPALL.TRN, which gives the ranges and distribution types for sampled variables. Output from LHS appears in both ASCII and binary format. The ASCII file of most interest is the LHS2_DRSPALL.TRN file that lists the results of the LHS sampling in tabular format. A listing of this file is given in Appendix LHS2_DRSPALL.TRN. The binary output appears as 30 individual files (1 per vector) that serve as input to DRSPALL.

The next step requires submitting one DRSPALL run per vector. This is typically done in batch mode. This analysis ran 2 samples of 30 vectors each, requiring a total of 60 DRSPALL runs. All runs were executed to 900 seconds in DRSPALL time. This run time was determined by repeated trial and error in the model development process. Inspection of the output will reveal that drilling, tensile failure, fluidization, and spall releases to the surface all settle to steady values by 900 seconds. As such, there is no new information gained from running the code out longer.

Post-processing DRSPALL output takes two primary paths. The binary data from 30 runs can be summarized into one aggregate ASCII table for querying and analysis in a database or spreadsheet. Alternatively, the binary data may be read directly into a plotting program like BLOT (WIPP PA, 1996a), or preprocessed for input to SPLAT (WIPP PA, 1996b) for direct observation of history or spatial variables.

2.3 Output variable definitions

A comprehensive list of variable definitions is given in Appendix VARIABLE GLOSSARY. Of interest in this sensitivity study are:

1. Radial variables
    a. Cuttings radius (CUTRAD)
    b. Cavity radius (CAVRAD)
    c. Tensile radius (TENSRAD)
2. Pressure variables
    a. Cavity pressure in repository (CAVPRS)
    b. Flowing bottomhole pressure in wellbore (BOTPRS)
3. Equivalent uncompacted volumes
    a. Total (TOTVOLEQ)
    b. Cuttings (CUTVOLEQ)
    c. Spallings (SPLVOLEQ)

2.3.1 Radial variables

The radius is a key variable to understand in the DRSPALL model because spatial variables in the 1-D cylindrical and spherical geometries are all expressed as a function of radius. The origin for the cylindrical geometry is a line down the center of the borehole denoting the axis of symmetry (Figure 2-3a). The origin for the spherical repository domain is a point where the axis of the drill bit first touches the top of the repository (Figure 2-3b). The three primary radial variables in DRSPALL output are the drill cuttings radius, cavity radius, and the tensile-failed radius. The relationship among these three is demonstrated in Figure 2-3. The easiest place to start is with the cutting radius. This represents the position of the drill bit face in the repository. In most cases run here, drilling is the only mechanism that expands the cavity radius, so the drill radius and cavity radius will overlay. In the event of spallings, however, the cavity radius may actually grow larger than the drilled radius, as depicted in Figure 2-3. This implies that the spallings mechanism has removed material ahead of the drill bit. A third radial variable, tensile-failed radius, is also important to monitor because this variable identifies solid material that has failed due to the stress state, but has not mobilized into the flow stream. This may or may not be larger than the cavity radius, but it can never be smaller. Figure 2-3 and 2-4 show a situation in which material has failed out ahead of the bit, but has not fluidized and therefore forms a bed of disaggregated material subject to fluidization as the gas velocity reaches a sufficiently high value.

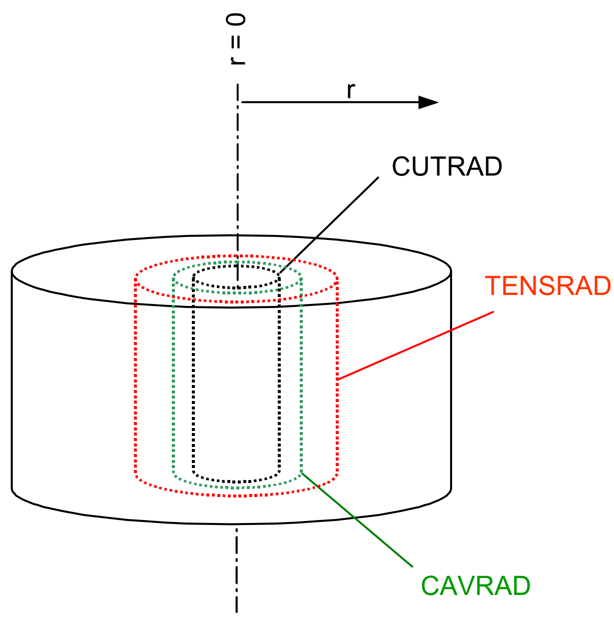

Figure 2-3. Radial variables in cylindrical geometry.

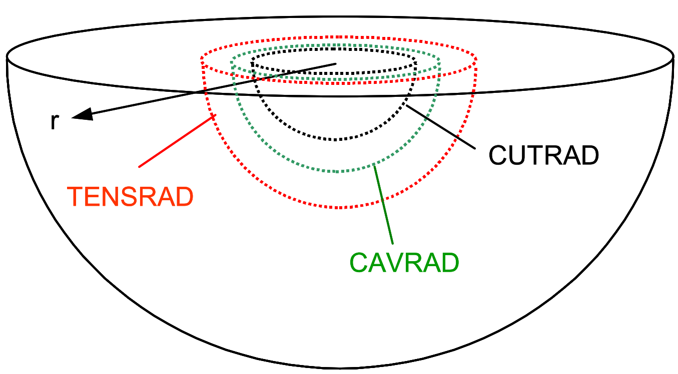

Figure 2-4. Radial variables in spherical geometry.

2.3.1.1 *Mapping the cuttings radius in DRSPALL geometry*

The cuttings radius in the one-dimensional DRSPALL geometry is mapped to the cuttings in a real three-dimensional system by conserving the surface area of the expanding cavity. For the cylindrical geometry, this involves starting with a narrow cylinder that extends through the repository height along the drilling axis, and expanding the radius as the real bit penetrates downward. For the spherical geometry, this requires defining a small hemisphere that has its origin at the point where the drillbit would first intersect the repository, and expanding this hemisphere radially as the bit proceeds. Drilling continues in both geometries for the amount of time required for a real bit to penetrate the entire depth of the repository. This implies that the rate of areal expansion of the drilled cavity is the same in all systems. More detail on the mapping among geometries is given in the Design Document for DRSPALL, document version 1.10 (WIPP PA, 2003).

2.3.2 *Pressure variables*

The two pressure variables of interest prior to bit penetration are the "pseudo-" cavity pressure in the repository, and the flowing bottomhole pressure in the wellbore. The pseudo-cavity is a small volume created in the repository in order to avoid forcing the gas to flow to a single point (spherical geometry) or line (cylindrical geometry) at the origin of the domain. See the DRSPALL Design Document, v1,.10 (WIPP PA, 2003) for a more detailed explanation of the pseudo-cavity. Upon bit penetration, the cavity and well bottom define the same region in the model domain, and thus evaluate to the same pressure.

2.3.3 *Equivalent volumes*

DRSPALL calculates the mass of repository solids ejected to the land surface. For the purpose of comparing these release masses to releases from CCA and PAVT analyses, the DRSPALL expelled masses are converted to "equivalent uncompacted volume" units:

$$V_{eq} = \frac{m_s}{\rho_s(1-\phi_o)} \tag{2.1}$$

where V_{eq} is the equivalent volume prior to compaction, m_s is the solids mass ejected at the surface, ρ_s is the solids density, and ϕ_o is the porosity of a waste-filled room prior to closure. Values of ρ_s = 2650 kg/m3 (Appendix DEFAULTS) and ϕ_o = 0.85 (DOE, 1996: Appendix PAR, Table PAR-38) are used in this analysis.

DRSPALL distinguishes between equivalent uncompacted volume of repository removed by all processes (TOTVOLEQ), and material released by spallings (SPLVOLEQ), by subtracting the equivalent volume of material removed by drilling action (CUTVOLEQ), or cuttings, from TOTVOLEQ. This is shown schematically for the hemispherical repository geometry in Figure 2-5.

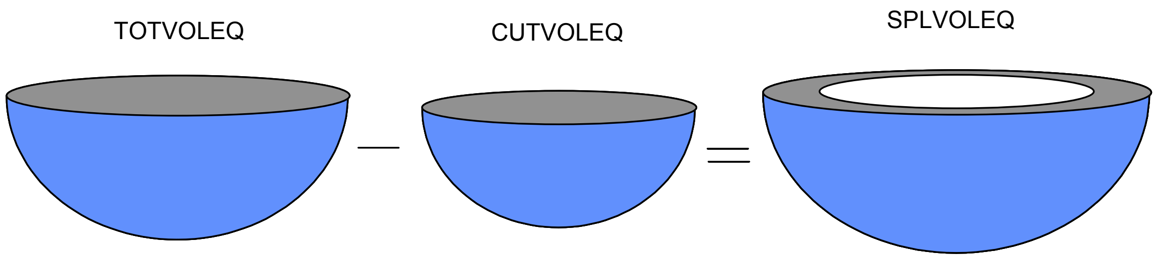

Figure 2-5. Schematic of the relationship among TOTVOLEQ, CUTVOLEQ, and SPLVOLEQ.

2.4 System specifications

This analysis was run on the Open VMS 7.3-1 operating system at Sandia National Laboratories, Carlsbad, NM. Runs were submitted to Compaq Alpha ES40, ES45, and 8400 machines, with a total of 20 processors available for computations. 60 vectors were executed in all, requiring about 277 hours of computational time spread over all 20 processors or roughly 48 hours of wall clock time.

3 RESULTS AND DISCUSSION – SPHERICAL GEOMETRY

3.1 First sample: Initial Repository Pressure = 8 – 15 MPa

The results of the first LHS sampling are summarized in Table 3-1. The 8-character variable names shown in the top row of Table 3-1 are defined in Appendix VARIABLE GLOSSARY. Note that the values for each variable fall within the bounds given in Table 2-1. The values in this table were extracted from the LHS output file LHS2_DRSPALL.TRN, listed in its entirety in APPENDIX LHS2_DRSPALL.TRN.

While there are many output variables of potential interest in the spallings model, the item of most concern from a TSPA and regulatory standpoint is the volume of spalled solids that is released to the surface. Shown in Table 3-2 is the summary of spallings releases for the 8-15 MPa runs. Note that only one vector (v007) gave a nonzero release, and the equivalent spalled volume is 0.24 m^3.

Table 3.1. Results of 8-15 MPa LHS sampling. A glossary of variable names is given in Appendix VARIABLE GLOSSARY.

VEC	REPIPRES	REPIPOR	REPIPERM	POISRAT	TENSLSTR	INITMDEN	MUDVISCO	MUDSOLMX	MUDSOLVE	DRILRATE	MUDPRATE	DDZPERM	WALLROUG	SHAPEFAC	PARTDIAM
1	1.44E+07	5.38E-01	1.05E-12	4.11E-01	1.30E+05	1.29E+03	1.86E-02	6.28E-01	-1.66E+00	3.28E-03	2.20E-02	1.04E-15	4.28E-04	8.80E-01	7.88E-03
2	1.12E+07	5.97E-01	6.20E-14	4.00E-01	1.43E+05	1.26E+03	1.56E-02	6.00E-01	-1.77E+00	5.64E-03	2.13E-02	4.28E-14	1.19E-03	9.95E-01	6.90E-03
3	1.18E+07	5.64E-01	8.53E-13	3.57E-01	1.48E+05	1.22E+03	2.53E-02	5.97E-01	-1.67E+00	4.10E-03	1.77E-02	3.22E-14	1.61E-03	2.45E-01	8.13E-03
4	1.04E+07	6.09E-01	7.71E-13	3.82E-01	1.67E+05	1.32E+03	8.66E-03	6.19E-01	-1.71E+00	5.84E-03	1.67E-02	2.08E-14	6.69E-05	2.01E-01	5.91E-03
5	9.27E+06	5.00E-01	2.72E-13	4.17E-01	1.25E+05	1.31E+03	9.75E-03	6.10E-01	-1.26E+00	4.04E-03	1.76E-02	6.65E-15	2.60E-03	7.05E-01	4.51E-03
6	1.46E+07	6.35E-01	3.41E-13	3.83E-01	1.27E+05	1.37E+03	2.81E-02	5.93E-01	-1.39E+00	4.54E-03	2.25E-02	5.62E-14	8.78E-05	5.02E-01	7.27E-03
7	1.39E+07	3.93E-01	1.13E-13	4.19E-01	1.60E+05	1.27E+03	1.93E-02	6.34E-01	-1.54E+00	5.18E-03	2.10E-02	1.83E-15	1.53E-03	1.73E-01	8.77E-03
8	1.46E+07	4.53E-01	3.73E-13	3.85E-01	1.45E+05	1.20E+03	1.46E-02	6.40E-01	-1.44E+00	5.63E-03	1.88E-02	7.67E-14	2.11E-03	5.33E-01	4.71E-03
9	1.26E+07	5.68E-01	8.00E-14	4.03E-01	1.52E+05	1.25E+03	1.24E-02	6.29E-01	-1.36E+00	3.01E-03	1.74E-02	8.67E-14	5.51E-05	5.86E-01	6.61E-03
10	9.42E+06	3.75E-01	5.60E-13	4.23E-01	1.35E+05	1.35E+03	8.26E-03	6.06E-01	-1.79E+00	3.56E-03	2.17E-02	2.87E-14	1.02E-04	1.08E-01	2.33E-03
11	8.23E+06	4.34E-01	2.61E-13	4.29E-01	1.23E+05	1.20E+03	2.74E-02	6.37E-01	-1.69E+00	5.12E-03	2.28E-02	3.89E-14	1.28E-04	7.94E-01	3.52E-03
12	1.34E+07	4.65E-01	1.19E-12	3.64E-01	1.42E+05	1.23E+03	1.62E-02	6.31E-01	-1.61E+00	3.16E-03	1.66E-02	1.90E-15	2.20E-04	9.41E-01	5.62E-03
13	1.16E+07	5.52E-01	5.15E-14	3.59E-01	1.69E+05	1.34E+03	1.36E-02	6.21E-01	-1.50E+00	5.24E-03	2.36E-02	9.62E-15	5.95E-04	9.31E-01	2.98E-03
14	1.08E+07	4.60E-01	3.29E-14	4.08E-01	1.63E+05	1.26E+03	1.15E-02	5.99E-01	-1.23E+00	3.50E-03	2.32E-02	4.79E-14	1.17E-03	8.93E-01	6.15E-03
15	1.02E+07	3.69E-01	1.51E-13	3.51E-01	1.32E+05	1.28E+03	1.83E-02	6.27E-01	-1.43E+00	4.19E-03	2.20E-02	3.50E-15	1.98E-03	3.29E-01	3.22E-03
16	8.11E+06	4.93E-01	1.40E-13	3.54E-01	1.65E+05	1.31E+03	2.97E-02	6.22E-01	-1.54E+00	4.35E-03	2.07E-02	5.00E-15	8.58E-05	6.76E-01	4.90E-03
17	1.40E+07	4.15E-01	2.66E-14	3.98E-01	1.55E+05	1.36E+03	1.32E-02	5.97E-01	-1.76E+00	3.07E-03	2.11E-02	2.27E-15	7.88E-04	6.56E-01	2.62E-03
18	9.61E+06	3.59E-01	4.73E-13	3.72E-01	1.36E+05	1.37E+03	2.50E-02	6.32E-01	-1.26E+00	4.85E-03	2.03E-02	6.87E-14	4.54E-04	5.76E-01	8.20E-03
19	1.05E+07	5.12E-01	2.24E-13	4.26E-01	1.54E+05	1.34E+03	2.61E-02	6.04E-01	-1.31E+00	5.34E-03	1.63E-02	1.24E-15	2.99E-04	7.34E-01	5.26E-03
20	1.23E+07	6.01E-01	1.78E-13	3.70E-01	1.20E+05	1.32E+03	1.07E-02	6.12E-01	-1.21E+00	4.96E-03	1.94E-02	3.16E-15	1.52E-04	2.93E-01	1.48E-03
21	1.31E+07	5.21E-01	3.08E-14	4.22E-01	1.61E+05	1.15E+03	2.37E-02	6.17E-01	-1.33E+00	4.58E-03	2.00E-02	1.08E-14	3.65E-04	4.33E-01	1.06E-03
22	1.26E+07	5.34E-01	1.76E-14	3.91E-01	1.33E+05	1.18E+03	2.87E-02	6.17E-01	-1.51E+00	3.86E-03	1.90E-02	2.82E-15	1.44E-04	1.50E-01	9.71E-03
23	9.96E+06	6.53E-01	3.77E-14	3.79E-01	1.30E+05	1.30E+03	2.23E-02	6.24E-01	-1.74E+00	3.73E-03	1.91E-02	2.31E-14	3.09E-03	2.74E-01	4.15E-03
24	8.85E+06	6.27E-01	6.76E-13	4.12E-01	1.41E+05	1.24E+03	1.73E-02	6.13E-01	-1.28E+00	4.29E-03	2.39E-02	1.43E-15	6.83E-04	6.34E-01	9.20E-03
25	8.49E+06	6.47E-01	7.24E-14	3.75E-01	1.47E+05	1.17E+03	5.23E-03	6.36E-01	-1.46E+00	3.81E-03	1.97E-02	7.85E-15	5.39E-04	4.24E-01	7.36E-03
26	8.95E+06	4.05E-01	1.30E-12	3.88E-01	1.59E+05	1.15E+03	2.33E-02	5.91E-01	-1.57E+00	3.39E-03	1.81E-02	1.60E-14	9.20E-04	4.84E-01	3.88E-03
27	1.12E+07	4.81E-01	2.00E-14	3.66E-01	1.22E+05	1.19E+03	2.13E-02	6.02E-01	-1.59E+00	5.47E-03	1.70E-02	1.39E-14	1.83E-04	7.68E-01	1.85E-03
28	1.29E+07	3.83E-01	1.03E-13	3.62E-01	1.28E+05	1.19E+03	6.80E-03	6.12E-01	-1.63E+00	4.68E-03	2.31E-02	4.13E-15	6.06E-05	8.45E-01	8.93E-03
29	1.35E+07	5.78E-01	1.50E-12	3.93E-01	1.50E+05	1.16E+03	2.05E-02	6.07E-01	-1.38E+00	4.81E-03	2.42E-02	5.41E-15	2.29E-04	3.59E-01	2.13E-03
30	1.20E+07	4.28E-01	4.33E-14	4.03E-01	1.39E+05	1.24E+03	6.17E-03	5.94E-01	-1.40E+00	5.79E-03	1.84E-02	1.33E-14	2.94E-04	3.82E-01	9.66E-03

Table 3-2. Summary of equivalent uncompacted spall volumes (m^3) calculated for the 8-15 MPa sensitivity runs.

Vector	SPLVOLEQ	Vector	SPLVOLEQ
20	0	**14**	0
7	0.2386	**16**	0
15	0	**17**	0
1	0	**18**	0
2	0	**19**	0
3	0	**21**	0
4	0	**22**	0
5	0	**23**	0
6	0	**24**	0
8	0	**25**	0
9	0	**26**	0
10	0	**27**	0
11	0	**28**	0
12	0	**29**	0
13	0	**30**	0

In addition to looking at the summary output, it is instructive to review the progress of selected individual vectors in order to better understand the mechanisms controlling the release volumes. Vectors 020 and 007 are chosen here for a closer look.

3.1.1 Vector 020

Vector 020 has an initial repository pressure of P_I =12.3 MPa, and a resulting equivalent uncompacted spall volume of SPLVOLEQ = 0 m^3. The following series of three figures (Figures 3-1 to 3-3) monitors the progress of several history variables. Included are plots of fluid pressure, radii of repository features, and uncompacted volumes.

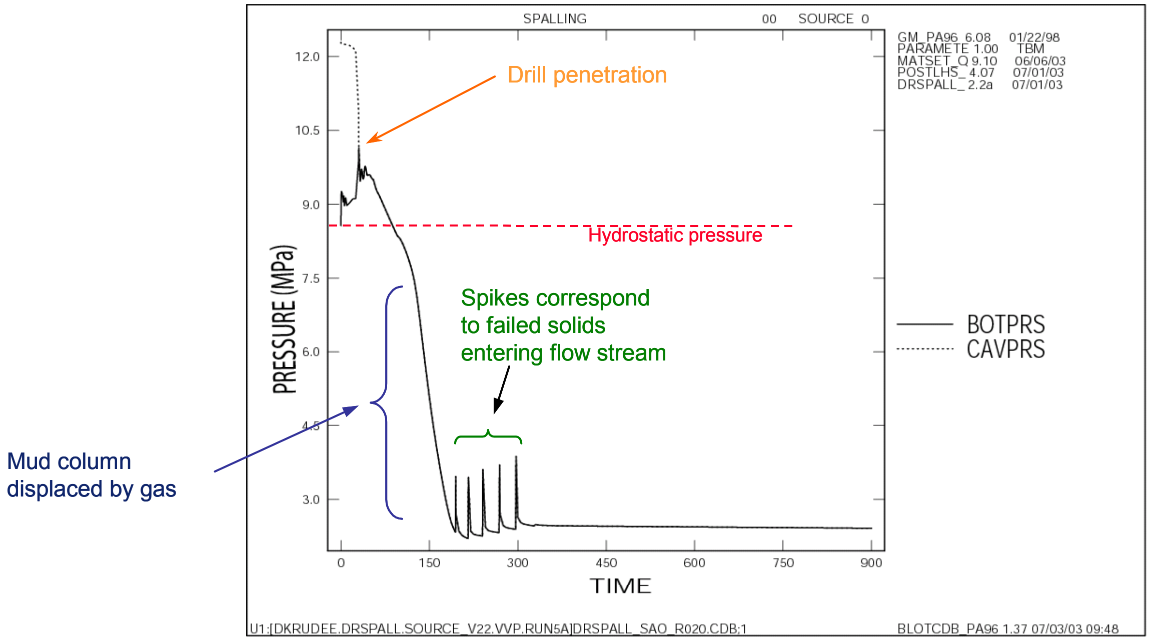

Figure 3-1. Pressure history plot for v020.

Figure 3-1 displays the history variables well bottomhole pressure (BOTPRS) and cavity pressure (CAVPRS) for vector 020. Labeled for reference on this plot is the hydrostatic pressure at the well bottom. Notice that at time = 0, the well starts near hydrostatic pressure, while the cavity pressure representing the face of the repository soon to be penetrated by the drill bit starts at 12.3 MPa (sampled initial repository pressure, REPIPRES). As time progresses and the drill bit approaches the repository, the pressures converge due to gas bleed through the DDZ and become equivalent when the drill actually penetrates the repository. The bottomhole pressure continues to drop as the mud column is displaced by gas and blown out of the borehole. In the field, this circumstance would be recognized by the driller as an increasing mud return rate provoking the closing of the blowout preventer. For the purpose of the WIPP PA, driller intervention is precluded and no steps are therefore taken by the hypothetical driller. Once the mud is displaced, the bottomhole pressure stabilizes to less than 3 MPa as gas blowdown continues. Several spikes in the pressure plot appear between 150 and 300 seconds. These correspond to solids failure and entrainment into the flow stream. Combined factors such as increases in mixture density, mixture viscosity, and numerical noise upon addition of discrete quantities of solids to the largely gas flow stream cause the spikes.

Figure 3-2 displays three radii that describe the progress of drilling (CUTRAD), material failure (TENSRAD), and cavity growth (CAVRAD) in the hemispherical repository domain. All radii start at zero and remain there until the bit intersects the repository at about 40 seconds. The drill bit proceeds though the repository domain until drilling stops at about 320 seconds. The endpoint for drilling is set by the simple formula:

$$\text{drilling time} = \text{repository height/drill penetration rate} \tag{3.1}$$

Repository height varies with porosity, and porosity is a sampled variable. As such, repository height is an indirectly sampled variable. In figure 3-2, the final drilled radius is about 0.49 m. Between 175 and 300 seconds, some stepping of the CAVRAD and TENSRAD variables is observed. This indicates that several tensile failure events expand the cavity momentarily ahead of the drill bit, but drilling eventually catches up so that all three variables overlay after 320 seconds. These steps will also correspond with the spikes observed in the pressure history plot (Figure 3-1).

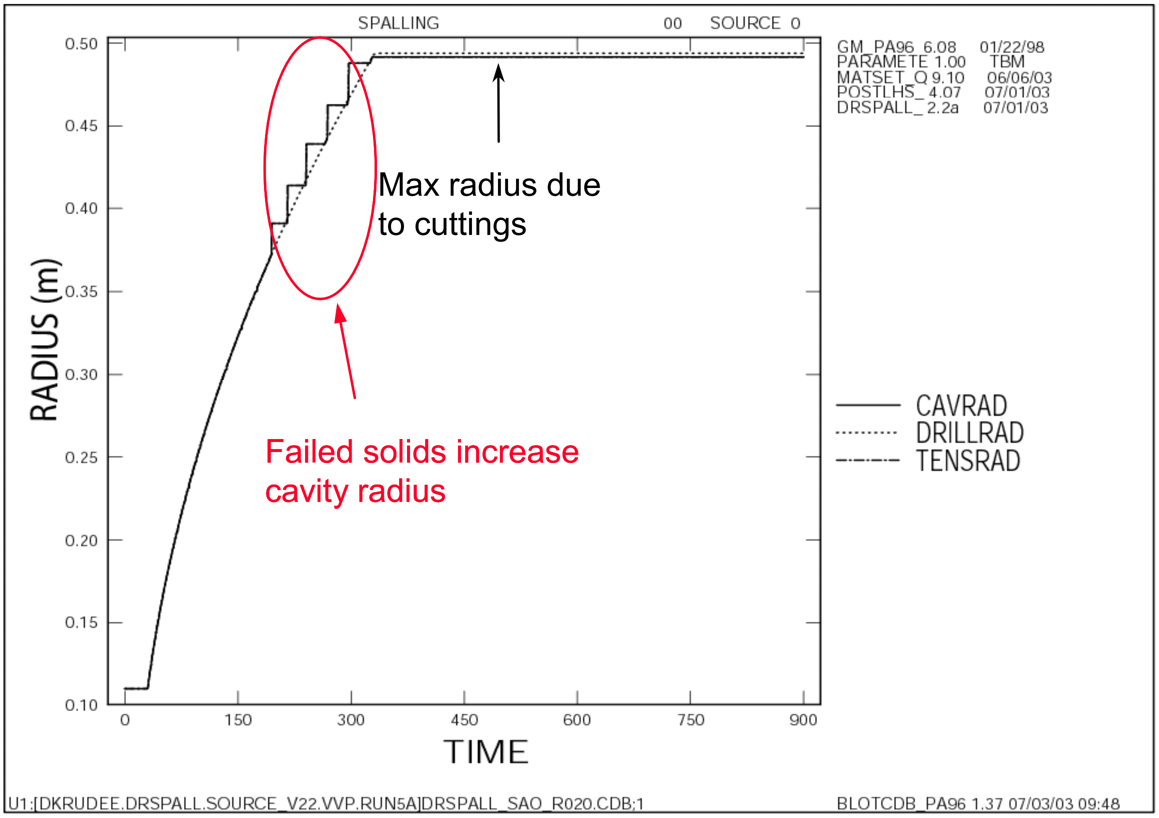

Figure 3-2. Radius variables history plot for v020.

Equivalent uncompacted volumes for v020 are shown as a function of time in Figure 3-3. Three variables, CUTVOLEQ, SPLVOLEQ, and TOTVOLEQ are displayed. All start at zero, and only increase after drilling begins in the repository at ~40 seconds. Notice that CUTVOLEQ and TOTVOLEQ overlay while SPLVOLEQ = 0 until about 175 seconds when the first spalling failure occurs. SPLVOLEQ spikes five times between 175 and 320 seconds, but in every case, drilling eventually excavates the volume spalled and the total spalled volume is reduced to zero. While the material removed by spalling is actually transported up the borehole as soon as it is fluidized, the mass accounting in the code assumes that such material would have eventually been removed by drilling, and therefore is not counted as spalled material in the final report at 900 seconds.

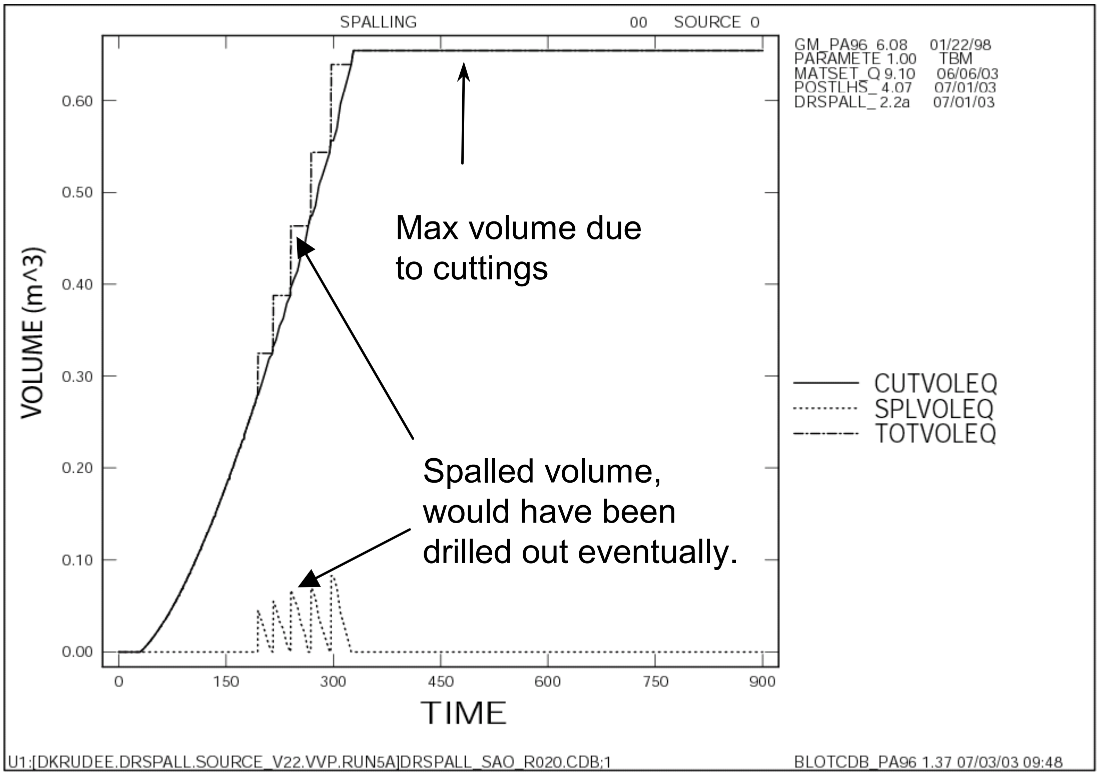

Figure 3-3. Equivalent volumes history plot for v020.

3.1.2 Vector 007

While vector 020 exhibited no ultimate spallings volumes at 900 seconds, vector 007 did have a final volume of SPLVOLEQ = 0.24 m^3. Here we inspect the history variables in v007 closely to see what leads to a spalling event.

Figure 3-4 shows the pressures as a function of time. Repository pressure and bottomhole pressure converge at the time of drill penetration. Similarly to v020, the mud column blows out and bottomhole pressure decreases to below 3.0 MPa. Also, some temporary spall failure is indicated by the spikes between 175 and 300 seconds.

Figure 3-5 shows that the three radii of interest for vector 007 overlay until about 200 seconds when the tensile and cavity radii expand to ~0.46 m. The drilling stops at ~0.40 m, resulting in spalled material at 900 seconds. The match between the cavity radius and tensile radius implies that fluidization occurs immediately after tensile failure. Inspection of the superficial gas velocity (WBSUPVEL) relative to the minimum fluidization velocity (FLUIDVEL) in Figure 3-6 confirms that fluidization should occur at virtually all times after 150 seconds.

Final equivalent uncompacted volumes for v007 are shown in Figure 3-7. The final cavity volume is 0.79 m^3, and after subtracting cuttings, the remaining spalled volume is 0.24 m^3.

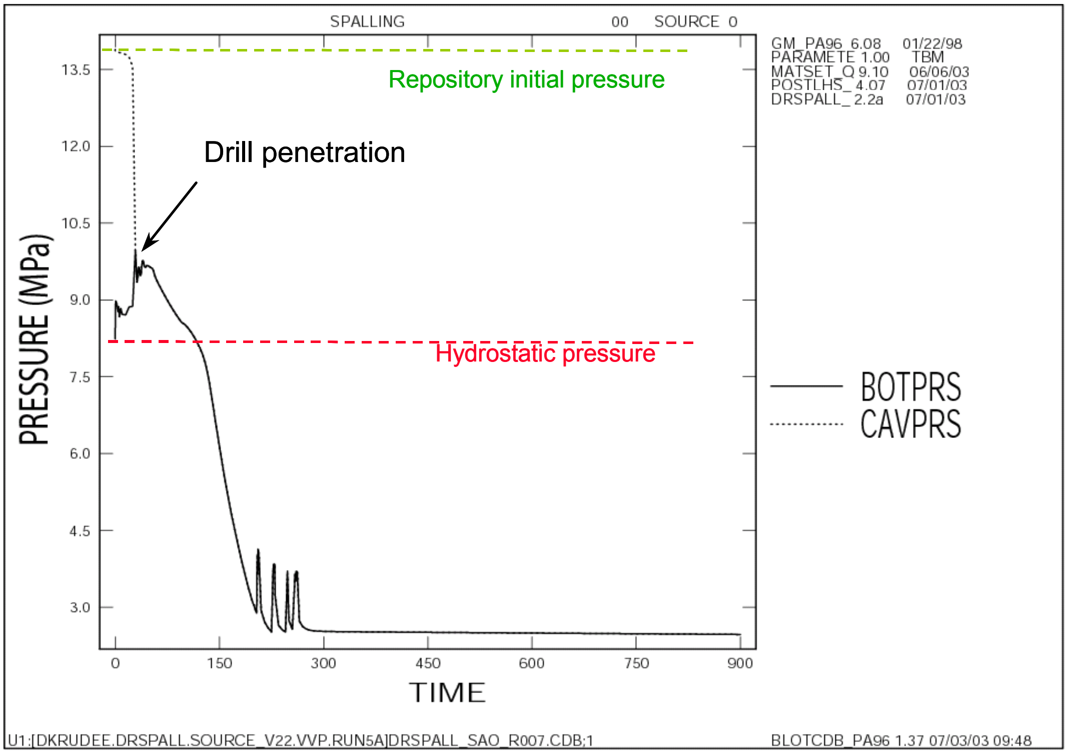

Figure 3-4. Pressure history plot for v007.

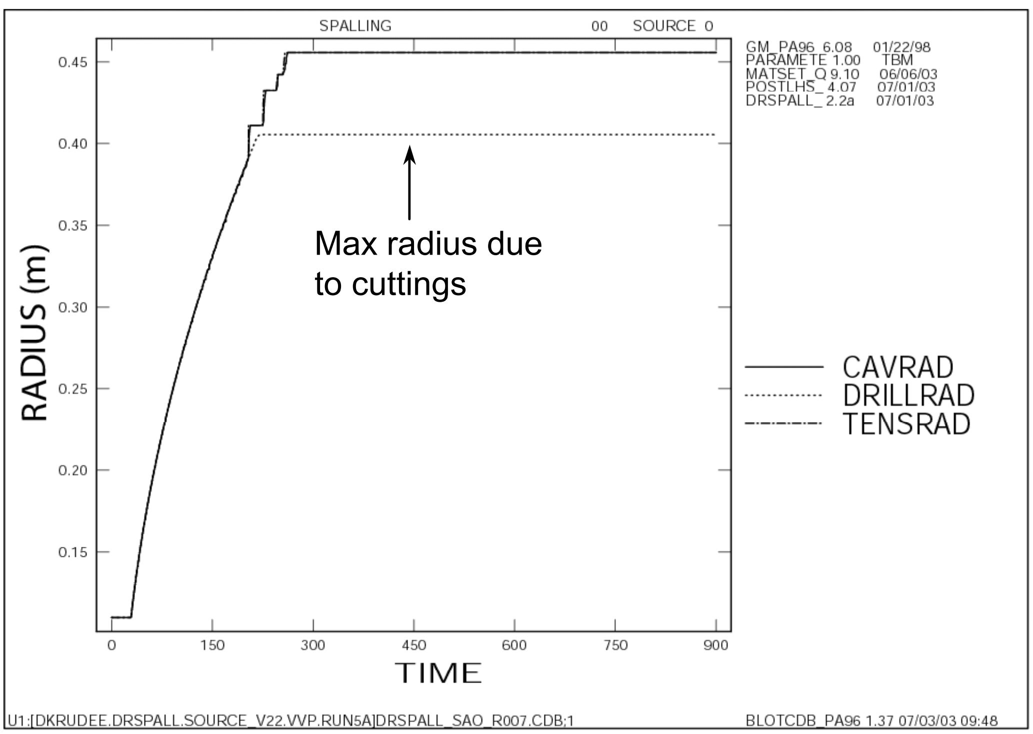

Figure 3-5. Radius variables history plot for v007.

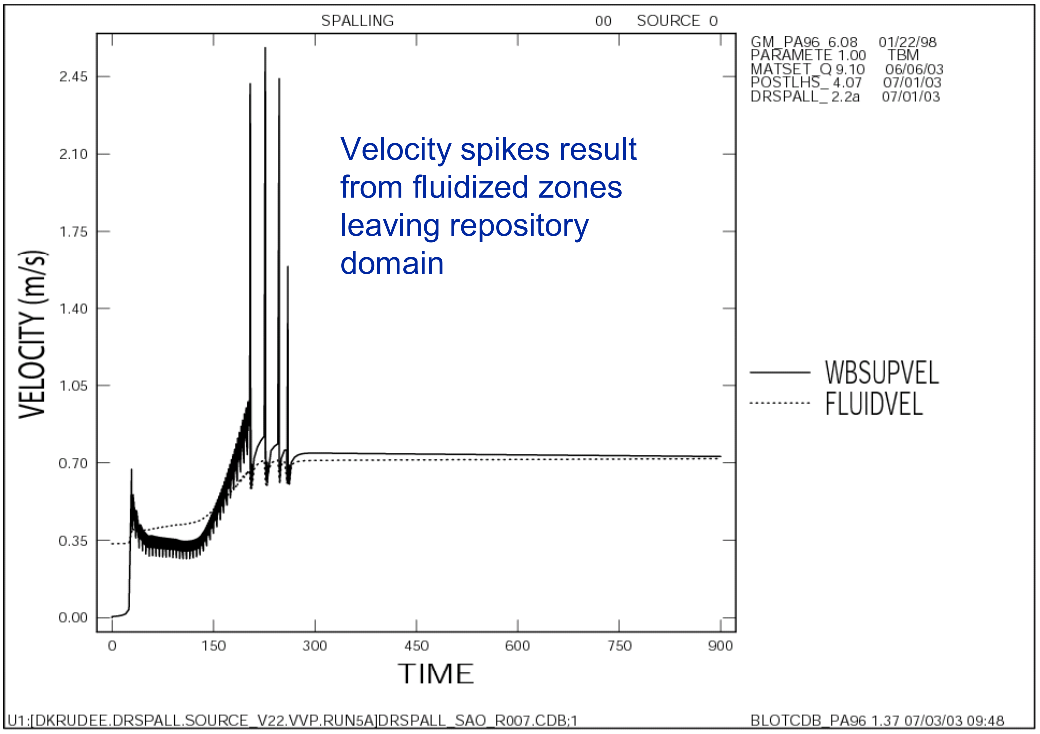

Figure 3-6. Velocity history plot for v007.

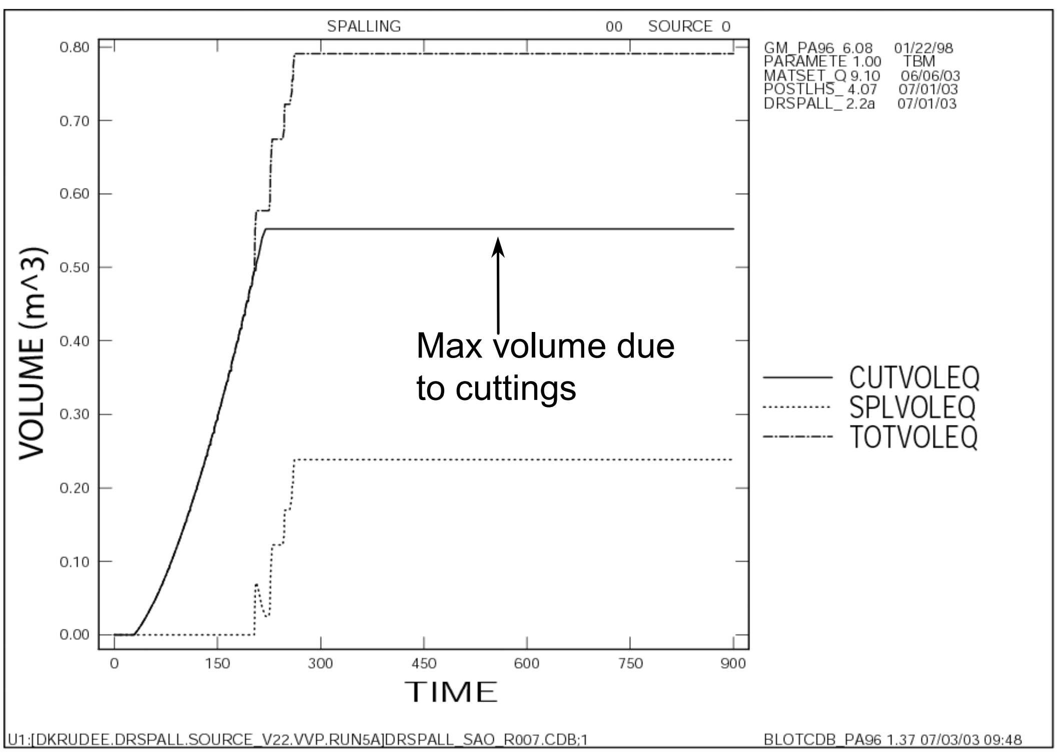

Figure 3-7. Equivalent uncompacted volume plot for v007.

3.2 Second sample: Initial Repository Pressure = 12 – 15 MPa

The range for repository initial pressure is the only variable that changes in this sampling, now raised to 12-15 MPa. As such, all of the other values will be the same vector-by-vector (see Table 3-1). The new pressure sampling is shown in Table 3-3.

Table 3-3. Sampled pressures for high-pressure sensitivity matrix.

vector	Repository Pressure (Pa)	vector	Repository pressure (Pa)
1	1.47E+07	16	1.20E+07
2	1.33E+07	17	1.45E+07
3	1.36E+07	18	1.27E+07
4	1.30E+07	19	1.31E+07
5	1.25E+07	20	1.38E+07
6	1.47E+07	21	1.41E+07
7	1.45E+07	22	1.39E+07
8	1.48E+07	23	1.28E+07
9	1.39E+07	24	1.24E+07
10	1.26E+07	25	1.22E+07
11	1.21E+07	26	1.24E+07
12	1.43E+07	27	1.33E+07
13	1.35E+07	28	1.40E+07
14	1.32E+07	29	1.43E+07
15	1.29E+07	30	1.37E+07

When executed in DRSPALL, these 30 vectors resulted in just three nonzero releases. The summary results are presented in Table 3-4. Note that v007 was again a release vector, with a doubling of release volume observed with an increase in pressure from 13.9 to 14.5 MPa. Vectors 020 and 015 now exhibit nonzero releases, with values of 1.20 and 0.05 m^3 equivalent uncompacted spall volumes, respectively.

Table 3-4. Summary of equivalent uncompacted spall volumes (m^3) calculated for the 8-15 MPa and 12-15MPa sensitivity runs.

Vector	SPLVOLEQ		Vector	SPLVOLEQ	
	8-15 MPa	*12-15 MPa*		*8-15 MPa*	*12-15 MPa*
20	0	1.2026	**14**	0	0
7	0.2386	0.49153	**16**	0	0
15	0	0.049454	**17**	0	0
1	0	0	**18**	0	0
2	0	0	**19**	0	0
3	0	0	**21**	0	0
4	0	0	**22**	0	0
5	0	0	**23**	0	0
6	0	0	**24**	0	0
8	0	0	**25**	0	0
9	0	0	**26**	0	0
10	0	0	**27**	0	0
11	0	0	**28**	0	0
12	0	0	**29**	0	0
13	0	0	**30**	0	0

3.2.1 Vector 020, high pressure

Initial repository pressure was increased relative to the first run from 12.3 MPa to 13.8 MPa. This resulted in an increase in SPLVOLEQ from 0 to 1.2 m^3. Starting with the radius variables (Figure 3-8), it is evident that the tensile and cavity radii separate from the drilled radius after 150 seconds and climb to a stable value of ~0.70 m. Recall that the initiation of failure in the low-pressure v020 (Figure 3-2) also occurred around 150 seconds, but the stress state induced by the lower pressure gradient was not sufficient to propagate the failure more than 2 or 3 cm ahead of the drill bit. In the high-pressure case, the failure and subsequent fluidization (Figure 3-9) caused the cavity to grow rapidly to a radius of 0.70 m, where it then stabilized. The fact that the cavity growth ceased but superficial velocity exceeds fluidization velocity implies that the cavity is stabilized by the stress state, with no more failure occurring. Any failed and bedded material has been entrained and transported to the surface.

Volume history for v020, high pressure, is shown in Figure 3-10. At 150 seconds, the TOTVOLEQ grows along with the cavity radius to a stable volume of ~1.8 m3. SPLVOLEQ reaches a peak of ~1.4 m^3 at 250 seconds, but decreases to 1.2 m^3 as the drill excavates some of the volume that spalled.

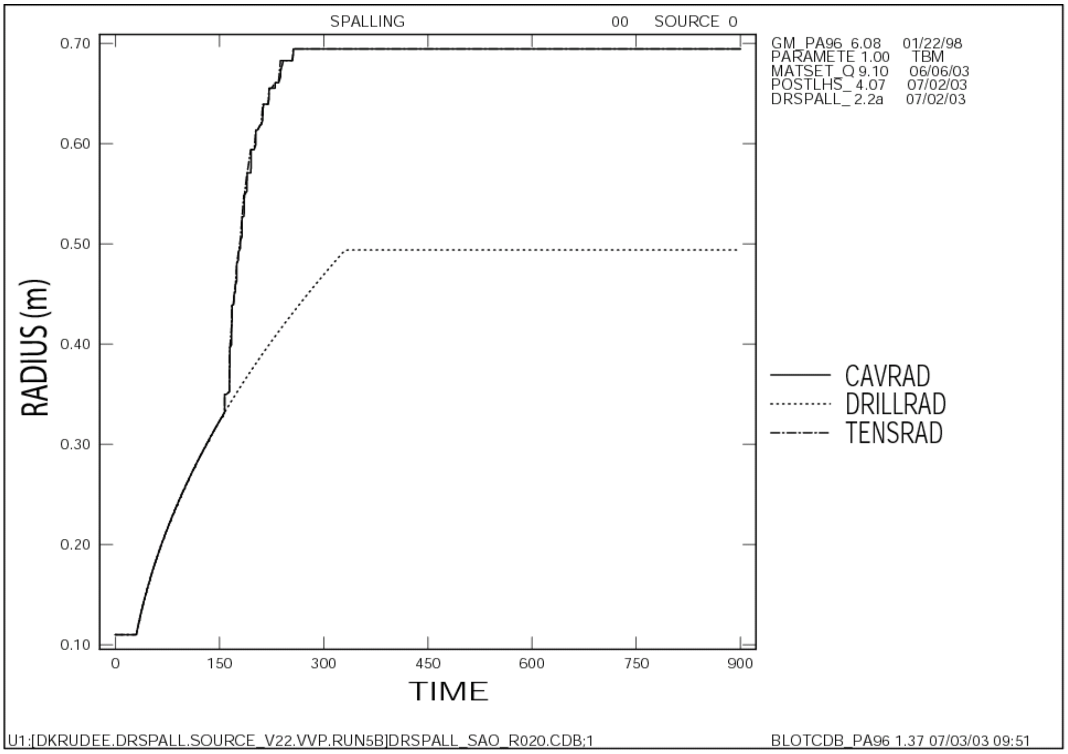

Figure 3-8. Radius variables history plot for v020, high pressure case.

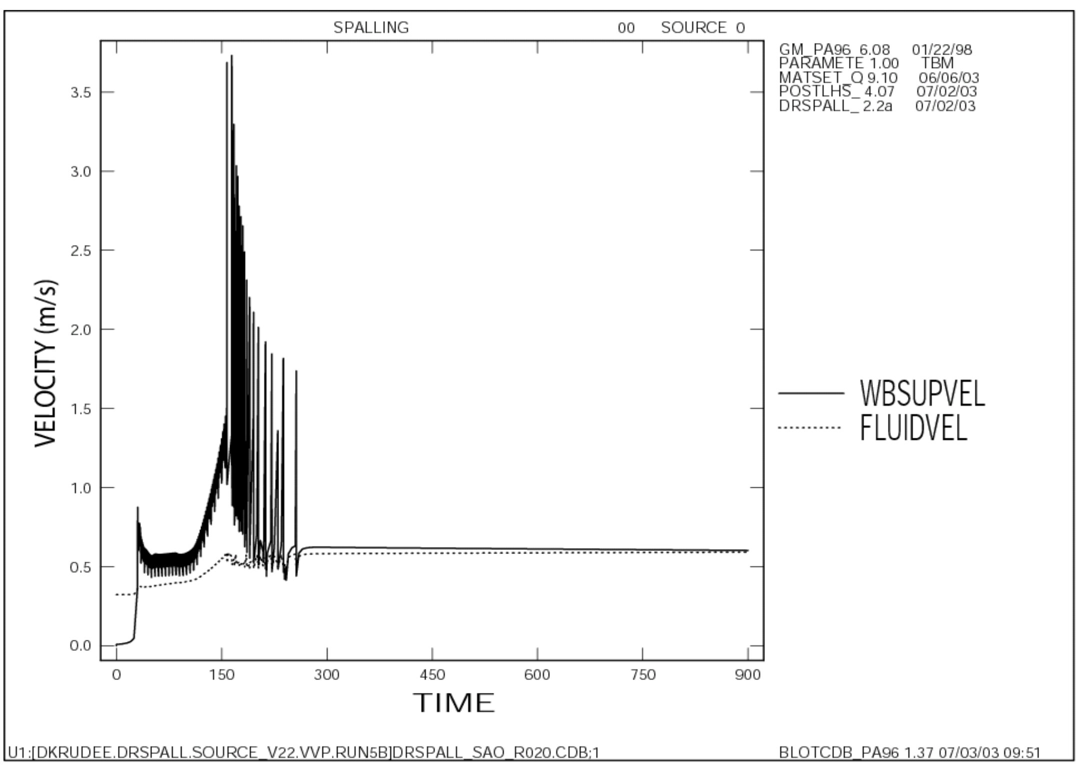

Figure 3-9. Velocity history plot for v020, high pressure case.

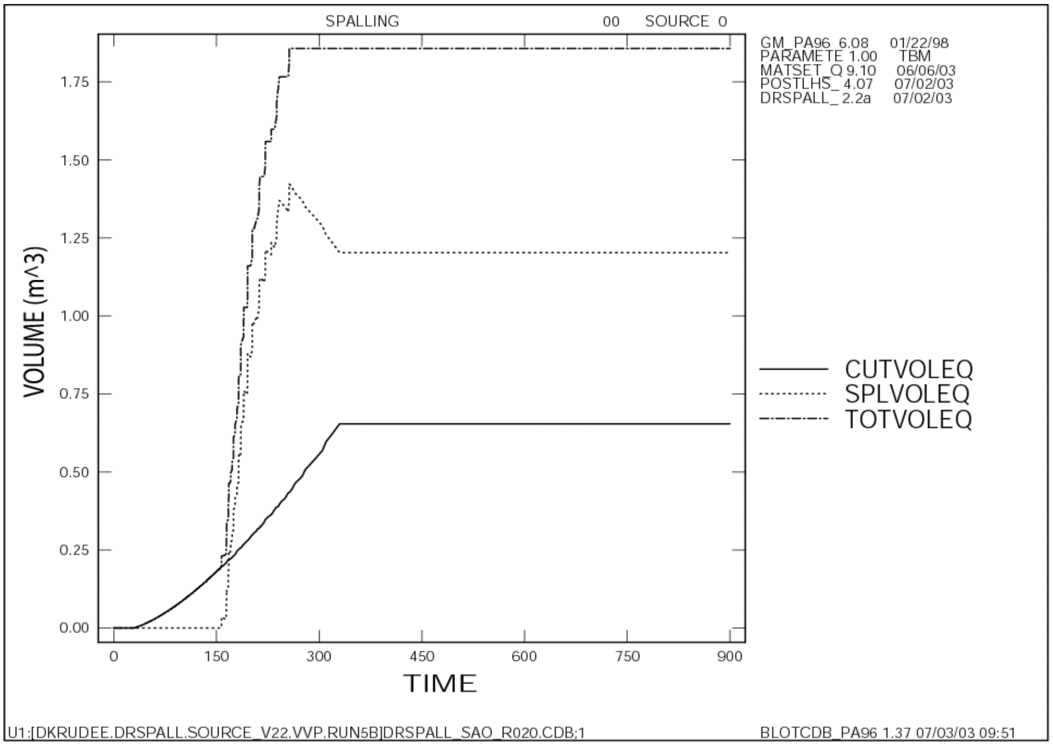

Figure 3-10. Equivalent uncompacted volume history plot for v020, high pressure case.

3.2.2 Vector 007, high pressure

A doubling of spall volume was observed in v007 due to an increase in repository pressure from 13.9 to 14.5 MPa. Inspection of the radius variables plot (Figure 3-11) shows that the failed radius settles to a slightly larger value (0.51 m) than the cavity radius (0.50 m), while the drilled radius stopped at 0.40 m. There is apparently failed, bedded material in this vector that does not entrain into the wellbore flow stream. Confirmation of this can be found in the velocity history plot (Figure 3-12), where the superficial velocity lies below the minimum fluidization velocity after 300 seconds. This cavity is therefore stabilized by the fluidized bed mechanism. The equivalent uncompacted cavity volume stabilized to TOVOLEQ = 1.05 m^3 after 300 seconds, while the equivalent uncompacted spall volume reached a stable value of SPLVOLEQ = 0.49 m^3.

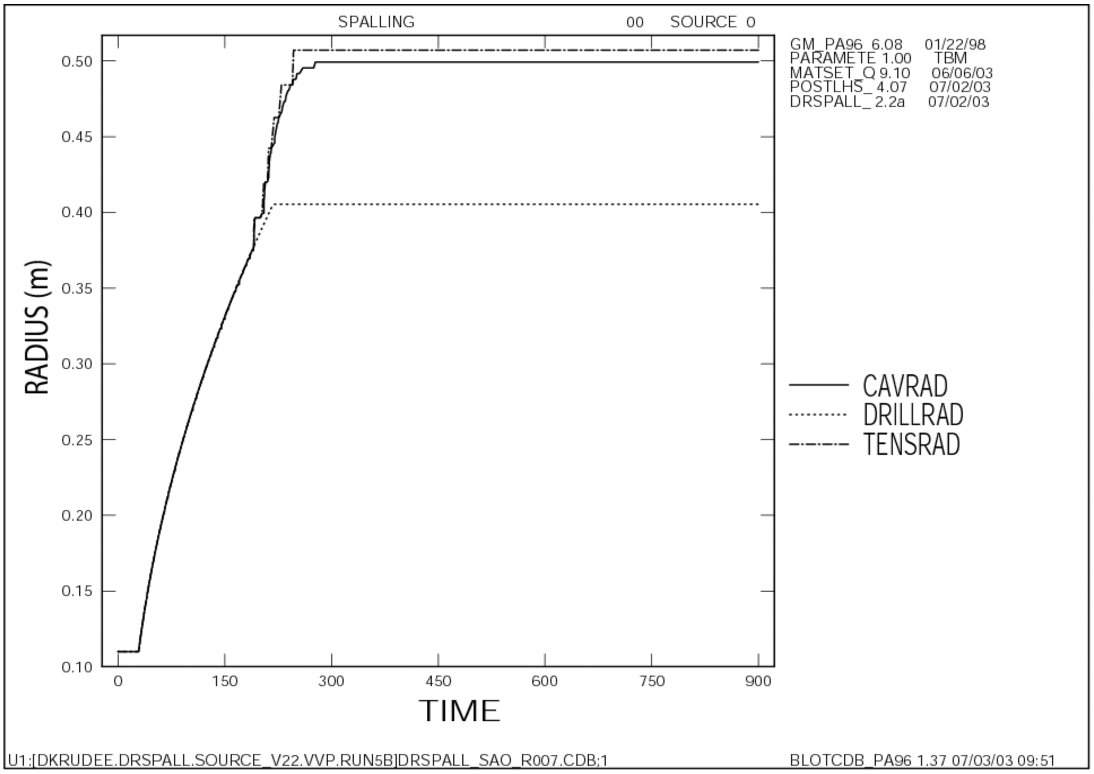

Figure 3-11. Radius variables history plot for v007, high pressure case.

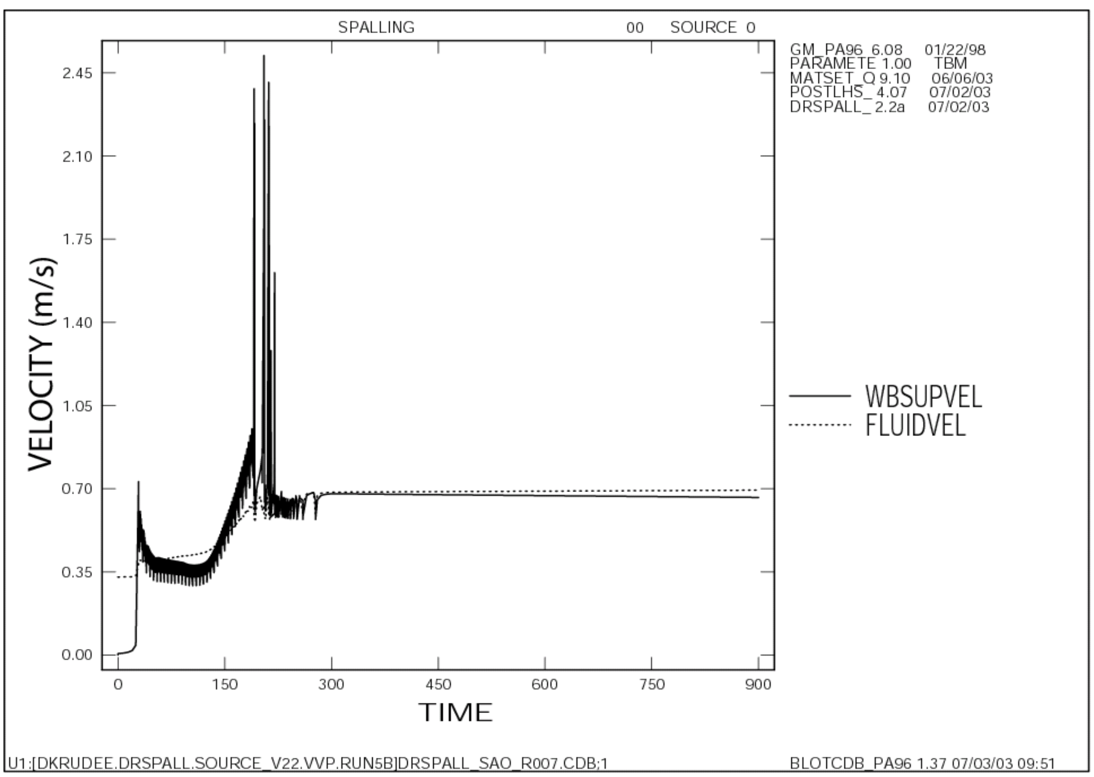

Figure 3-12. Velocity history plot for v007, high pressure case.

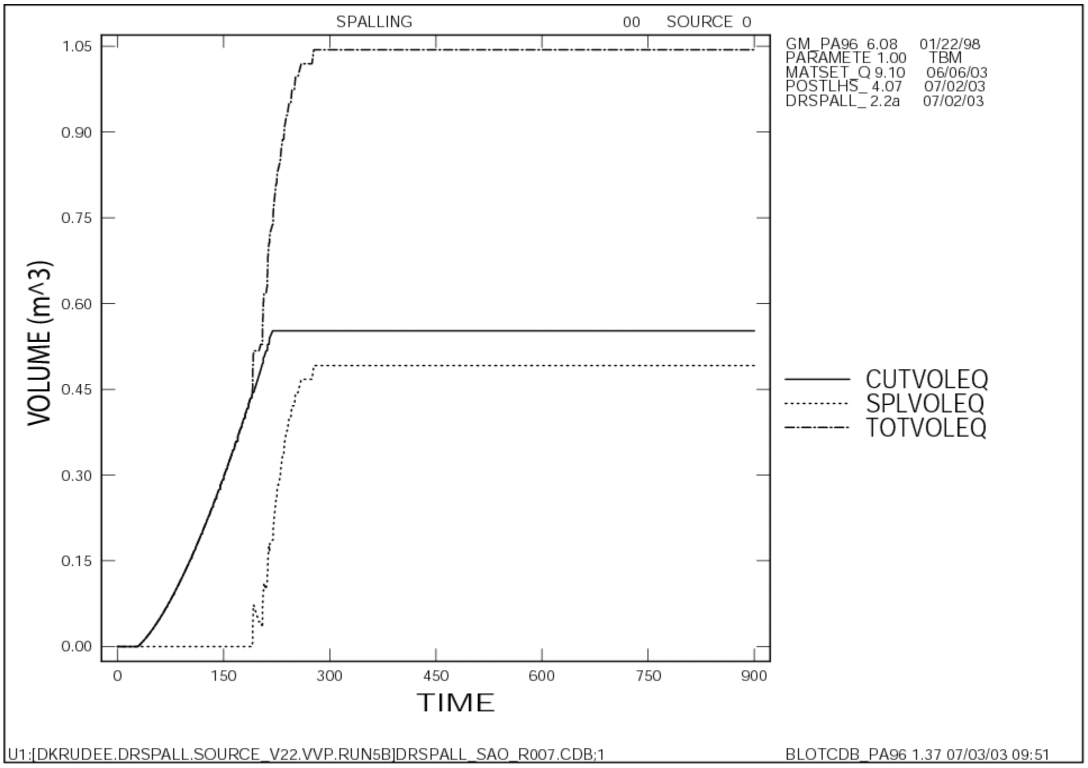

Figure 3-13. Equivalent uncompacted volume history plot for v007, high pressure case.

3.3 Scatterplots

In addition to reviewing lists of final output variables, model sensitivity may also be explored by using scatterplots. A selected dependent variable such as equivalent uncompacted spall volume (SPLVOLEQ) at a late time in the run, typically 900 seconds, is plotted as a function of an independent variable such as initial repository pressure (REPIPRES) . In this format, it is possible to explore possible correlations between the input and output variable by visual inspection the results of all 60 vectors on one set of axes. For the data shown here, the following dependent variables were explored:

- equivalent uncompacted spall volume
- tensile radius – cutting radius

…as a function of the following independent variables:

- repository initial pressure
- repository permeability
- waste tensile strength
- particle diameter × shape factor

3.3.1 Variables controlling equivalent uncompacted spall volume

3.3.1.1 Repository initial pressure

Figure 3-14 shows SPLVOLEQ at 900 seconds plotted as a function of REPIPRES. Each symbol in this figures corresponds to one vector, so there are 60 symbols on this plot. While only 4 vectors of the 60 give nonzero spall releases, it is apparent that no vectors with REPIPRES < 12 MPa exhibited spallings. Repository pressure is a critical variable in the spallings model for several reasons. First, the stress state in the porous solid is a direct function of the pressure gradient formed between the far field and the wellbore. A larger pressure gradient leads to higher stresses and more potential failure. Second, mobilization of tensile-failed solids requires a sufficient gas velocity for the loose particles to mobilize into the flow stream by fluidized bed theory. A minimum fluidization velocity defined by the Ergun (1952) model must be exceeded in order to mobilize waste. The gas velocity at the cavity face that causes fluidization is directly proportional to the pressure gradient at the cavity wall. Therefore, the repository pressure relative to the wellbore pressure is a critical variable impacting the equivalent uncompacted spall volume releases.

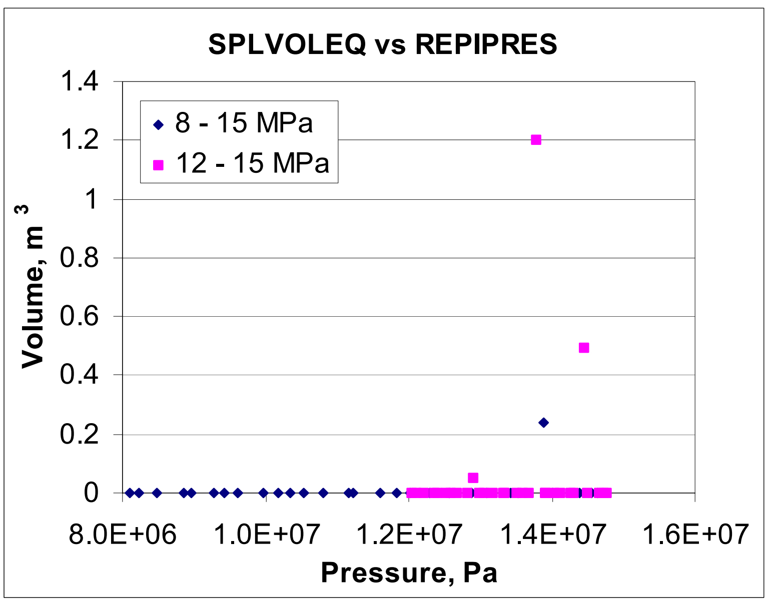

Figure 3-14. Scatterplot of SPLVOLEQ vs. REPIPRES for all 60 vectors.

3.3.1.2 Waste tensile strength

Also potentially important in determining SPLVOLEQ is the tensile strength of waste. Figure 3-15 shows a scatterplot with TENSLSTR as the independent variable. With only four release vectors out of 60, the data above the zero axis are sparse, and it is difficult to find a correlation. The highest release did coincide with the lowest tensile strength vector (v020) from the high-pressure runs (REPIPRES = 13.8 MPa), but no release was observed for the same vector at a slightly lower pressure (REPIPRES = 12.3 MPa).

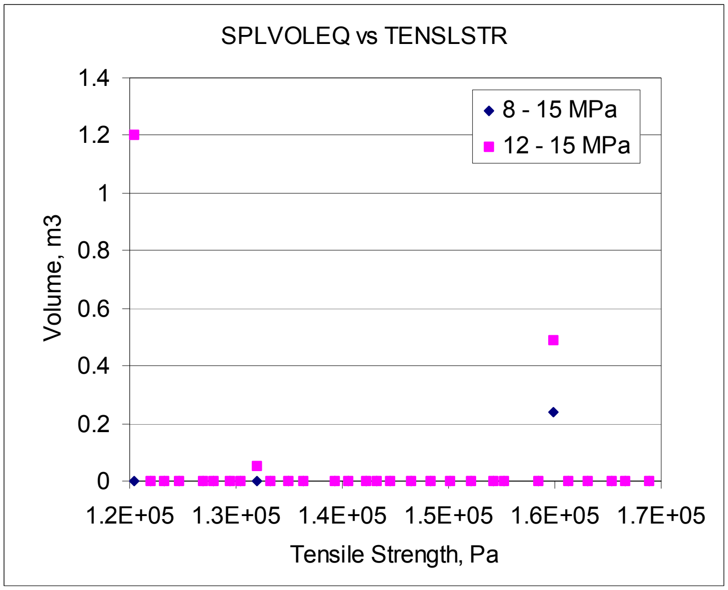

Figure 3-15. Scatterplot of SPLVOLEQ vs. TENSLSTR for all 60 vectors.

3.3.1.3 Particle diameter and shape factor

Particle diameter and shape factor can become important to spall release volumes through their impact on the minimum fluidization velocity calculated by Ergun's equation (Ergun, 1952, Hansen et al., 2003). These two factors appear as a product in Ergun's model, and have the general effect of lowering the minimum fluidization velocity as their product is lowered. In physical terms, small or non-spherical particles in a packed bed are more likely to fluidize than large, spherical particles. The scatterplot shown in Figure 3-16 shows the relationship between the product PARTDIAM*SHAPEFAC and the equivalent uncompacted spall volume. It is difficult from this figure to clearly identify a relationship between the independent and dependent variables. Note that the independent variable axis is plotted on a logarithmic scale, so most of the activity appears to occur below a product of 2.0E-3 m. Recall that particle diameter is varied from 1 mm to 1 cm, while shape factor is varied from 0.1 to 1.0. There is no conclusive relationship indicated in this figure.

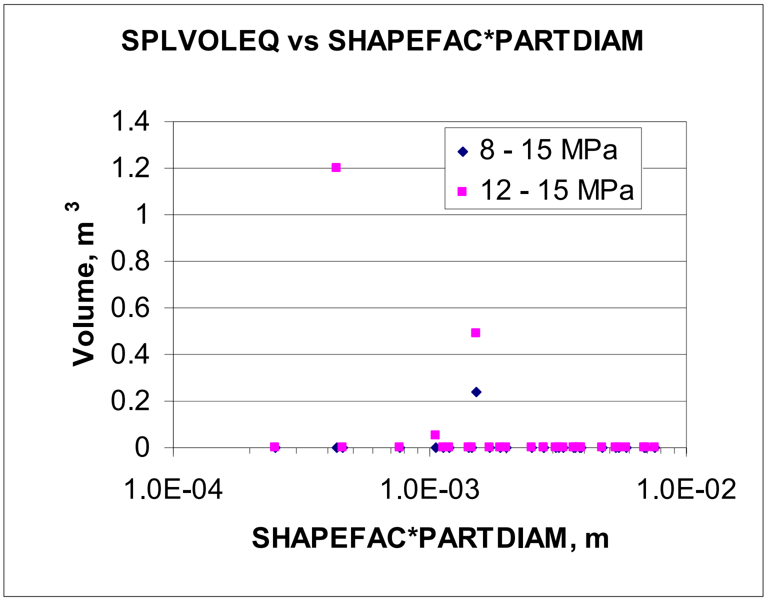

*Figure 3-16. Scatterplot of SPLVOLEQ vs. SHAPEFAC*PARTDIAM for all 60 vectors.*

3.3.2 Variables controlling tensile radius

It is illustrative for this analysis to define a new dependent variable by computing the difference between the tensile-failed radius and the cavity radius. This new variable is depicted schematically in Figure 3-17. While not of particular interest to TSPA results, the difference between these two variables indicates the extent to which the repository material failed ahead of the ultimate drilled radius. This gives an indication of the potential for spallings, independent of how much material was actually moved up the borehole. Tensile failure is a necessary precursor to spall release. In this sensitivity sample where the spall releases are mostly zero, this new intermediate variable helps to visualize the coupled mechanisms that control spall releases, and provides more resolution to the output.

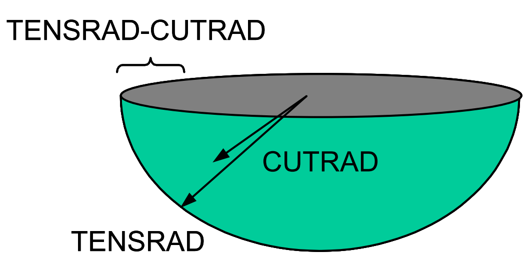

Figure 3-17. Schematic of definition of TENSRAD-CUTRAD output variable.

3.3.2.1 Repository initial pressure

The sensitivity of TENSRAD-CUTRAD to repository initial pressure is illustrated in Figure 3-18. Notice that a distinct break occurs at about 11 MPa. Below this pressure, no failure was observed in any vector. Above this pressure, about half of the vectors exhibited failure. This indicates a strong relationship between pressure and failure, consistent with the design of the conceptual model.

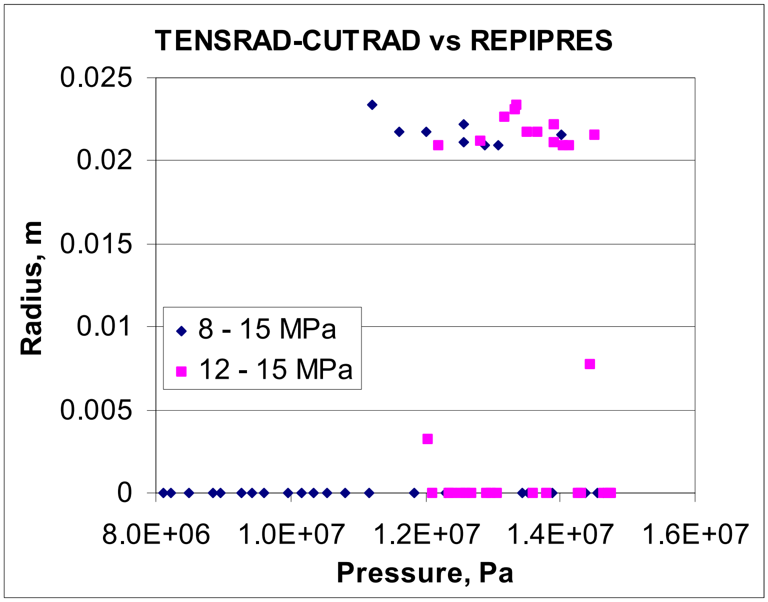

Figure 3-18. Scatterplot of TENSRAD-CUTRAD vs. REPIPRES for all 60 vectors.

3.3.2.2 Tensile strength

The sensitivity of TENSRAD-CUTRAD to waste tensile strength is illustrated in Figure 3-19. No particular correlation is observed, with failure apparently just as likely over the range of tensile strength (0.12-0.17 MPa) examined.

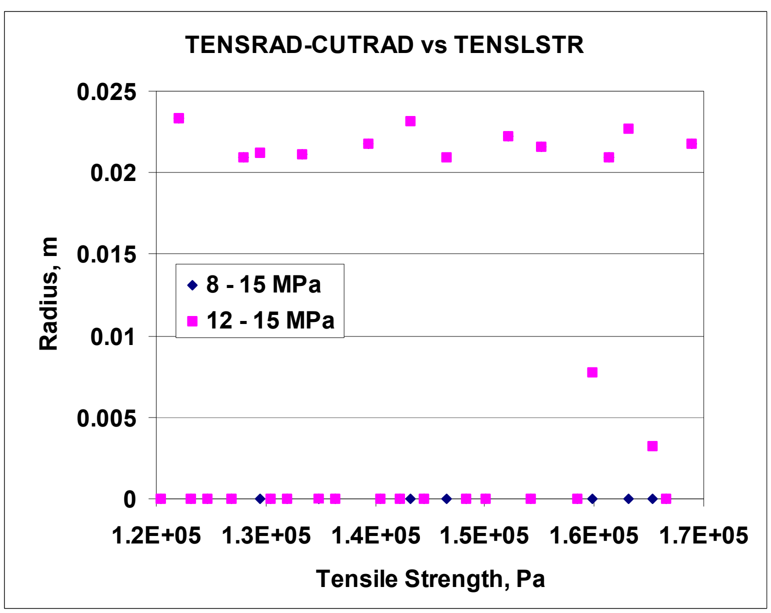

Figure 3-19. Scatterplot of TENSRAD-CUTRAD vs. TENSLSTR for all 60 vectors.

3.3.2.3 Repository permeability

Plotting the TENSRAD-CUTRAD against repository permeability illustrates an important relationship in the spallings model. No failure is observed for waste material with permeability above k = 2E-13 m^2. Alternatively, many failures are observed at permeability below k = 2E-13 m^2. This is consistent with the design of the conceptual model that would suggest more failure due to higher pressure gradients in less permeable media.

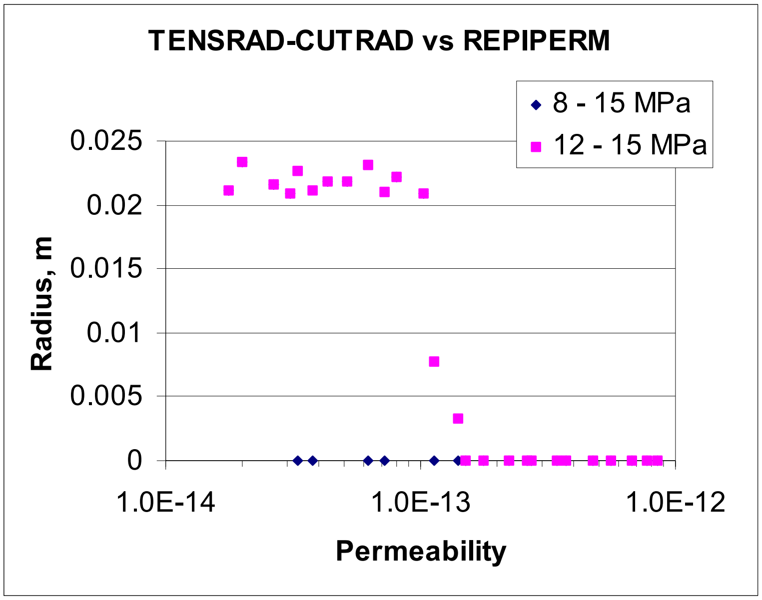

Figure 3-20. Scatterplot of TENSRAD-CUTRAD vs. REPIPERM for all 60 vectors.

4 RESULTS AND DISCUSSION – CYLINDRICAL GEOMETRY

In a real three-dimensional system, the drilling process creates a cylindrical borehole through the waste repository that constantly increases in length and possibly grows radially due to caving and spalling processes. To rigorously simulate a borehole that grows axially, radially, or both, under isotropic homogenous conditions would require a large, computationally-intensive two-dimensional axial-symmetric model. The probabilistic framework in which the spallings model is applied requires many executions, resulting in a necessary balance between model sophistication and computational efficiency. Development of a one-dimensional model geometry was seen as a strategy that would promote computational speed but still include all of the critical mechanisms proposed in the conceptual model. Therefore, two one-dimensional geometric models (hemispherical, cylindrical) are implemented in DRSPALL, with the geometry selected by the user. At early time just prior to and just after penetration, the repository domain is best modeled with hemispherical flow and stress state assumptions. As the bit approaches the floor of the repository the one-dimensional cylindrical assumption is more appropriate. In spite of this, only one geometry may be used per execution in the current DRSPALL model. The purpose of this discussion is to compare the results of cylindrical versus spherical repository geometry for the same set of input parameters.

4.1 Cylindrical vs. Spherical Geometry

The effect of the geometry on specific model setup parameters is demonstrated in Figure 4-1, which compares equivalent radius and enclosed volume for the two geometries as a function of drill bit penetration depth. Recall that the equivalence to the actual wellbore geometry drilled into the repository assumes conservation of cavity surface area (§ 2.3.1.1). The result is that neither the drilled radius nor the drilled volume is conserved. Surface area is conserved to provide consistency in the coupling of the wellbore and repository models with respect to gas flow. At early times for cylindrical geometry, the wellbore cavity is modeled as a very small diameter cylinder with a length equal to the repository height. As drilling proceeds, the actual 3-D wellbore cavity in the repository increases while radius remains constant. In the one-dimensional DRSPALL model, however, the wellbore cavity length is fixed and the radius increases to conserve surface area. When the drill bit reaches the repository floor at a depth of 1.5 m, the radius and volume for cylindrical geometry is slightly larger than the actual 3-D wellbore because the circular surface area at the bottom of the wellbore is included in the circumferential surface area of the cylindrical geometry model. In spherical geometry the equivalent radius and volume are considerably larger than that of the actual 3-D wellbore cavity. Recall that a sphere has the largest ratio of volume to surface area of any geometric shape, so for a given surface area, the volume of a hemisphere will be larger than that of a cylinder.

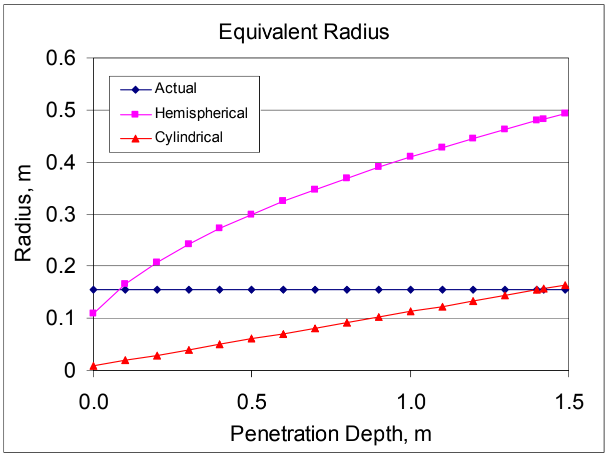

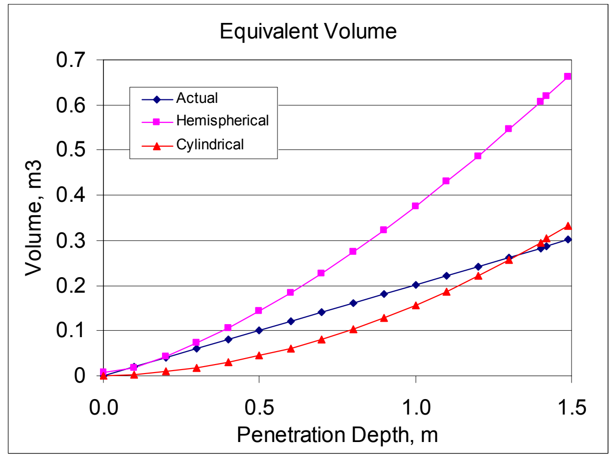

Figure 4-1. Equivalent radius and volume for one-dimensional hemispherical and cylindrical geometries

Figure 4-2 shows the effect of geometry on the radial elastic stress. Recall that the radial elastic stress ($\sigma_{er}(r)$) represents the stress distribution as a function of radius r in a thick-walled shell, determined by the geometry and the boundary conditions. The formula used in DRSPALL (WIPP PA, 2003) appears as:

$$\sigma_{er}(r) = \left\{ \sigma_{ff} \left[1 - \left(\frac{r_c}{r} \right)^m \right] + p_c \left(\frac{r_c}{r} \right)^m \right\} \tag{4.1}$$

where σ_{ff} is the far-field stress outer boundary condition, r_c is the cavity (inner wall) radius, m is the geometry exponent (cyl: m = 2, sph: m = 3), and p_c is the cavity pressure inner boundary condition. A spreadsheet was used to calculate stress profiles using Eq. 4.1 and the boundary conditions corresponding to a bit penetration depth of 0.7, with the resulting profiles shown in Figure 4-2. Three curves are shown: (1) cylindrical geometry with r_c = 0.082m, (2) hemispherical geometry with r_c =0.35 m, and (3) cylindrical geometry with r_c =0.35 m.

There are two major factors contributing to the differences in the stress profiles. One factor arises from the conservation of cavity surface area during drilling, which results in a much smaller equivalent cavity radius in cylindrical geometry (r_c = 0.082m) versus spherical geometry (r_c = 0.35m) at a given bit penetration depth. The inner boundaries in curves 1 and 2 correspond to the respective equivalent cavity radii for a real bit penetration depth of 0.7m. This smaller equivalent cavity radius results in larger compressive radial elastic stresses and a steeper stress gradient near the wellbore than in the spherical geometry. The other factor is the geometry. For the same cavity radius (compare curves 2 and 3 with R_c = 0.35m), the cylindrical geometry has lower compressive stresses and gradients near the wellbore than the spherical (compare curves). The differing radius case (curve 1 vs. 2) is representative of the sensitivity results presented in § 4.2. The effect of these differences on effective stress and tensile failure will be dependent on the pore pressure profile, which is a function of both geometry and time.

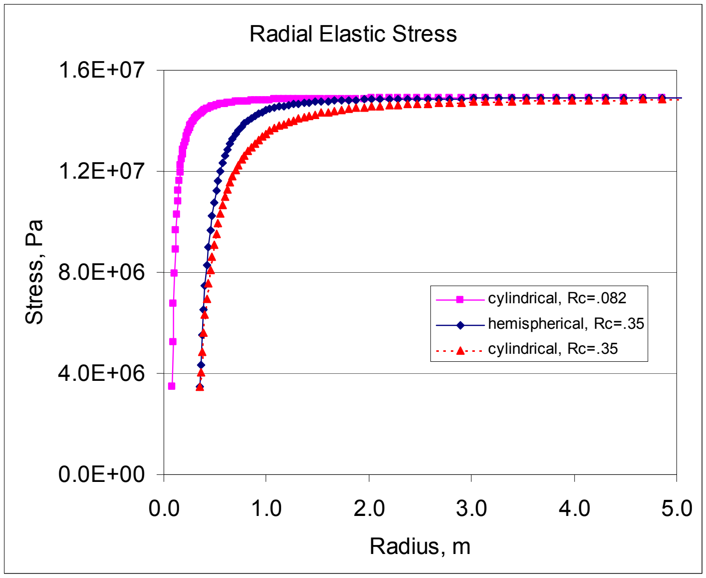

Figure 4-2. Radial elastic stress profiles for one-dimensional hemispherical and cylindrical geometries

For the discussions in the remainder of this section, the two sets of 30 runs used in the original sensitivity study presented in Section 3 were repeated with only the geometry input flag switched from hemispherical to cylindrical. All other sampled and numerical modeling parameters remained the same. The result was that zero spall release was calculated for all 60 vectors when using cylindrical geometry as compared to 4 vectors that had nonzero spall release when using spherical geometry (1 for 8-15MPa set and 3 for the 12-15MPa set). The summary of releases comparing the geometries for the 30 high pressure (12-15 MPa) runs is shown in Table 4-1.

Table 4-1. Summary of equivalent uncompacted spall volumes (m^3) calculated for the 12-15 MPa sensitivity runs for spherical and cylindrical geometries.

Vector	SPLVOLEQ (12-15 MPa)		Vector	SPLVOLEQ (12-15 MPa)	
	Spherical	*Cylindrical*		*Spherical*	*Cylindrical*
20	1.2026	0	**14**	0	0
7	0.49153	0	**16**	0	0
15	0.049454	0	**17**	0	0
1	0	0	**18**	0	0
2	0	0	**19**	0	0
3	0	0	**21**	0	0
4	0	0	**22**	0	0
5	0	0	**23**	0	0
6	0	0	**24**	0	0
8	0	0	**25**	0	0
9	0	0	**26**	0	0
10	0	0	**27**	0	0
11	0	0	**28**	0	0
12	0	0	**29**	0	0
13	0	0	**30**	0	0

The effect of the geometry is demonstrated below in section 4.1 by comparing histories (variable versus time) and profiles (variable versus repository radius) of intermediate results for vector 020 from the high-pressure sampled set, which had the largest spall release in the original sensitivity study.

4.2 Vector 020 cylindrical vs. spherical results

In this section histories and profiles of intermediate results are compared to demonstrate the effect of the one-dimensional model geometries. Profiles were taken at 160 seconds or just after tensile failure began with spherical geometry. Note these profiles will have almost the same cavity surface area but different repository inner radii and drilled volumes because of the equivalent geometry assumption that conserves surface area.

4.2.1 History variables

Figure 4-3 shows bottomhole (BOTPRS) and cavity (CAVPRS) pressure histories for (a) the spherical geometry, and (b) the cylindrical geometry. Differences first appear at runtime ~20 sec, or 10 sec prior to bit penetration. While in the spherical geometry, cavity pressure at the face of the waste decreases from 14 to 10 MPa right before penetration, in cylindrical geometry, the cavity pressure decreases to ~13.5 MPa right before penetration. This implies that the pore pressure near point of penetration is higher in the cylindrical case than in the spherical case, and the pressure gradients will be lower at the time of intrusion. Consequently, the wellbore in the cylindrical case sees a much higher repository pressure upon penetration. Eventually, bottomhole pressure stabilizes at a lower value with the cylindrical repository geometry after 300 seconds. The spikes in pressure between 150 and 250s for the hemispherical case are due to fluidized waste entering the wellbore.

The difference in bottom hole pressure just prior to penetration is due to the wellbore numerical diffusion implementation at the bottom of the wellbore. The effect is amplified in the cylindrical case because of the smaller timesteps and smaller equivalent cavity radius relative to the spherical runs. Subsequent adjustments to the diffusion model have shown marked improvement in comparisons of early time bottom hole pressure. The effect of these adjustments on the spherical case was less significant and tended to reduce spall. These modifications will be incorporated in the results presented in the Sensitivity Analysis Report - Part II.

Figure 4-4 shows equivalent uncompacted spall (SPLVOLEQ), cuttings (CUTVOLEQ) and total (TOTVOLEQ) volume histories and clearly reveals the spall releases in the hemispherical case (1.2 m^3 at 900 seconds). Also evident is the difference in cuttings volume (final spherical CUTVOLEQ = 0.66 m^3, cylindrical CUVOLEQ = $0.33m^3$) because the equivalent geometries do not conserve volume. Similar results are shown for cavity radius (CAVRAD), tensile failure radius (TENSRAD) and equivalent drilling radius (DRILLRAD) in Figure 4-5. The fact that CAVRAD and TENSRAD overlay in Figure 4-4a after 150 seconds indicates that any solid material that failed in tension was also fluidized.

Figure 4-6 shows fluidization velocity threshold (FLUIDVEL) and superficial pore velocity (WBSUPVEL) histories for the cell next to the wellbore. The cell comprising the cavity wall varies as material is drilled or fails and fluidizes. Visible in the cylindrical geometry is the lower pore velocity at the time of penetration as a result of the lower pressure gradient. Late time pore velocity is higher in the cylindrical case because the wellbore interface is at a smaller radius (smaller flux area) due to no spall. In both geometries superficial gas velocity near the cavity face exceeded the fluidization threshold, indicating that for the spherical case, spall release was limited by cessation of failure rather than by the fluidization mechanism.

4.2.2 Spatial variables

Figure 4-7 shows pore pressure (POREPRS) and radial total elastic stress (RADELSTR) profiles at 160 sec or just after the initial tensile failure. The effect of the geometry on gradients is apparent in pore pressure profiles, with the spherical case showing steeper gradients near the wellbore. This would also be expected in the elastic stress profile, however, the very small effective radius in the cylindrical geometry is strongly influencing the behavior near the well as was demonstrated earlier.

Figure 4-8 shows radial effective stress (RADEFSTR) and radial seepage stress (RADSPSTR) profiles over the entire repository domain at 160s. Figures 4-9 and 4-10 zoom in on radial effective stress in the region near the cavity wall where the tensile phase develops. Note that on these last two figures the abscissa is relative to the wall rather than the center axis of the wellbore. Also, recall that radial effective stress is calculated from the elastic stress minus the pore pressure (Figure 4-7) plus the seepage stress and that its average value (over a characteristic length= 2.0 cm for this study) is compared to the tensile cutoff value to determine material failure. Therefore, its behavior is important in determining the effect of geometry on spall release. The seepage stress component is very similar for both geometries, indicating that the combined effects of geometry and differential pressure are similar in the two geometries. The peak compressive radial effective stress, however, is more than twice as large in the cylindrical case indicating the pore pressure has dropped more in the interior of the repository relative to the elastic stress. This is also evident in Figure 4-7. Close examination of the region near the cavity interface shows that radial effective stress does not go into tension in cylindrical geometry. In contrast, in the spherical geometry the phasing and relative gradients of the stress components develops a tensile phase right at the cavity interface that covers 2.2 cm and 9 zones. It is in this region that the average tensile stress will eventually exceed the tensile limit and cause failure.

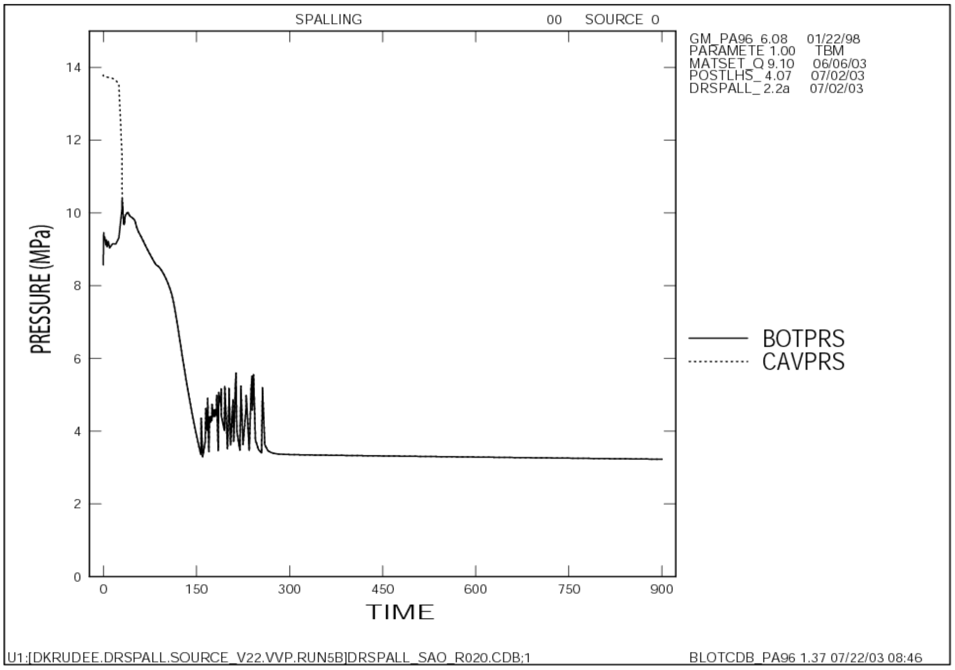

(a) Hemispherical

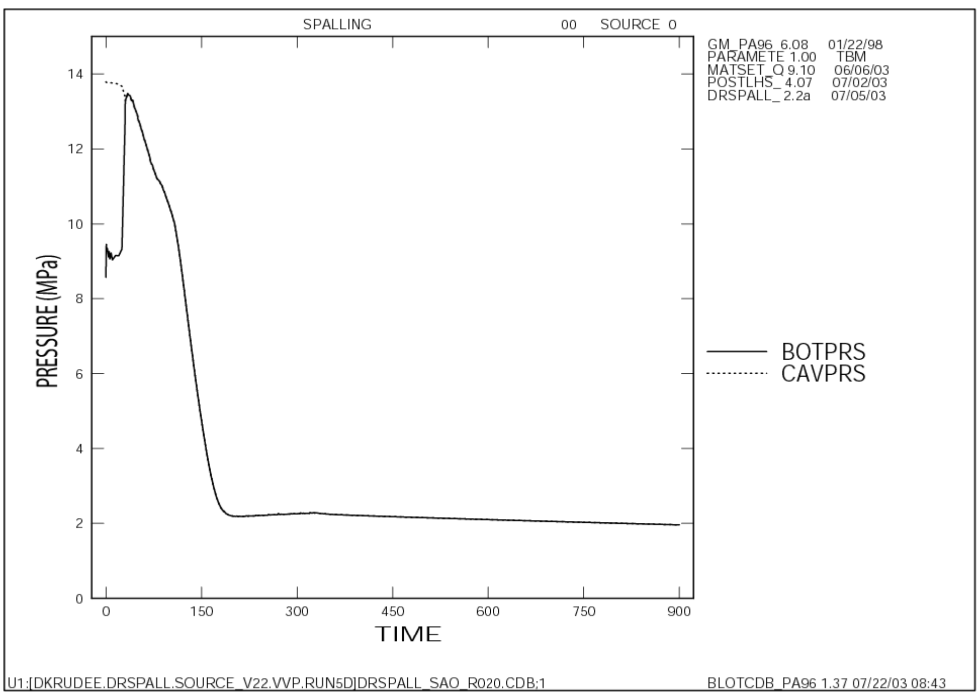

(b) Cylindrical

Figure 4-3. Bottomhole and cavity pressure histories

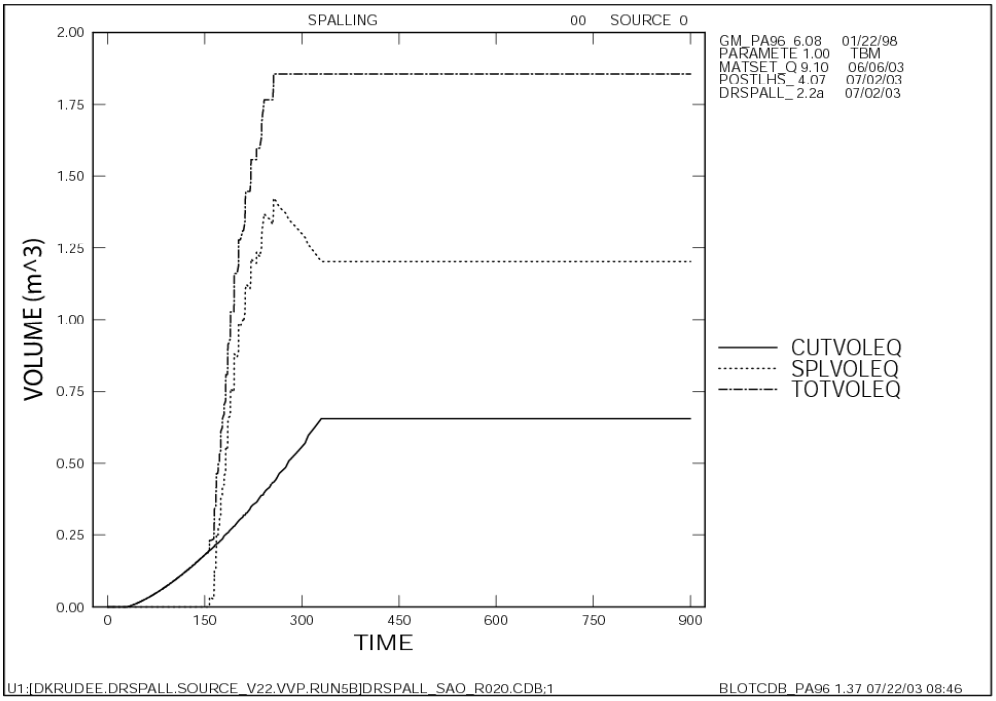

(a) Hemispherical

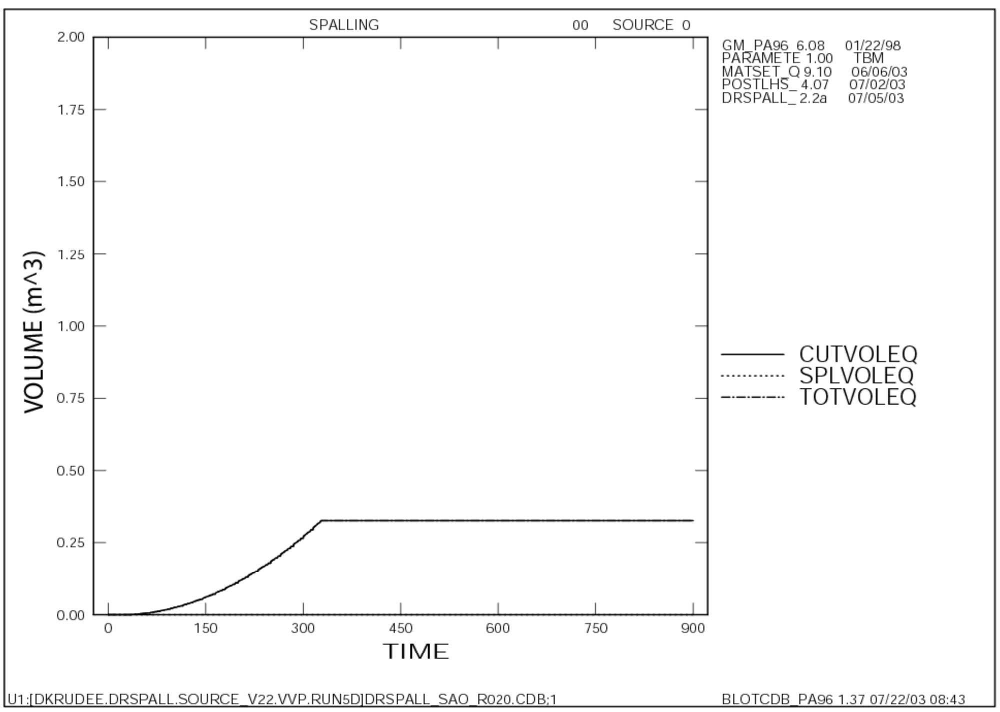

(b) Cylindrical

Figure 4-4. Cuttings, spall and total equivalent uncompacted volume histories

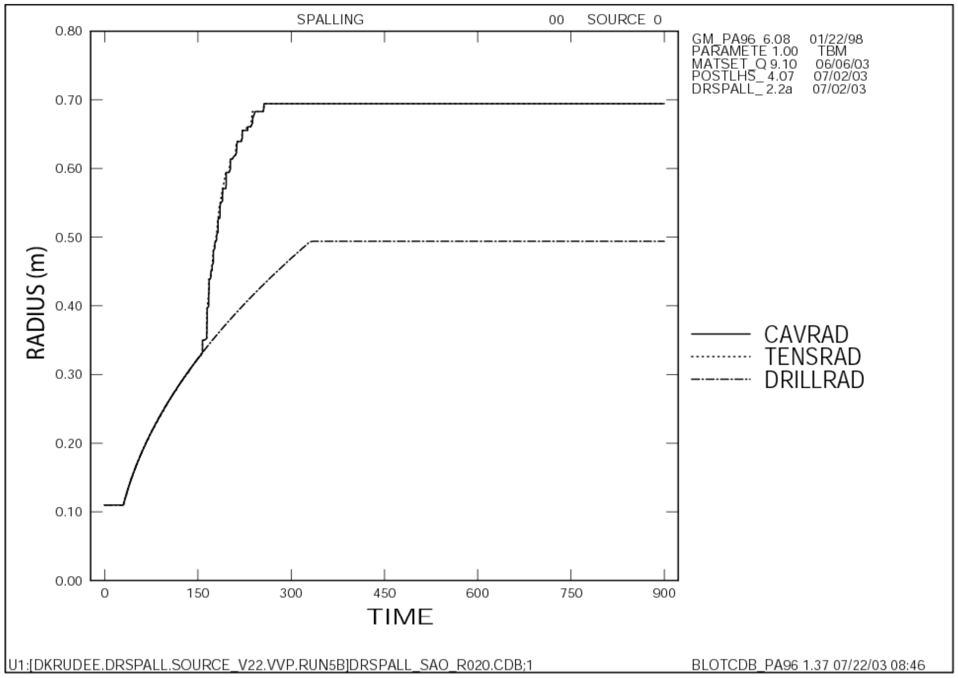

(a) Hemispherical

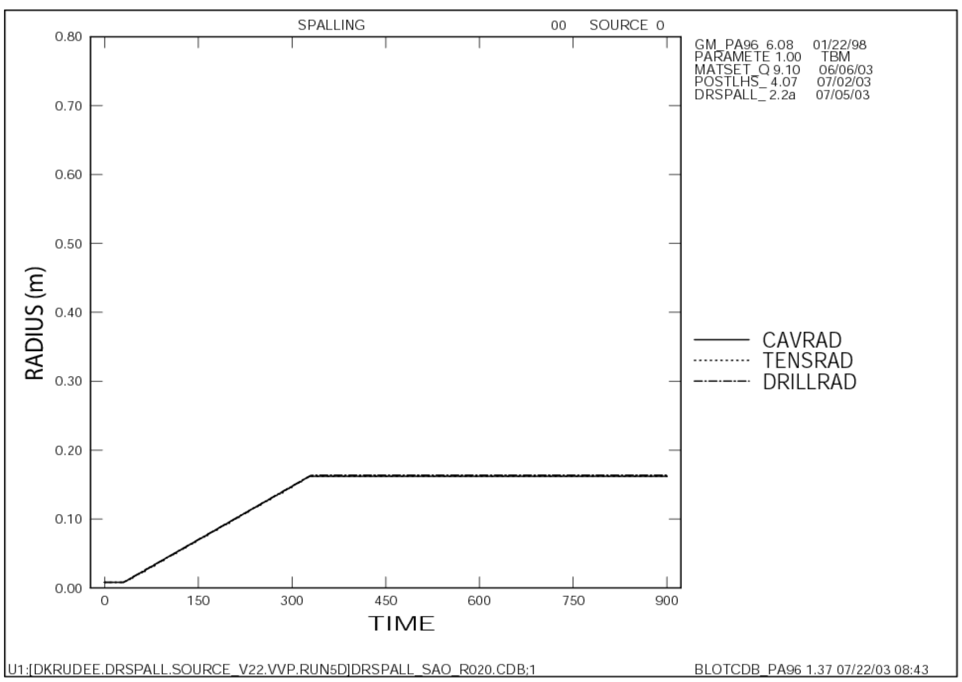

(b) Cylindrical

Figure 4-5. Cavity, tensile and equivalent drilling radii histories

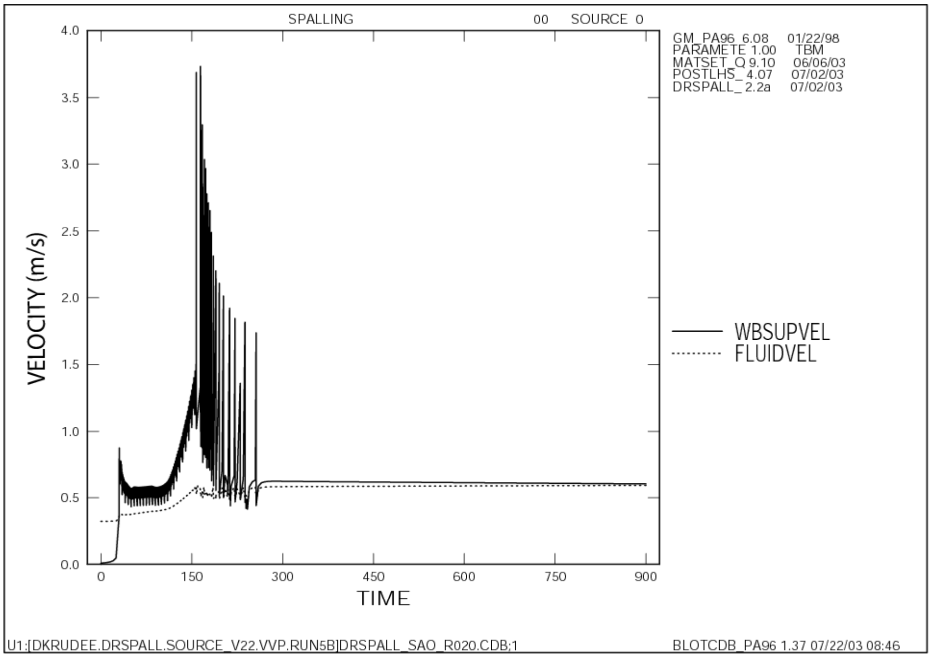

(a) Hemispherical

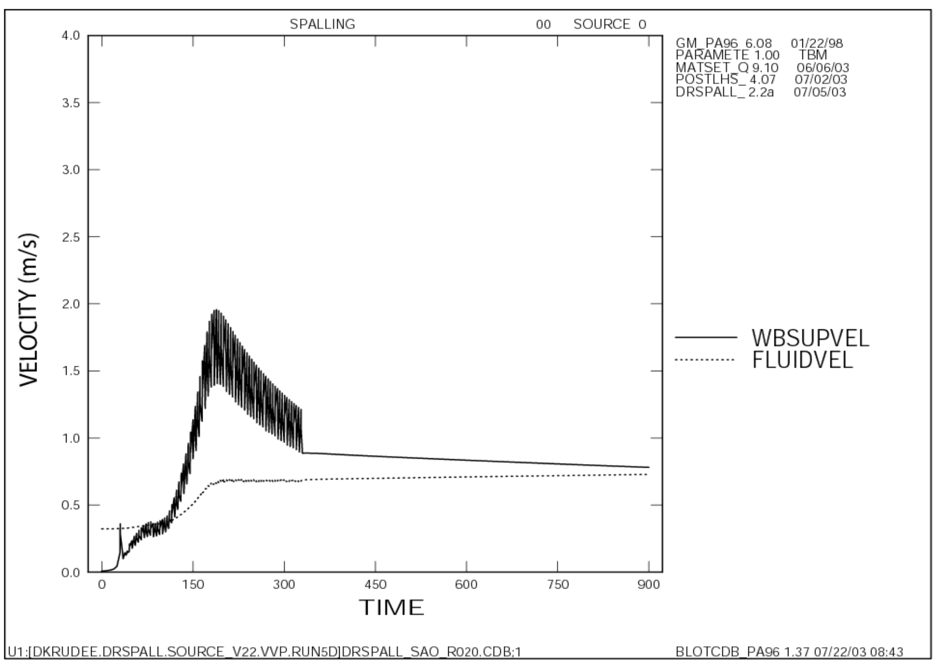

(b) Cylindrical

Figure 4-6. Fluidization threshold and superficial pore velocity histories

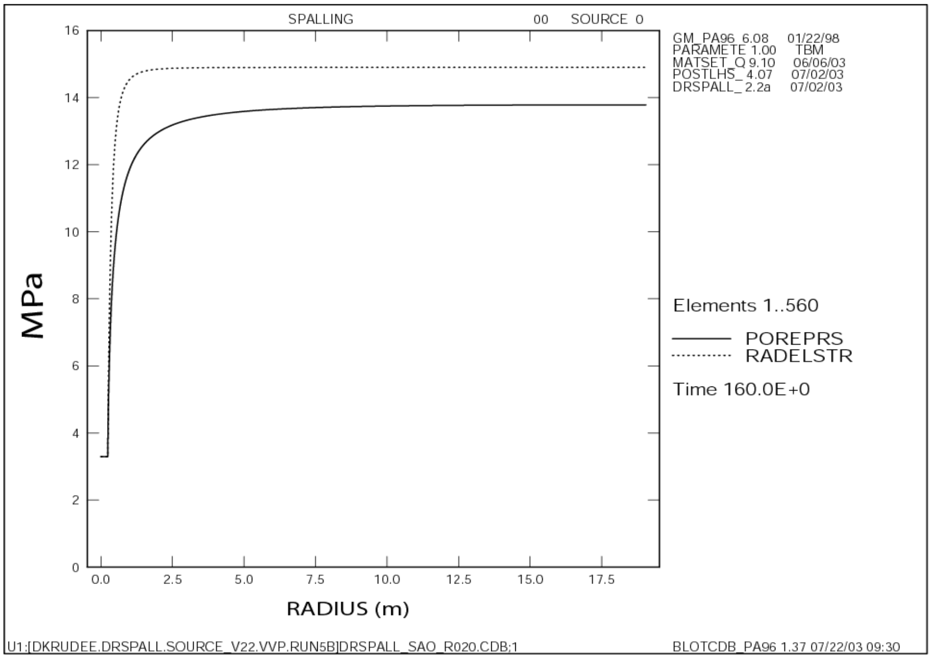

(a) Hemispherical

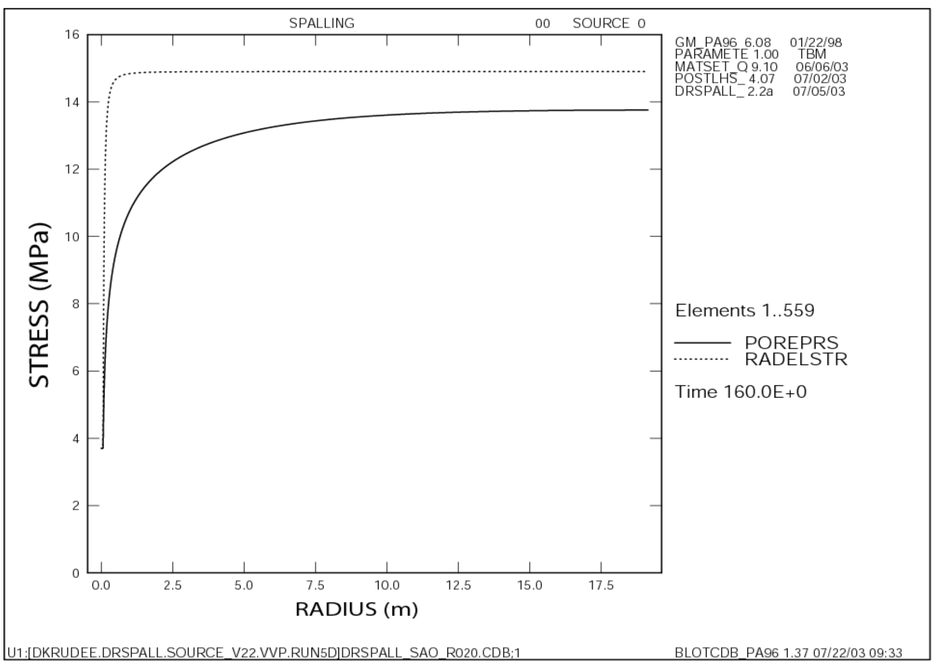

(b) Cylindrical

Figure 4-7. Pore pressure and radial elastic (total) stress profiles for entire repository domain.

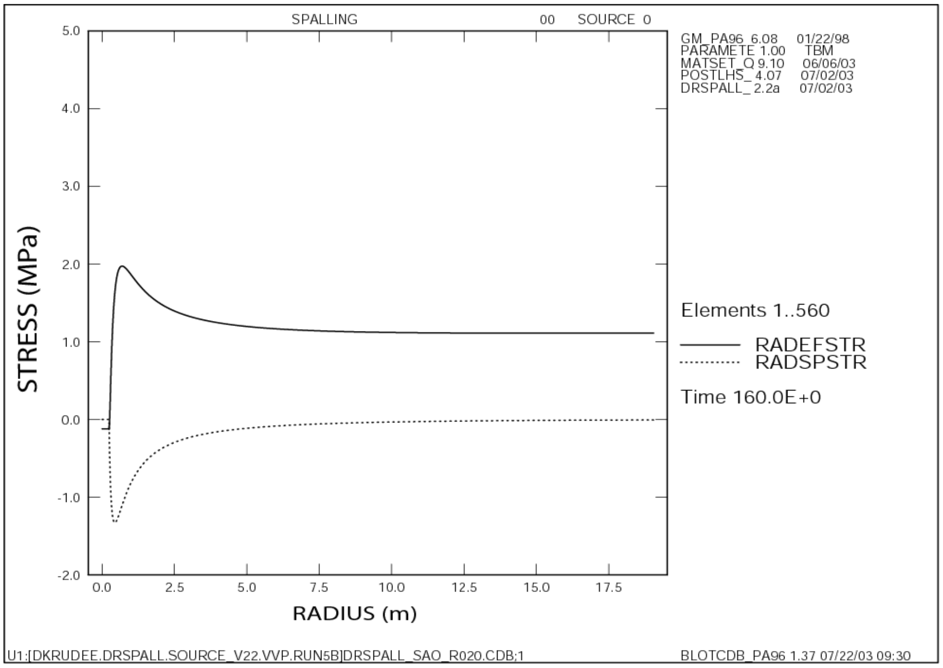

(a) Hemispherical

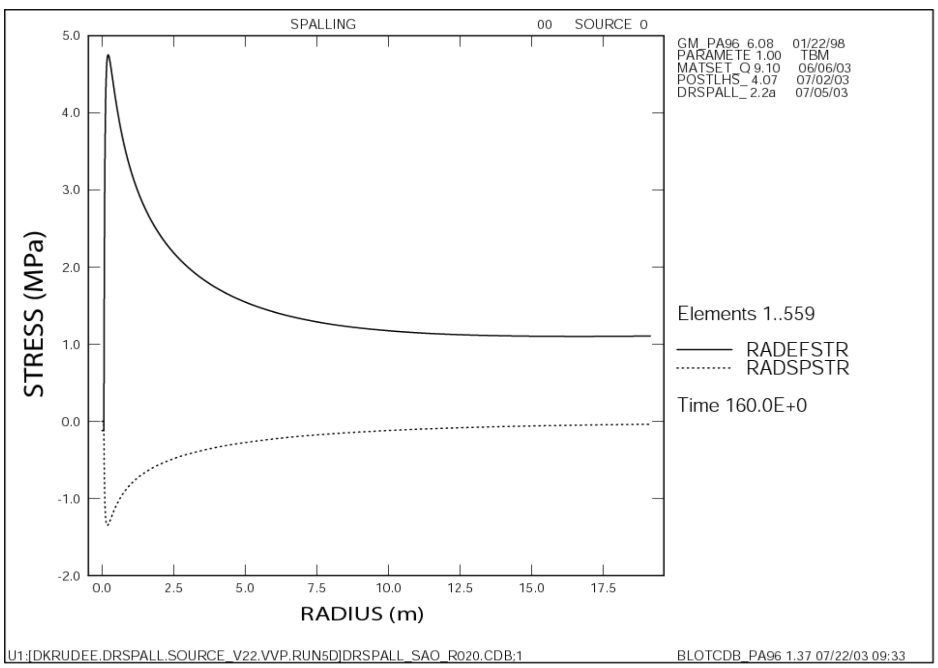

(b) Cylindrical

Figure 4-8. Radial effective and seepage stress profiles for entire repository domain.

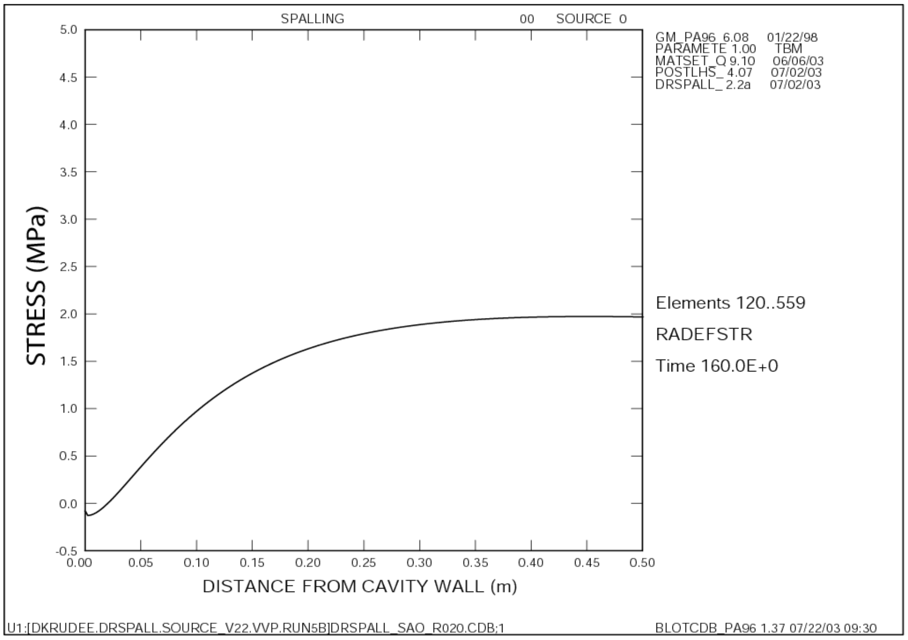

(a) Hemispherical

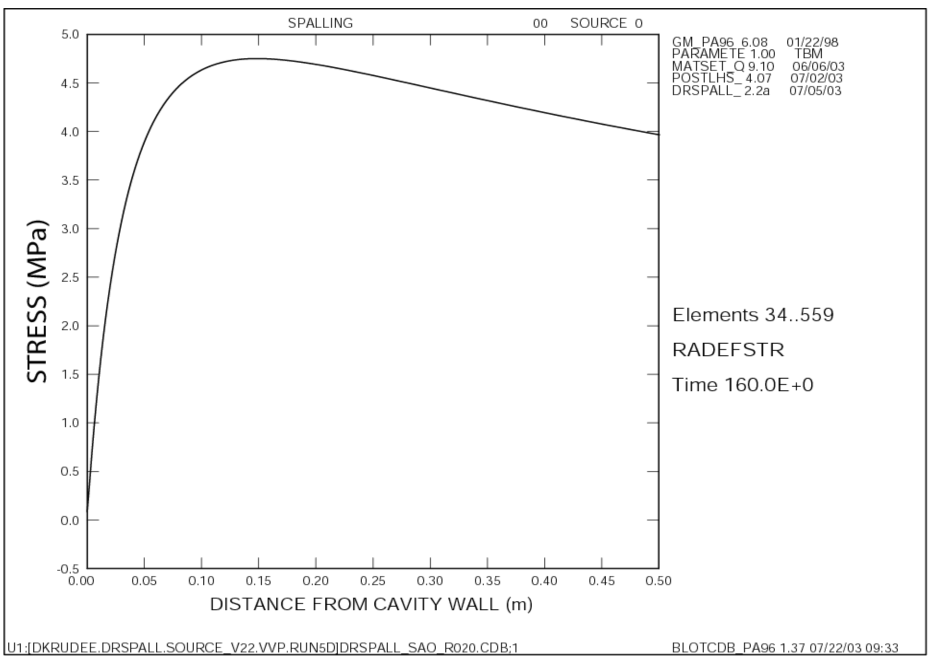

(b) Cylindrical

Figure 4-9. Radial effective stress profile (magnification 1)

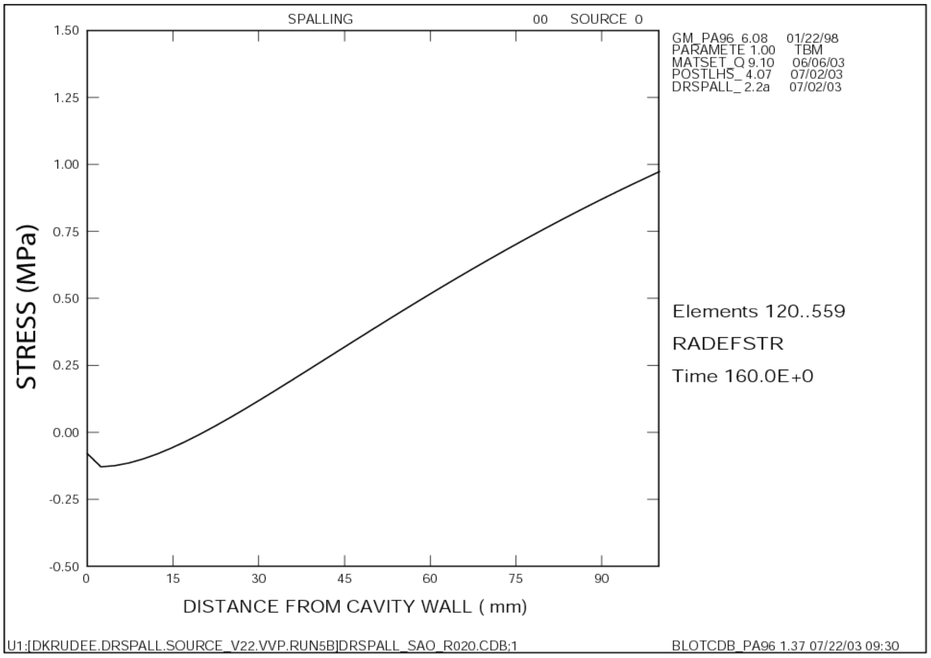

(a) Hemispherical

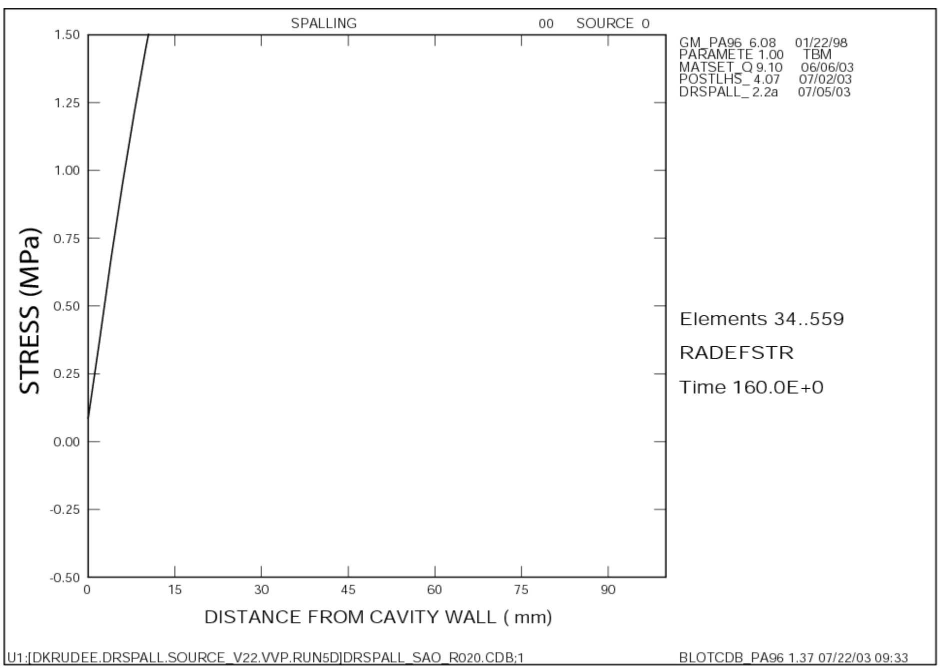

(b) Cylindrical

Figure 4-10. Radial effective stress profile (magnification 2)

5 SUMMARY

The sensitivity analysis presented here indicates that the DRSPALL model shows a sensitivity to input parameters that is consistent with the conceptual model. Key parameters include repository pressure and repository permeability. Both of these factors are expected to directly affect the magnitude of tensile stresses, and the fluidization capacity of the system, which will, in turn, affect spall release volumes. No particular correlation was observed between spall release volumes and waste tensile strength or particle diameter × shape factor over the range of input values examined (see Table 2-1). Most of the release volumes were actually zero (see Tables 3-4 and 4-1) . This implies that spall releases are expected only in a small region of the parameter space.

The results of this sensitivity analysis allow for the following specific conclusions.

1. Spall volumes resulting from the sampled input parameters given in Table 2-1 ranged from 0 to 1.2 m^3 equivalent uncompacted volume.
2. No tensile failure was observed for
   a. REPIPRES < 11 MPa
   b. REPIPERM > 2E-13 m^2
3. No spall releases were observed for
   a. REPIPRES < 12 MPa
   b. Cylindrical geometry
4. No particular correlation of SPLVOLEQ was observed for
   a. the product PARTDIAM*SHAPEFAC
5. No correlation of SPLVOLEQ or TENSRAD-CUTRAD was observed for
   a. TENSLSTR varied from 0.12 to 0.17 MPa
6. The selected one-dimensional geometry has a significant effect on the calculation of spall release due its affect on pressure and stress gradients.
7. Spherical geometry is more likely to result in spall release, and is thus conservative relative to releases for the study shown here

REFERENCES

DOE (U.S. Department of Energy). 1996. *Title 40 CFR Part 191 Compliance Certification Application for the Waste Isolation Pilot Plant*. DOE/CAO-1996-2184. Carlsbad, NM: United Stated Department of Energy, Waste Isolation Pilot Plant, Carlsbad Area Office. Vols I-XXI.

Ergun, S. 1952. Fluid Flow Through Packed Columns. *Chemical Engineering Progress*. 48: 89-94.

Hansen, F.D., Pfeifle, T.W., Lord, D.L. 2003. *Parameter Justification Report for DRSPALL*. Carlsbad, NM: Sandia National Laboratories.

Helton, J. Davis, F.L. 2002. *Latin Hypercube Sampling and the Propagation of Uncertainty in Analyses of Complex Systems.* SAND2001-0417. Albuquerque, NM: Sandia National Laboratories.

WIPP PA (Performance Assessment). 1996a. *User's Manual for BLOTCDB Version 1.37, Document Version 1.00*, WPO# 37501. Carlsbad, NM: Sandia National Laboratories.

WIPP PA (Performance Assessment). 1996b. *User's Manual for SPLAT Version 1.02, Document Version 1.01*, WPO# 40960. Carlsbad, NM: Sandia National Laboratories.

WIPP PA (Performance Assessment). 2003. *Design Document for DRSPALL version 1.00, Document Version 1.10.* ERMS# 529878. Carlsbad, NM: Sandia National Laboratories.

APPENDIX DEFAULTS

	Parameter	Units	Source	MATERIAL	PROPERTY	Distribution	Median	Low	High
1	Land Elevation	m	NEW			Constant	1.037E+03		
2	Repository Top	m	NEW			Constant	3.847E+02		
3	DRZ Permeability	m2	CCA PA database	DRZ_1	PRMX_LOG	LogUniform	1.122E-16	3.981E-20	3.162E-13
4	Initial Gas Pressure	Pa	BRAGFLO			Uniform	1.145E+07	8.000E+06	1.490E+07
5	Far-Field In-Situ Stress	Pa	NEW			Constant	1.490E+07		
6	Porosity	-	BRAGFLO			Uniform	5.050E-01	3.500E-01	6.600E-01
7	Permeability	m2	NEW RANGE			LogUniform	2.400E-13	2.400E-14	2.400E-12
8	Biot Beta	--	NEW			Constant	1.000E+00		
9	Poisson's Ratio	--	NEW			Uniform	3.900E-01	3.500E-01	4.300E-01
10	Cohesion	Pa	NEW			Constant	1.400E+05		
11	Friction Angle	deg	NEW			Constant	4.580E+01		
12	Tensile Strength	Pa	NEW VALUE			Uniform	1.450E+05	1.200E+05	1.700E+05
13	Particle Diameter	m	NEW			LogUniform	1.000E-02	1.000E-03	1.000E-01
14	Gas Viscosity	Pa*s	CCA PA database	H2	VISCO	Constant	8.934E-06		
15	Mud Density	kg/m3	CCA PA database	DRILLMUD	DNSFLUID	Cumulative	1.210E+03	1.140E+03	1.380E+03
16	Mud Viscosity	Pa*s	CCA PA database	DRILLMUD	VISCO	Cumulative	1.100E-02	5.000E-03	3.000E-02
17	Pipe roughness	m	NEW			Constant	5.000E-05		
18	Wellbore roughness	m	NEW			Loguniform	3.937E-04	5.000E-05	3.100E-03
19	Max. Solids Vol. Fraction	--	NEW			Uniform	6.150E-01	5.900E-01	6.400E-01
20	Solids Viscosity Exponent	--	NEW			Uniform	-1.500E+00	-1.800E+00	-1.200E+00
21	Bit Diameter	m	CCA PA database	BOREHOLE	DIAMMOD	Constant	3.112E-01		
22	Pipe Diameter	m	CCA PA database	BOREHOLE	PIPED	Constant	1.143E-01		
23	Collar Diameter	m	CCA PA database	BOREHOLE	COLDIA	Constant	2.032E-01		
24	Pipe Inside Diameter	m	NEW			Constant	9.718E-02		
25	Collar Length	m	CCA PA database	BOREHOLE	L1	Constant	1.829E+02		
26	Drilling Rate	m/s	NEW			Uniform	4.445E-03	2.963E-03	5.927E-03
27	Mud Pump Rate	m3/s	NEW			Uniform	2.018E-02	1.615E-02	2.422E-02
28	DDZ Thickness	m	NEW			Constant	1.600E-01		
29	DDZ Permeability	m2	NEW			LogUniform	1.000E-14	1.000E-15	1.000E-13

30	Stop Drilling Exit Vol Rate	m3/s	NEW			Constant	1.000E+03		
31	Stop Pumping Exit Vol rate	m3/s	NEW			Constant	1.000E+03		
32	π	-	CCA PA database	REFCON	PI	Constant	3.142E+00		
33	Atmospheric pressure	Pa	NEW			Constant	1.017E+05		
34	Gravitational constant	m/s2	CCA PA database	REFCON	GRAVACC	Constant	9.807E+00		
35	Water Compressibility	1/Pa	CCA PA database	BRINESAL	COMPRES	Constant	3.100E-10		
36	Gas Constant	J/kg K	CCA PA database	BLOWOUT	RGAS	Constant	4.116E+03		
37	Repository Temperature	K	CCA PA database	BLOWOUT	TREPO	Constant	3.000E+02		
38	Waste Density	kg/m3	CCA PA database	BLOWOUT	RHOS	Constant	2.650E+03		
39	Salt Density	kg/m3	NEW			Constant	2.180E+03		
40	Shape Factor	--	NEW			Uniform	5.500E-01	1.000E-01	1.000E+00
41	Bit Nozzle Number	--	NEW			Constant	3.000E+00		
42	Bit Nozzle Diameter	m	NEW			Constant	1.111E-02		

APPENDIX LHS2_DRSPALL.TRN

The following is a listing of the ASCII output file LHS2_DRSPALL.TRN created by running LHS. Also created are 30 output binary files (1 per vector) that are not listed here. Note that the sampled parameter names, distributions, and ranges are given on the first page of this listing. Below this appears a table of the new parameter values computed by LHS, followed by a similar table showing the rank of a particular value within the distribution of 30 values. Rank = 1 corresponds to the lowest value in the distribution, while rank = 30 corresponds to the highest value. The final collection of tables show the histograms for each sampled variable.

U1:[DKRUDEE.DRSPALL.LHSJUL1]LHS2_DRSPALL.TRN;36
1-JUL-2003 19:15:52.72

```
1

    TITLE DRSPALL SENSITIVITY SAMPLING

    RANDOM SEED =   585364674

    NUMBER OF VARIABLES =  15

    NUMBER OF OBSERVATIONS =   30
0   THE SAMPLE INPUT VECTORS WILL BE PRINTED ALONG WITH THEIR CORRESPONDING RANKS
0   HISTOGRAMS OF THE ACTUAL SAMPLE WILL BE PLOTTED FOR EACH INPUT VARIABLE
0   THE CORRELATION MATRICES (RAW DATA AND RANK CORRELATIONS) WILL BE PRINTED
1

    TITLE DRSPALL SENSITIVITY SAMPLING

    VARIABLE  DISTRIBUTION          RANGE            LABEL
0       1     UNIFORM           8.0000E+06 TO   1.4850E+07  DR_SPALL  REPIPRES
0       2     UNIFORM           0.3500     TO   0.6600      DR_SPALL REPIPOR
0       3     LOGUNIFORM        1.7000E-14 TO   1.7000E-12  DR_SPALL  REPIPERM
0       4     UNIFORM           0.3500     TO   0.4300      DR_SPALL  POISRAT
0       5     LOGUNIFORM        1.2000E+05 TO   1.7000E+05  DR_SPALL  TENSLSTR
0       6     UNIFORM            1140.     TO    1380.      DR_SPALL  INITMDEN
0       7     UNIFORM           5.0000E-03 TO   3.0000E-02  DR_SPALL  MUDVISCO
0       8     UNIFORM           0.5900     TO   0.6400      DR_SPALL  MUDSOLMX
0       9     UNIFORM           -1.800     TO   -1.200      DR_SPALL  MUDSOLVE
0      10     UNIFORM           2.9600E-03 TO   5.9300E-03  DR_SPALL  DRILRATE
0      11     UNIFORM           1.6100E-02 TO   2.4200E-02  DR_SPALL  MUDPRATE
0      12     LOGUNIFORM        1.0000E-15 TO   1.0000E-13  DR_SPALL  DDZPERM
0      13     LOGUNIFORM        5.0000E-05 TO   3.1000E-03  DR_SPALL  WALLROUG
```

```
0      14     UNIFORM            0.1000     TO    1.000      DR_SPALL SHAPEFAC
0      15     UNIFORM            1.0000E-03 TO   1.0000E-02  DR_SPALL PARTDIAM
1TITLE DRSPALL SENSITIVITY SAMPLING
0LATIN HYPERCUBE SAMPLE INPUT VECTORS
```

	RUN NO.	X(1)	X(2)	X(3)	X(4)	X(5)	X(6)	X(7)	X(8)	X(9)	X(10)
0	1	1.438E+07	5.384E-01	1.049E-12	4.112E-01	1.304E+05	1.290E+03	1.859E-02	6.280E-01	-1.655E+00	3.282E-03
0	2	1.117E+07	5.965E-01	6.201E-14	3.997E-01	1.432E+05	1.257E+03	1.556E-02	6.002E-01	-1.770E+00	5.637E-03
0	3	1.184E+07	5.643E-01	8.527E-13	3.572E-01	1.483E+05	1.216E+03	2.526E-02	5.966E-01	-1.671E+00	4.104E-03
0	4	1.035E+07	6.092E-01	7.705E-13	3.819E-01	1.666E+05	1.318E+03	8.659E-03	6.185E-01	-1.711E+00	5.839E-03
0	5	9.268E+06	4.999E-01	2.722E-13	4.166E-01	1.247E+05	1.312E+03	9.751E-03	6.096E-01	-1.261E+00	4.039E-03
0	6	1.456E+07	6.346E-01	3.413E-13	3.829E-01	1.269E+05	1.372E+03	2.805E-02	5.930E-01	-1.389E+00	4.540E-03
0	7	1.389E+07	3.930E-01	1.133E-13	4.188E-01	1.599E+05	1.273E+03	1.931E-02	6.340E-01	-1.539E+00	5.179E-03
0	8	1.464E+07	4.528E-01	3.733E-13	3.849E-01	1.445E+05	1.196E+03	1.463E-02	6.399E-01	-1.443E+00	5.626E-03
0	9	1.257E+07	5.682E-01	8.004E-14	4.034E-01	1.521E+05	1.247E+03	1.238E-02	6.292E-01	-1.357E+00	3.013E-03
0	10	9.421E+06	3.748E-01	5.597E-13	4.225E-01	1.349E+05	1.349E+03	8.264E-03	6.059E-01	-1.788E+00	3.563E-03
0	11	8.232E+06	4.335E-01	2.608E-13	4.293E-01	1.232E+05	1.204E+03	2.739E-02	6.367E-01	-1.686E+00	5.120E-03
0	12	1.343E+07	4.653E-01	1.188E-12	3.642E-01	1.423E+05	1.227E+03	1.615E-02	6.311E-01	-1.607E+00	3.161E-03
0	13	1.160E+07	5.522E-01	5.154E-14	3.590E-01	1.689E+05	1.335E+03	1.359E-02	6.210E-01	-1.496E+00	5.242E-03
0	14	1.081E+07	4.597E-01	3.293E-14	4.077E-01	1.631E+05	1.263E+03	1.151E-02	5.986E-01	-1.232E+00	3.502E-03
0	15	1.017E+07	3.686E-01	1.510E-13	3.512E-01	1.320E+05	1.284E+03	1.833E-02	6.266E-01	-1.426E+00	4.192E-03
0	16	8.108E+06	4.931E-01	1.403E-13	3.536E-01	1.653E+05	1.306E+03	2.966E-02	6.222E-01	-1.544E+00	4.348E-03
0	17	1.401E+07	4.151E-01	2.660E-14	3.976E-01	1.552E+05	1.361E+03	1.318E-02	5.968E-01	-1.756E+00	3.067E-03
0	18	9.606E+06	3.593E-01	4.734E-13	3.720E-01	1.364E+05	1.366E+03	2.498E-02	6.321E-01	-1.256E+00	4.851E-03
0	19	1.053E+07	5.119E-01	2.238E-13	4.262E-01	1.542E+05	1.343E+03	2.608E-02	6.042E-01	-1.309E+00	5.342E-03
0	20	1.229E+07	6.013E-01	1.778E-13	3.703E-01	1.204E+05	1.324E+03	1.069E-02	6.123E-01	-1.208E+00	4.956E-03
0	21	1.309E+07	5.213E-01	3.077E-14	4.218E-01	1.613E+05	1.148E+03	2.374E-02	6.167E-01	-1.328E+00	4.582E-03
0	22	1.257E+07	5.343E-01	1.763E-14	3.914E-01	1.333E+05	1.176E+03	2.873E-02	6.172E-01	-1.508E+00	3.856E-03
0	23	9.963E+06	6.530E-01	3.765E-14	3.787E-01	1.295E+05	1.298E+03	2.232E-02	6.242E-01	-1.736E+00	3.725E-03
0	24	8.850E+06	6.266E-01	6.761E-13	4.120E-01	1.405E+05	1.242E+03	1.731E-02	6.134E-01	-1.281E+00	4.287E-03
0	25	8.486E+06	6.469E-01	7.238E-14	3.754E-01	1.465E+05	1.167E+03	5.231E-03	6.361E-01	-1.463E+00	3.808E-03
0	26	8.953E+06	4.049E-01	1.304E-12	3.875E-01	1.585E+05	1.148E+03	2.327E-02	5.909E-01	-1.571E+00	3.393E-03
0	27	1.122E+07	4.813E-01	1.996E-14	3.662E-01	1.220E+05	1.186E+03	2.130E-02	6.022E-01	-1.593E+00	5.472E-03
0	28	1.288E+07	3.828E-01	1.029E-13	3.620E-01	1.279E+05	1.189E+03	6.803E-03	6.115E-01	-1.628E+00	4.679E-03
0	29	1.353E+07	5.783E-01	1.498E-12	3.931E-01	1.501E+05	1.159E+03	2.051E-02	6.073E-01	-1.379E+00	4.808E-03
0	30	1.202E+07	4.280E-01	4.326E-14	4.029E-01	1.393E+05	1.235E+03	6.171E-03	5.944E-01	-1.404E+00	5.788E-03

```
1TITLE DRSPALL SENSITIVITY SAMPLING
0LATIN HYPERCUBE SAMPLE INPUT VECTORS
```

	RUN NO.	X(11)	X(12)	X(13)	X(14)	X(15)
0	1	2.198E-02	1.037E-15	4.283E-04	8.799E-01	7.877E-03
0	2	2.126E-02	4.275E-14	1.185E-03	9.946E-01	6.897E-03
0	3	1.773E-02	3.216E-14	1.607E-03	2.454E-01	8.133E-03
0	4	1.670E-02	2.083E-14	6.685E-05	2.012E-01	5.907E-03
0	5	1.763E-02	6.650E-15	2.601E-03	7.045E-01	4.510E-03
0	6	2.253E-02	5.619E-14	8.783E-05	5.017E-01	7.274E-03
0	7	2.096E-02	1.834E-15	1.529E-03	1.727E-01	8.766E-03

0	8	1.880E-02	7.667E-14	2.111E-03	5.325E-01	4.714E-03
0	9	1.741E-02	8.671E-14	5.510E-05	5.862E-01	6.605E-03
0	10	2.168E-02	2.872E-14	1.021E-04	1.077E-01	2.326E-03
0	11	2.284E-02	3.890E-14	1.275E-04	7.944E-01	3.523E-03
0	12	1.657E-02	1.903E-15	2.199E-04	9.413E-01	5.617E-03
0	13	2.362E-02	9.618E-15	5.954E-04	9.313E-01	2.976E-03
0	14	2.324E-02	4.794E-14	1.170E-03	8.925E-01	6.153E-03
0	15	2.204E-02	3.502E-15	1.979E-03	3.289E-01	3.217E-03
0	16	2.066E-02	4.995E-15	8.580E-05	6.764E-01	4.903E-03
0	17	2.110E-02	2.274E-15	7.877E-04	6.563E-01	2.617E-03
0	18	2.028E-02	6.865E-14	4.536E-04	5.761E-01	8.200E-03
0	19	1.633E-02	1.237E-15	2.990E-04	7.336E-01	5.262E-03
0	20	1.939E-02	3.162E-15	1.523E-04	2.932E-01	1.476E-03
0	21	2.003E-02	1.076E-14	3.647E-04	4.332E-01	1.055E-03
0	22	1.896E-02	2.821E-15	1.441E-04	1.498E-01	9.714E-03
0	23	1.910E-02	2.311E-14	3.088E-03	2.738E-01	4.145E-03
0	24	2.392E-02	1.425E-15	6.829E-04	6.339E-01	9.202E-03
0	25	1.968E-02	7.852E-15	5.391E-04	4.237E-01	7.361E-03
0	26	1.814E-02	1.595E-14	9.197E-04	4.839E-01	3.880E-03
0	27	1.696E-02	1.386E-14	1.834E-04	7.683E-01	1.851E-03
0	28	2.308E-02	4.129E-15	6.057E-05	8.454E-01	8.925E-03
0	29	2.419E-02	5.414E-15	2.289E-04	3.590E-01	2.130E-03
0	30	1.837E-02	1.331E-14	2.935E-04	3.820E-01	9.659E-03

1TITLE DRSPALL SENSITIVITY SAMPLING
0RANKS OF LATIN HYPERCUBE SAMPLE INPUT VECTORS

	RUN NO.	X(1)	X(2)	X(3)	X(4)	X(5)	X(6)	X(7)	X(8)	X(9)	X(10)
0	1	28.	19.	27.	23.	8.	19.	17.	23.	8.	4.
0	2	14.	24.	9.	19.	16.	15.	13.	7.	2.	28.
0	3	17.	21.	26.	3.	19.	10.	25.	4.	7.	12.
0	4	11.	26.	25.	12.	29.	23.	5.	18.	5.	30.
0	5	6.	15.	19.	25.	4.	22.	6.	12.	27.	11.
0	6	29.	28.	20.	13.	5.	30.	28.	2.	21.	16.
0	7	26.	5.	13.	26.	25.	17.	18.	27.	14.	23.
0	8	30.	10.	21.	14.	17.	8.	12.	30.	18.	27.
0	9	20.	22.	11.	21.	21.	14.	9.	24.	23.	1.
0	10	7.	3.	23.	28.	11.	27.	4.	10.	1.	7.
0	11	2.	9.	18.	30.	3.	9.	27.	29.	6.	22.
0	12	24.	12.	28.	6.	15.	11.	14.	25.	10.	3.
0	13	16.	20.	8.	4.	30.	25.	11.	19.	16.	24.
0	14	13.	11.	5.	22.	27.	16.	8.	6.	29.	6.
0	15	10.	2.	15.	1.	9.	18.	16.	22.	19.	13.
0	16	1.	14.	14.	2.	28.	21.	30.	20.	13.	15.
0	17	27.	7.	3.	18.	23.	28.	10.	5.	3.	2.
0	18	8.	1.	22.	9.	12.	29.	24.	26.	28.	20.
0	19	12.	16.	17.	29.	22.	26.	26.	9.	25.	25.
0	20	19.	25.	16.	8.	1.	24.	7.	14.	30.	21.

0	21	23.	17.	4.	27.	26.	2.	23.	16.	24.	17.
0	22	21.	18.	1.	16.	10.	5.	29.	17.	15.	10.
0	23	9.	30.	6.	11.	7.	20.	21.	21.	4.	8.
0	24	4.	27.	24.	24.	14.	13.	15.	15.	26.	14.
0	25	3.	29.	10.	10.	18.	4.	1.	28.	17.	9.
0	26	5.	6.	29.	15.	24.	1.	22.	1.	12.	5.
0	27	15.	13.	2.	7.	2.	6.	20.	8.	11.	26.
0	28	22.	4.	12.	5.	6.	7.	3.	13.	9.	18.
0	29	25.	23.	30.	17.	20.	3.	19.	11.	22.	19.
0	30	18.	8.	7.	20.	13.	12.	2.	3.	20.	29.

1TITLE DRSPALL SENSITIVITY SAMPLING
0RANKS OF LATIN HYPERCUBE SAMPLE INPUT VECTORS

RUN NO.		X(11)	X(12)	X(13)	X(14)	X(15)
0	1	22.	1.	16.	26.	23.
0	2	20.	25.	24.	30.	20.
0	3	7.	23.	26.	5.	24.
0	4	3.	20.	3.	4.	17.
0	5	6.	13.	29.	21.	12.
0	6	24.	27.	5.	14.	21.
0	7	18.	4.	25.	3.	26.
0	8	10.	29.	28.	15.	13.
0	9	5.	30.	1.	17.	19.
0	10	21.	22.	6.	1.	5.
0	11	25.	24.	7.	24.	9.
0	12	2.	5.	11.	29.	16.
0	13	28.	15.	19.	28.	7.
0	14	27.	26.	23.	27.	18.
0	15	23.	9.	27.	8.	8.
0	16	17.	11.	4.	20.	14.
0	17	19.	6.	21.	19.	6.
0	18	16.	28.	17.	16.	25.
0	19	1.	2.	14.	22.	15.
0	20	13.	8.	9.	7.	2.
0	21	15.	16.	15.	12.	1.
0	22	11.	7.	8.	2.	30.
0	23	12.	21.	30.	6.	11.
0	24	29.	3.	20.	18.	28.
0	25	14.	14.	18.	11.	22.
0	26	8.	19.	22.	13.	10.
0	27	4.	18.	10.	23.	3.
0	28	26.	10.	2.	25.	27.
0	29	30.	12.	12.	9.	4.
0	30	9.	17.	13.	10.	29.

1   TITLE DRSPALL SENSITIVITY SAMPLING
0   HISTOGRAM FOR VARIABLE NO. 1   UNIFORM   DISTRIBUTION

```
     MIDPOINT          FREQ.

    8085000.             2    XX
    8414999.             1    X
    8744999.             1    X
    9074999.             1    X
    9404999.             2    XX
    9734999.             1    X
   0.1006500E+08         2    XX
   0.1039500E+08         2    XX
   0.1072500E+08         1    X
   0.1105500E+08         2    XX
   0.1138500E+08         0
   0.1171500E+08         2    XX
   0.1204500E+08         1    X
   0.1237500E+08         1    X
   0.1270500E+08         2    XX
   0.1303500E+08         2    XX
   0.1336500E+08         2    XX
   0.1369500E+08         0
   0.1402500E+08         2    XX
   0.1435500E+08         1    X
   0.1468500E+08         2    XX
0                       30


      MIN            MAX           RANGE           MEAN          MEDIAN        VARIANCE

    8107682.      0.1463851E+08   6530831.      0.1141358E+08  0.1140833E+08  0.3985014E+13

1   TITLE DRSPALL SENSITIVITY SAMPLING
0  HISTOGRAM FOR VARIABLE NO.  2     UNIFORM         DISTRIBUTION

     MIDPOINT          FREQ.

   0.3525000             1    X
   0.3675000             2    XX
   0.3825001             1    X
   0.3975001             2    XX
   0.4125001             1    X
   0.4275001             2    XX
   0.4425001             0
   0.4575001             2    XX
   0.4725001             1    X
   0.4875002             2    XX
   0.5025002             1    X
   0.5175002             2    XX
```

```
   0.5325001            2    XX
   0.5475001            1    X
   0.5625001            2    XX
   0.5775001            1    X
   0.5925001            1    X
   0.6075001            2    XX
   0.6225001            1    X
   0.6375000            1    X
   0.6525000            2    XX
0                      30

      MIN            MAX           RANGE           MEAN           MEDIAN        VARIANCE

   0.3592504      0.6529922      0.2937418      0.5049652      0.5059057      0.7999992E-02

1   TITLE DRSPALL SENSITIVITY SAMPLING
0  HISTOGRAM FOR VARIABLE NO.  3     LOGUNIFORM      DISTRIBUTION

     MIDPOINT          FREQ.

   0.3699998E-13       10    XXXXXXXXXX
   0.1109999E-12        4    XXXX
   0.1849999E-12        2    XX
   0.2589999E-12        3    XXX
   0.3329998E-12        1    X
   0.4069998E-12        1    X
   0.4809997E-12        1    X
   0.5549997E-12        1    X
   0.6289996E-12        0
   0.7029996E-12        1    X
   0.7769995E-12        1    X
   0.8509994E-12        1    X
   0.9249994E-12        0
   0.9989994E-12        0
   0.1072999E-11        1    X
   0.1146999E-11        0
   0.1220999E-11        1    X
   0.1294999E-11        1    X
   0.1368999E-11        0
   0.1442999E-11        0
   0.1516999E-11        1    X
0                      30

      MIN            MAX           RANGE           MEAN           MEDIAN        VARIANCE
```

```
   0.1763018E-13  0.1498357E-11  0.1480727E-11  0.3667784E-12  0.1643786E-12  0.1769211E-24

1   TITLE DRSPALL SENSITIVITY SAMPLING
0  HISTOGRAM FOR VARIABLE NO.  4     UNIFORM         DISTRIBUTION

     MIDPOINT          FREQ.

   0.3529499             2    XX
   0.3568499             1    X
   0.3607499             2    XX
   0.3646499             2    XX
   0.3685499             1    X
   0.3724499             1    X
   0.3763499             1    X
   0.3802499             2    XX
   0.3841498             2    XX
   0.3880498             1    X
   0.3919498             2    XX
   0.3958498             1    X
   0.3997498             1    X
   0.4036498             2    XX
   0.4075498             1    X
   0.4114498             2    XX
   0.4153498             1    X
   0.4192498             1    X
   0.4231498             2    XX
   0.4270498             1    X
   0.4309497             1    X
0                       30


      MIN            MAX           RANGE           MEAN          MEDIAN        VARIANCE

   0.3512448      0.4293006      0.7805583E-01  0.3900402      0.3894181      0.5430857E-03

1   TITLE DRSPALL SENSITIVITY SAMPLING
0  HISTOGRAM FOR VARIABLE NO.  5     LOGUNIFORM      DISTRIBUTION

     MIDPOINT          FREQ.

    121200.0             2    XX
    123600.0             2    XX
    126000.0             1    X
    128400.0             2    XX
    130800.0             1    X
    133200.0             2    XX
    135600.0             2    XX
```

```
    138000.0             0
    140400.0             2    XX
    142800.0             2    XX
    145200.0             1    X
    147600.0             2    XX
    150000.0             1    X
    152400.0             1    X
    154800.0             2    XX
    157200.0             0
    159600.0             2    XX
    162000.0             2    XX
    164400.0             1    X
    166800.0             1    X
    169200.0             1    X
0                       30

      MIN            MAX           RANGE           MEAN          MEDIAN        VARIANCE

    120370.0       168878.5       48508.51       143374.6       142759.0      0.2096278E+09

1   TITLE DRSPALL SENSITIVITY SAMPLING
0  HISTOGRAM FOR VARIABLE NO.  6     UNIFORM         DISTRIBUTION

     MIDPOINT          FREQ.

    1149.500             2    XX
    1160.500             1    X
    1171.500             2    XX
    1182.500             1    X
    1193.500             2    XX
    1204.500             1    X
    1215.500             1    X
    1226.500             1    X
    1237.500             2    XX
    1248.500             1    X
    1259.500             2    XX
    1270.500             1    X
    1281.500             1    X
    1292.500             1    X
    1303.500             2    XX
    1314.500             2    XX
    1325.500             1    X
    1336.500             1    X
    1347.500             2    XX
    1358.500             1    X
    1369.500             2    XX
```

```
0                       30


      MIN            MAX           RANGE           MEAN          MEDIAN        VARIANCE

    1147.682       1372.191       224.5092       1259.770       1259.989       4754.800

1   TITLE DRSPALL SENSITIVITY SAMPLING
0  HISTOGRAM FOR VARIABLE NO.  7     UNIFORM         DISTRIBUTION

     MIDPOINT          FREQ.

   0.5399999E-02         1    X
   0.6599999E-02         2    XX
   0.7799999E-02         1    X
   0.8999999E-02         1    X
   0.1020000E-01         2    XX
   0.1140000E-01         1    X
   0.1260000E-01         2    XX
   0.1380000E-01         1    X
   0.1500000E-01         2    XX
   0.1620000E-01         1    X
   0.1740000E-01         1    X
   0.1860000E-01         2    XX
   0.1980000E-01         1    X
   0.2100000E-01         2    XX
   0.2220000E-01         1    X
   0.2340000E-01         2    XX
   0.2460000E-01         1    X
   0.2580000E-01         2    XX
   0.2700000E-01         1    X
   0.2820000E-01         2    XX
   0.2940000E-01         1    X
0                       30


      MIN            MAX           RANGE           MEAN          MEDIAN        VARIANCE

   0.5230680E-02  0.2965956E-01  0.2442888E-01  0.1758024E-01  0.1781625E-01  0.5233707E-04

1   TITLE DRSPALL SENSITIVITY SAMPLING
0  HISTOGRAM FOR VARIABLE NO.  8     UNIFORM         DISTRIBUTION

     MIDPOINT          FREQ.

   0.5916002             1    X
   0.5940002             2    XX
```

```
   0.5964001            2    XX
   0.5988001            1    X
   0.6012001            2    XX
   0.6036001            1    X
   0.6060001            1    X
   0.6084000            1    X
   0.6108000            2    XX
   0.6132000            2    XX
   0.6156000            1    X
   0.6180000            2    XX
   0.6204000            1    X
   0.6227999            1    X
   0.6251999            1    X
   0.6275999            2    XX
   0.6299999            2    XX
   0.6323999            1    X
   0.6347998            1    X
   0.6371998            2    XX
   0.6395998            1    X
0                      30

      MIN           MAX          RANGE          MEAN          MEDIAN        VARIANCE

   0.5908749     0.6398594     0.4898453E-01  0.6150166     0.6150127     0.2086004E-03

1   TITLE DRSPALL SENSITIVITY SAMPLING
0  HISTOGRAM FOR VARIABLE NO.  9     UNIFORM         DISTRIBUTION

     MIDPOINT          FREQ.

   -1.783500            2    XX
   -1.754500            1    X
   -1.725500            2    XX
   -1.696500            1    X
   -1.667500            2    XX
   -1.638500            1    X
   -1.609500            1    X
   -1.580500            2    XX
   -1.551500            2    XX
   -1.522500            1    X
   -1.493500            1    X
   -1.464500            1    X
   -1.435500            2    XX
   -1.406500            1    X
   -1.377500            2    XX
   -1.348500            1    X
```

```
   -1.319499             2    XX
   -1.290499             1    X
   -1.261499             2    XX
   -1.232499             1    X
   -1.203499             1    X
0                       30

      MIN            MAX           RANGE           MEAN          MEDIAN        VARIANCE

   -1.787823      -1.208417      0.5794060      -1.499879      -1.501855      0.3027242E-01

1   TITLE DRSPALL SENSITIVITY SAMPLING
0  HISTOGRAM FOR VARIABLE NO. 10     UNIFORM         DISTRIBUTION

     MIDPOINT          FREQ.

   0.3010000E-02         2    XX
   0.3150000E-02         1    X
   0.3290000E-02         1    X
   0.3430000E-02         1    X
   0.3570000E-02         2    XX
   0.3710000E-02         1    X
   0.3850000E-02         2    XX
   0.3990000E-02         1    X
   0.4130000E-02         2    XX
   0.4270000E-02         1    X
   0.4410000E-02         1    X
   0.4550000E-02         2    XX
   0.4690000E-02         1    X
   0.4830000E-02         2    XX
   0.4970001E-02         1    X
   0.5110001E-02         2    XX
   0.5250001E-02         1    X
   0.5390001E-02         1    X
   0.5530001E-02         1    X
   0.5670001E-02         2    XX
   0.5810001E-02         2    XX
0                       30

      MIN            MAX           RANGE           MEAN          MEDIAN        VARIANCE

   0.3012818E-02  0.5838518E-02  0.2825700E-02  0.4433378E-02  0.4444232E-02  0.7353703E-06

1   TITLE DRSPALL SENSITIVITY SAMPLING
0  HISTOGRAM FOR VARIABLE NO. 11     UNIFORM         DISTRIBUTION
```

```
     MIDPOINT          FREQ.

   0.1618500E-01         1    X
   0.1657500E-01         2    XX
   0.1696500E-01         1    X
   0.1735500E-01         1    X
   0.1774500E-01         2    XX
   0.1813500E-01         1    X
   0.1852500E-01         1    X
   0.1891500E-01         3    XXX
   0.1930500E-01         1    X
   0.1969500E-01         1    X
   0.2008501E-01         1    X
   0.2047501E-01         2    XX
   0.2086501E-01         1    X
   0.2125501E-01         2    XX
   0.2164501E-01         1    X
   0.2203501E-01         2    XX
   0.2242501E-01         1    X
   0.2281501E-01         1    X
   0.2320501E-01         2    XX
   0.2359501E-01         1    X
   0.2398501E-01         1    X
   0.2437501E-01         1    X
0                       30

      MIN            MAX           RANGE           MEAN          MEDIAN        VARIANCE

   0.1633179E-01  0.2419202E-01  0.7860230E-02  0.2017193E-01  0.2015741E-01  0.5583186E-05

1   TITLE DRSPALL SENSITIVITY SAMPLING
0  HISTOGRAM FOR VARIABLE NO. 12     LOGUNIFORM      DISTRIBUTION

     MIDPOINT          FREQ.

   0.2149999E-14        10    XXXXXXXXXX
   0.6449998E-14         4    XXXX
   0.1075000E-13         2    XX
   0.1505000E-13         3    XXX
   0.1935000E-13         1    X
   0.2364999E-13         1    X
   0.2794999E-13         1    X
   0.3224999E-13         1    X
   0.3654999E-13         0
   0.4084999E-13         2    XX
```

```
   0.4514999E-13         0
   0.4944999E-13         1    X
   0.5374999E-13         0
   0.5804999E-13         1    X
   0.6234999E-13         0
   0.6664999E-13         1    X
   0.7094999E-13         0
   0.7524999E-13         1    X
   0.7954999E-13         0
   0.8384999E-13         0
   0.8814999E-13         1    X
0                       30


      MIN            MAX           RANGE           MEAN          MEDIAN        VARIANCE

   0.1036870E-14  0.8671365E-13  0.8567678E-13  0.2114528E-13  0.1018933E-13  0.5792042E-27

1   TITLE DRSPALL SENSITIVITY SAMPLING
0  HISTOGRAM FOR VARIABLE NO. 13     LOGUNIFORM      DISTRIBUTION

     MIDPOINT          FREQ.

   0.7500000E-04         8    XXXXXXXX
   0.2250000E-03         6    XXXXXX
   0.3750000E-03         2    XX
   0.5250000E-03         3    XXX
   0.6750001E-03         1    X
   0.8250001E-03         1    X
   0.9750001E-03         1    X
   0.1125000E-02         2    XX
   0.1275000E-02         0
   0.1425000E-02         0
   0.1575000E-02         2    XX
   0.1725000E-02         0
   0.1875000E-02         0
   0.2025000E-02         1    X
   0.2175000E-02         1    X
   0.2325000E-02         0
   0.2475000E-02         0
   0.2625000E-02         1    X
   0.2775000E-02         0
   0.2925000E-02         0
   0.3075000E-02         1    X
0                       30
```

```
     MIN            MAX            RANGE            MEAN           MEDIAN         VARIANCE

   0.5510329E-04  0.3087521E-02  0.3032418E-02  0.7382859E-03  0.3964929E-03  0.6506905E-06

1   TITLE DRSPALL SENSITIVITY SAMPLING
0  HISTOGRAM FOR VARIABLE NO. 14     UNIFORM         DISTRIBUTION

     MIDPOINT          FREQ.

   0.1100000            1    X
   0.1540000            2    XX
   0.1979999            1    X
   0.2419999            1    X
   0.2859999            2    XX
   0.3299999            1    X
   0.3739999            2    XX
   0.4179999            2    XX
   0.4619999            1    X
   0.5059999            1    X
   0.5499999            1    X
   0.5939999            2    XX
   0.6379998            2    XX
   0.6819998            1    X
   0.7259998            2    XX
   0.7699997            1    X
   0.8139997            1    X
   0.8579997            2    XX
   0.9019997            1    X
   0.9459996            2    XX
   0.9899996            1    X
0                      30

     MIN            MAX            RANGE            MEAN           MEDIAN         VARIANCE

   0.1076704      0.9945842      0.8869138      0.5501117      0.5542962      0.6719758E-01

1   TITLE DRSPALL SENSITIVITY SAMPLING
0  HISTOGRAM FOR VARIABLE NO. 15     UNIFORM         DISTRIBUTION

     MIDPOINT          FREQ.

   0.1075000E-02        1    X
   0.1505000E-02        1    X
   0.1935000E-02        2    XX
   0.2365000E-02        1    X
   0.2795000E-02        2    XX
```

```
   0.3225000E-02         1    X
   0.3655000E-02         1    X
   0.4085000E-02         2    XX
   0.4515000E-02         2    XX
   0.4945000E-02         1    X
   0.5375000E-02         1    X
   0.5805000E-02         2    XX
   0.6235000E-02         1    X
   0.6665000E-02         1    X
   0.7095000E-02         2    XX
   0.7525000E-02         1    X
   0.7955000E-02         2    XX
   0.8385000E-02         1    X
   0.8815000E-02         2    XX
   0.9245000E-02         1    X
   0.9675000E-02         2    XX
0                       30


      MIN            MAX           RANGE           MEAN          MEDIAN        VARIANCE

   0.1055460E-02  0.9714357E-02  0.8658896E-02  0.5495924E-02  0.5439280E-02  0.6745872E-05

1TITLE DRSPALL SENSITIVITY SAMPLING
0CORRELATIONS AMONG INPUT VARIABLES CREATED BY THE LATIN HYPERCUBE SAMPLE FOR RAW DATA                              PAGE   1
0    1  1.0000
0    2  0.0180  1.0000
0    3  0.0738  0.0326  1.0000
0    4  0.0009 -0.0589 -0.0327  1.0000
0    5  0.0021  0.0150  0.0760  0.0276  1.0000
0    6 -0.0450 -0.0143 -0.1909  0.0054 -0.0192  1.0000
0    7 -0.0348  0.0319  0.1273 -0.0256 -0.0098 -0.0457  1.0000
0    8 -0.0439 -0.0367 -0.0743 -0.0713 -0.0324 -0.0734  0.0098  1.0000
0    9 -0.0052  0.0813 -0.1153  0.0964  0.0065  0.0240 -0.0022  0.0174  1.0000
0   10  0.0131  0.0318 -0.2082 -0.0222  0.0041  0.0044  0.0088  0.0035  0.0905  1.0000
0   11  0.0355 -0.0561 -0.0134  0.0820 -0.0182  0.0718  0.0019  0.0107  0.0315 -0.0255  1.0000
0   12  0.0702 -0.0043 -0.1006  0.0540 -0.0103  0.0917  0.0463  0.1278  0.1064  0.0464 -0.0552  1.0000
0   13 -0.0840  0.0071 -0.1197 -0.0357 -0.0773  0.0518 -0.0279  0.1005 -0.0281 -0.0854 -0.0856  0.0727  1.0000
0   14  0.0051 -0.0623 -0.0576  0.0007  0.0136  0.0300 -0.0332 -0.0052  0.0188 -0.0186  0.1821  0.0580 -0.1174  1.0000
0   15  0.0812  0.0587 -0.0229  0.0206 -0.0345 -0.0432 -0.0312  0.0599  0.0403  0.0056 -0.0053  0.1142 -0.0439  0.0002  1.0000
0            1       2       3       4       5       6       7       8       9      10      11      12      13      14      15
0VARIABLES
0THE VARIANCE INFLATION FACTOR FOR THIS MATRIX IS  1.16
1TITLE DRSPALL SENSITIVITY SAMPLING
0CORRELATIONS AMONG INPUT VARIABLES CREATED BY THE LATIN HYPERCUBE SAMPLE FOR RANK DATA                             PAGE   1
0    1  1.0000
0    2  0.0131  1.0000
```

```
0    3 -0.0567  0.0002  1.0000
0    4  0.0024 -0.0554 -0.0020  1.0000
0    5  0.0091  0.0113 -0.0234  0.0327  1.0000
0    6 -0.0478 -0.0118  0.0461  0.0056 -0.0296  1.0000
0    7 -0.0185  0.0296  0.0834 -0.0238 -0.0087 -0.0554  1.0000
0    8 -0.0545 -0.0318  0.0670 -0.0625 -0.0185 -0.0634  0.0149  1.0000
0    9  0.0065  0.0727 -0.0145  0.1026  0.0073  0.0354 -0.0016  0.0136  1.0000
0   10  0.0167  0.0202 -0.0741 -0.0314  0.0029  0.0225  0.0167  0.0056  0.0808  1.0000
0   11  0.0256 -0.0496 -0.0109  0.0710 -0.0247  0.0794 -0.0087  0.0065  0.0287 -0.0283  1.0000
0   12 -0.1208  0.0234 -0.0318 -0.0363  0.0105 -0.0069 -0.0145 -0.0590 -0.0345  0.1244 -0.0541  1.0000
0   13 -0.0558 -0.0541 -0.0327  0.0225  0.0905 -0.0238 -0.0105  0.0011  0.0558 -0.0692  0.0274 -0.0140  1.0000
0   14 -0.0002 -0.0683 -0.0772  0.0131  0.0060  0.0305 -0.0300  0.0002  0.0229 -0.0113  0.1622 -0.0358 -0.0073  1.0000
0   15  0.0607  0.0483  0.0389  0.0140 -0.0105 -0.0483 -0.0158  0.0701  0.0416  0.0020 -0.0091 -0.0567 -0.0274 -0.0118  1.0000
0            1       2       3       4       5       6       7       8       9      10      11      12      13      14      15
0VARIABLES
0THE VARIANCE INFLATION FACTOR FOR THIS MATRIX IS  1.05
```

APPENDIX VARIABLE GLOSSARY

Glossary of DRSPALL variable names
Spallings Model Peer Review
July 7-12, 20003

Table VG-1. Property Names

Property Name	Drspall input parameter
SURFELEV	Land elevation
REPOSTOP	Repository top
REPOSTCK	Total thickness
DRZTCK	DRZ(disturbed Rock Zone) thickness
DRZPERM	DRZ permeability
REPOTRAD	Outer radius
REPIPRES	Initial gas pressure
FFPORPRS	Far-field Pore Pressure and Initial repository pressure
FFSTRESS	Far-field In-Situ Stress
REPIPOR	Repository initial porosity
REPIPERM	Repository initial permeability
BIOTBETA	Biot beta
PIOSRAT	Poisson's ratio
COHESION	Cohesion
FRICTANG	Friction angle
TENSLSTR	Tensile strength
PARTDIAM	Particle diameter
GASBSDEN	Gas base density
GASVISCO	Gas viscosity
INITMDEN	Initial mud density
MUDVISCO	Mud viscosity
WALLROUG	Wall roughness
MUDSOLMX	Max mud solids volume fraction
MUDSOLVE	Mud solids viscosity exponent
BITDIAM	Bit diameter
PIPEDIAM	Pipe diameter
COLRDIAM	Collar diameter
PIPEID	Pipe inside diameter
COLRLNGT	Collar length
EXITLEN	Exit pipe length
EXITDIA	Exit pipe diameter
DRILRATE	Drilling rate
INITBAR	Initial bit distance above repository

MUDPRATE	Mud pump rate
MAXPUMPP	Maximum allowed mud pump pressure
DDZTHICK	DDZ (Drill Damage Zone) thickness
DDZPERM	DDZ permeability
SDEVR	Stop drilling exit volume rate
SPEVR	Stop pumping exit volume rate
SDTIME	Stop drilling time
MAXTIME	Max run time
PI	Pi
REFPRES	Atmospheric pressure
GRAVACC	Gravity
RGAS	Gas constant
TREP0	Repository temperature
GASDENS0	Gas base density
COMPRES	Water compressibility
RHOS	Waste density
SALTDENS	Salt density
SHAPFAC	Shape factor
TENSVEL	Tensile velocity
BITNZNO	Bit nozzle number
BITNZDIA	Bit nozzle diameter
CHOKEFF	Choke efficiency
CAVRAD0	Initial cavity radius

Table VG-2. History Variables
(at a location or spatial integrated value)

History Variable Name	Description
PUMPRS	Pump pressure
BOTPRS	Well bottomhole pressure
CAVPRS	Cavity pressure
DRILLRAD	Drilled Radius (Geometry dependent Equivalent)
CAVRAD	Cavity Radius (Geometry dependent Equivalent)
TENSRAD	Tensile Radius (Geometry dependent Equivalent)
CUTRAD	Maximum Cuttings Radius (Geometry dependent Equivalent)
WBSUPVEL	Waste boundary superficial (Darcy) pore velocity
FLUIDVEL	Critical fluidization velocity
MUDEJVEL	Mud ejection velocity
WASWELL	Mass of Waste in Well
WASEJCT	Mass of Waste Ejected
CUTMASMX	Maximum possible Cuttings Mass
GASINJ	Mass of Gas Injected
WELLGAS	Mass of Gas in Well
GASEJCT	Mass of Gas Ejected
GASPOSN	Gas Position in Well
WASPOSN	Waste Position in Well
CPUTIME	CPU time
RUNSTEP	Run step Index
VOLSTORE	Volume of Waste in Storage (failed and fluidized but waiting release to wellbore)
GASTORE	Mass of Gas in Storage
WASTORE	Mass of Waste in Storage
WASINJ	Waste Injected into wellbore
GASCAV	Mass of gas in psuedo-cavity prior to penetration
SWELLGAS	Sum gas mass in each wellbore computational cell
SREPOGAS	Sum gas mass in each repository cell
GASTOTAL	Total gas in system
GASFROMW	Total gas from waste
CUTMASS	Mass of cuttings
SPLMASS	Mass of spalled material
TOTMASS	Mass of spalled and drilled waste
CUTVOLEQ	Cutting volume assuming uncompacted waste porosity=0.85
SPLVOLEQ	Spall volume assuming uncompacted waste porosity=0.85
TOTVOLEQ	Spall and drilled volume assuming uncompacted waste porosity=0.85
CUTRUVOL	True cuttings volume assuming uncompacted waste porosity=0.85 (no geometric equivalence)
CUTRUMAS	True cuttings mass (no geometric equivalence)

PUMPRATE	Mud pump rate
SHEARRAD	Maximum radius at which shear stress exceeded maximum
NOZLVEL	Bit nozzle (Choke) fluid velocity
WBUPVEL	Wellbore velocity at well bottom
FLUIDTIM	Fluidization time for first Intact cell
SWELLGAS	Summation of gas mass in each cell
WASFROMR	Mass of waste lost from repository due to drilling and spall
WASTOTAL	Total spalled and drilled waste in system
PITGAIN	Pit gain
MUDEJCT	Mass of mud ejected

TableVG- 3. Element Variables
(space and time dependent)

Element Variable Name	Where Variable Defined	Description
POREPRS	Repository	Repository pressure
RADEFSTR	Repository	Radial effective stress
TANEFSTR	Repository	Tangential effective stress
POREVEL	Repository	Pore velocity
RADELSTR	Repository	Radial elastic stress
TANELSTR	Repository	Tangential elastic stress
RADSPSTR	Repository	Radial seepage stress
TANSPSTR	Repository	Tangential seepage stress
FLUDSTRT	Repository	Fluidization start time
FLUDSTOP	Repository	Fluidization stop time
FAILSTRT	Repository	Failure start time
SUPRVEL	Repository	Superficial fluid velocity
FORCHRAT	Repository	Monitoring variable for Forchheimer assumption
WELLPRS	Wellbore	Well pressure
WELLVEL	Wellbore	Well velocity
WELLGSMS	Wellbore	Well gas Mass
WELLWSMS	Wellbore	Well waste Mass
WELLRHO	Wellbore	Well fluid density
WELLWSVF	Wellbore	Well waste volume fraction
WELLGSVF	Wellbore	Well gas volume fraction
WELLSAVF	Wellbore	Well salt volume fraction
WELLWSMF	Wellbore	Well waste mass fraction
WELLGSMF	Wellbore	Well gas mass fraction
WELLMDMF	Wellbore	Well mud mass fraction
WELLVOL	Wellbore	Well cell volume
COORD	Wellbore	Well cell center coordinate

Sensitivity Analysis Report - Part II
DRSPALL Version 1.00

Report for
Conceptual Model Peer Review
Convening
July 7-11, 2003

Authors:
David Lord, SNL
David Rudeen, GRAM, Inc.

September 2003

WIPP: 1.3.5.1.2.1:PUB:QA-L:524400

Table of Contents

List of Figures

List of Tables

Glossary of Acronyms

Acronym	*Definition*
DDZ	Drilling-damaged zone
DRSPALL	Computer code that implements the new conceptual model for spallings
LHS	Latin Hypercube Sampling
PA	Performance Assessment
SNL	Sandia National Laboratories
TSPA	Total System Performance Assessment
WIPP	Waste Isolation Pilot Plant

1 TEST OBJECTIVE

This report, Part II of a series, documents the DRSPALL sensitivity study and "response surface" built in support of the WIPP Spallings Model Conceptual Model Peer Review convened July 7-9, 2003, in Albuquerque, NM. This report series addresses the panel's requests to (i) capture the oral presentation "DRSPALL Sensitivity Study," given on July 9, 2003, in report format, and (ii) build a DRSPALL "response surface" based on sensitivities to key variables elucidated by Sensitivity Analysis Report - Part I (Lord and Rudeen 2003), hereafter referred to as simply Part I.

The objectives of this analysis (Part II) are:

1. To examine DRSPALL sensitivity to several key input parameters, including repository initial pressure (8.0 to 14.9 MPa), waste permeability (1.7E-14 to 1.7E-12 m^2), and waste tensile strength (0.01 to 1.0 MPa) varied over these specific input ranges specified by the peer review panel
2. To define a spallings "response surface" as a function of the stated parameter ranges

Successful completion of this sensitivity analysis will provide reassurance that the model will behave appropriately and stably when run in the broad parameter space encountered in the WIPP total system performance assessment (TSPA). Moreover, this analysis will allow close inspection for proper implementation of the conceptual model by illustrating reasonable relationships between key inputs such as pressure and tensile strength and outputs such as tensile failure radius and total spall release.

2 PROBLEM SETUP

This analysis focuses on the relationship between uncertain input parameters and code output, addressing what is referred to as subjective uncertainty in the Waste Isolation Pilot Plant Performance Assessment (WIPP PA) context. Uncertainties related to time of intrusion, number of previous intrusions, etc., are not addressed here. Rather, these will be handled when the code is integrated into the TSPA.

2.1 Parameter Sampling

Latin Hypercube Sampling (LHS) (Helton and Davis, 2002) was used to generate the sampled input parameters sets. Among the more than forty input parameters required to run DRSPALL, fifteen parameters were deemed sufficiently uncertain and potentially important to code output that they were sampled in the sensitivity analysis in Part I. As a result of the analysis presented in Part I, as well as consideration of parameters already sampled in WIPP PA, the list of sampled parameters was narrowed to nine in Part II, as shown in Table 2-1. Parameters sampled in Part I but held constant in Part II are listed in Table 2-2.

Table 2-1. Summary of sampled DRSPALL input variables, including range and distribution.

Variable Name	*Units*	*Distribution*	*Low*	*High*
Repository Gas Pressure	Pa	UNIFORM	8.00E+06	1.49E+07
Porosity of Waste	-	UNIFORM	3.50E-01	6.60E-01
Permeability of Waste	m^2	LOGUNIFORM	1.70E-14	1.70E-12
Tensile Strength of Waste	Pa	LOGUNIFORM	1.00E+04	1.00E+06
Initial Mud Density	kg/m3	UNIFORM	1.14E+03	1.38E+03
Initial Mud Viscosity	Pa*s	UNIFORM	5.00E-03	3.00E-02
DDZ Permeability	m^2	LOGUNIFORM	1.00E-15	1.00E-13
Particle Shape Factor	-	UNIFORM	1.00E-01	1.00E+00
Particle Diameter	m	UNIFORM	1.00E-03	1.00E-02

Table 2-2. Summary of DRSPALL input variables sampled in Part I, but held constant in Part II.

CAMDAT name	*Parameter name*	*Units*	*Value*
POISRAT	Poisson's ratio of waste	-	3.80E-01
MUDSOLMX	Max Solids Vol Fraction in Mud	-	6.15E-01
MUDSOLVE	Solids viscosity exponent	-	-1.50E+00
DRILRATE	Drill penetration rate	m/s	4.45E-03
MUDPRATE	Mud pump rate	m^3/s	2.02E-02
WALLROUG	Wall roughness	m	5.00E-05

The parameters listed in Table 2-2 did not emerge as drivers for tensile failure or spall releases in Part I. Rationale for selecting the constant values for the six parameters listed in Table 2-2 is as follows. For POISRAT, the mean value ($\nu = 0.38$) from measured data presented in Hansen et al (2003) was used. For the next four parameters listed, the mean values from the uniform distributions given in Part I were selected. For WALLROUGH, the lowest value of 5.0E-05 m was chosen from the loguniform distribution of 5.0E-5 to 3.1E-3 m because this represents a conservative assumption for spall releases. Smooth wellbore walls tend to allow quicker evacuation of fluids from the wellbore, which in turn, can lead to more repository failure and greater spall releases.

All input parameter values not listed in Tables 2-1 and 2-2 are constant in this analysis, and are given in Appendix INPUT.

2.2 Code flow for sensitivity study

The code flow for this study is the same as detailed in Part I of this report.

2.3 Output variable definitions

A comprehensive list of variable definitions is given in Appendix VARIABLE GLOSSARY. Selected variables are also defined in more detail in Part I for the purpose of understanding the variables of interest in the sensitivity study. One new variable, incremental spall volume, is defined below.

2.3.1 Incremental spall volume (SPLVOL2)

In addition to reporting the equivalent uncompacted spall volumes (SPLVOLEQ) defined in Part I, we have defined a new release variable (SPLVOL2) that quantifies the amount of solid material removed due to failure and fluidization mechanisms, regardless of whether it would eventually be drilled out by bit action. Recall that Part I defines the equivalent uncompacted spall volume as the difference between the final cavity volume (TOTVOLEQ) minus the drilled cavity volume (CUTVOLEQ). Figure 2-5 in Part I illustrates the determination of SPLVOLEQ schematically. In some vectors, repository material is removed ahead of the bit due to failure and fluidization, though such failed material that is eventually drilled out is not captured in the SPLVOLEQ variable at late time. An example of this is shown in Figure 2.3-1 where the equivalent uncompacted volume and incremental spall volume are plotted versus time for vector 040 (see Table 3-1). Note the seven spikes in the SPLVOLEQ curve between 150 and 300 seconds. These represent removal of repository material due to tensile failure and fluidization. This material transports up the wellbore and is ejected to the land surface in the same way that drilled material is, but just slightly earlier in time. SPLVOLEQ goes down each time because drilling catches up with the spalled cavity radius. The approach for the new incremental spall release variable is to monitor which repository computational zones are removed by the failure and fluidization mechanism, and which are removed by drilling. Therefore, SPLVOL2 cannot decrease, and its value represents the sum of all height of all the spikes in SPLVOLEQ shown in Figure 2.3-1. While the final cavity volume TOTVOLEQ is conserved, the new drilled volume (not a reported output variable) is subject to decreases relative to CUTVOLEQ, and SPLVOL2 is greater than or equal to SPLVOLEQ.

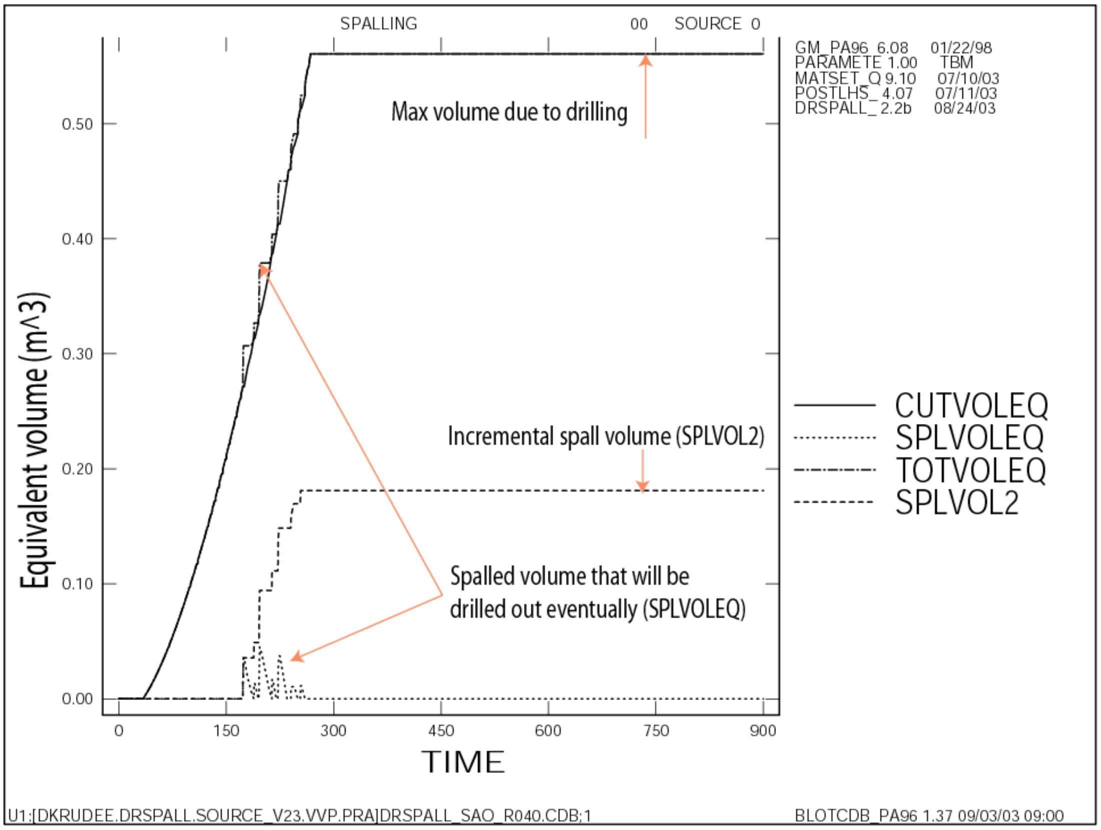

Figure 2.3-1. Volume history plot for vector 040 in spherical geometry annotated to illustrate the new incremental spallings volume (SPLVOL2) variable.

2.4 System specifications

This analysis was run on the Open VMS 7.3-1 operating system at Sandia National Laboratories, Carlsbad, NM. Runs were submitted to Compaq Alpha ES40, ES45, and 8400 machines, with a total of 20 processors available for computations. Fifty vectors using spherical geometry were executed, requiring about 477 hours computational time spread over all 20 processors or roughly 36 hours of wall clock time. Fifty vectors using cylindrical geometry required 273 hours CPU time or roughly 18 hrs wall clock time.

3 RESULTS AND DISCUSSION

3.1 LHS sampling results

The results of the sampling are summarized in Table 3-1. Recall that there are 50 vectors (rows) with 9 sampled variables (columns). Units are given in Part I, Appendix Defaults.

Table 3-1. Results of 8-15 MPa LHS sampling. A glossary of variable names is given in Appendix VARIABLE GLOSSARY.

VEC	REPIPRES	REPIPOR	REPIPERM	TENSLSTR	INITMDEN	MUDVISCO	DDZPERM	SHAPEFAC	PARTDIAM
1	1.06E+07	0.649	2.26E-14	4.13E+04	1293	1.30E-02	5.82E-15	0.236	6.83E-03
2	1.18E+07	0.450	3.50E-13	2.72E+04	1265	2.51E-02	2.28E-14	0.907	7.16E-03
3	9.30E+06	0.537	1.12E-12	3.25E+05	1229	1.05E-02	3.36E-14	0.734	4.89E-03
4	1.40E+07	0.553	9.42E-14	1.35E+05	1306	1.18E-02	9.80E-14	0.975	7.96E-03
5	1.20E+07	0.489	2.99E-14	1.25E+04	1270	1.89E-02	1.17E-15	0.936	5.28E-03
6	1.22E+07	0.392	1.05E-13	2.97E+04	1152	2.12E-02	9.96E-15	0.561	8.42E-03
7	8.29E+06	0.619	5.75E-14	2.41E+04	1378	2.70E-02	2.17E-15	0.474	9.83E-03
8	9.93E+06	0.408	2.11E-14	8.80E+05	1213	2.46E-02	4.16E-14	0.820	8.73E-03
9	1.32E+07	0.382	1.45E-12	1.27E+05	1297	1.93E-02	7.43E-15	0.419	8.88E-03
10	1.11E+07	0.615	1.82E-14	1.75E+04	1373	1.23E-02	4.37E-14	0.728	2.06E-03
11	8.85E+06	0.566	4.36E-13	1.71E+04	1238	1.48E-02	5.46E-14	0.354	4.63E-03
12	8.14E+06	0.522	3.75E-13	9.43E+04	1367	8.93E-03	3.71E-14	0.426	9.26E-03
13	1.44E+07	0.657	5.60E-14	6.18E+05	1223	2.05E-02	4.94E-14	0.661	1.14E-03
14	8.51E+06	0.584	1.36E-12	3.83E+04	1323	2.37E-02	3.07E-15	0.147	6.11E-03
15	9.41E+06	0.507	1.96E-13	5.22E+04	1315	1.03E-02	2.60E-14	0.797	3.37E-03
16	1.27E+07	0.363	2.83E-14	1.91E+04	1335	2.85E-02	1.08E-14	0.212	7.69E-03
17	1.46E+07	0.404	4.15E-13	4.10E+05	1363	2.43E-02	1.62E-14	0.881	7.37E-03
18	1.07E+07	0.419	1.05E-12	1.10E+04	1234	2.17E-02	6.16E-14	0.924	6.33E-03
19	1.04E+07	0.516	4.97E-14	3.43E+04	1353	1.95E-02	5.50E-15	0.569	3.67E-03
20	1.26E+07	0.606	8.07E-14	1.80E+05	1181	2.77E-02	2.65E-15	0.134	8.37E-03
21	1.48E+07	0.500	9.74E-13	6.77E+04	1281	2.62E-02	1.56E-15	0.604	3.00E-03
22	1.30E+07	0.524	8.28E-14	8.35E+04	1177	1.11E-02	1.08E-15	0.641	2.83E-03
23	1.16E+07	0.457	7.29E-14	9.61E+05	1309	1.36E-02	1.44E-14	0.450	1.50E-03
24	8.96E+06	0.497	2.29E-13	6.91E+05	1149	1.60E-02	1.96E-14	0.957	8.14E-03
25	9.90E+06	0.355	3.77E-14	1.37E+04	1255	1.35E-02	6.59E-14	0.293	2.40E-03
26	9.52E+06	0.439	1.78E-13	7.79E+04	1286	7.30E-03	1.69E-15	0.403	3.88E-03
27	1.36E+07	0.546	6.75E-14	1.51E+04	1186	2.65E-02	5.24E-15	0.540	3.21E-03
28	1.13E+07	0.397	1.23E-12	3.25E+04	1250	2.95E-02	1.23E-15	0.694	1.20E-03
29	9.69E+06	0.485	2.47E-14	3.58E+05	1339	2.30E-02	1.58E-14	0.864	5.57E-03
30	1.07E+07	0.430	1.61E-12	4.60E+05	1359	8.42E-03	2.78E-15	0.825	1.61E-03
31	1.41E+07	0.464	5.21E-13	1.03E+05	1197	1.66E-02	8.35E-14	0.514	6.49E-03
32	1.43E+07	0.587	7.85E-13	2.27E+05	1208	9.34E-03	7.60E-15	0.194	9.52E-03
33	1.28E+07	0.601	7.03E-13	1.11E+05	1301	2.59E-02	1.80E-14	0.850	5.11E-03
34	1.24E+07	0.444	2.71E-13	7.71E+05	1343	2.20E-02	3.39E-15	0.263	2.66E-03
35	1.09E+07	0.579	4.70E-13	5.63E+04	1201	1.53E-02	6.71E-15	0.305	4.57E-03

36	8.07E+06	0.631	6.32E-13	5.44E+05	1173	2.93E-02	4.17E-15	0.591	2.12E-03
37	1.24E+07	0.626	8.24E-13	6.19E+04	1332	1.77E-02	7.49E-14	0.108	5.40E-03
38	1.39E+07	0.636	5.75E-13	2.09E+04	1245	5.72E-03	8.97E-15	0.622	5.93E-03
39	1.13E+07	0.414	2.08E-13	2.68E+05	1277	2.08E-02	2.95E-14	0.374	4.25E-03
40	1.46E+07	0.436	1.67E-13	2.97E+05	1347	1.72E-02	3.82E-15	0.318	9.36E-03
41	1.03E+07	0.593	2.46E-13	4.65E+04	1252	7.61E-03	2.01E-15	0.989	6.71E-03
42	1.35E+07	0.561	3.50E-14	1.45E+05	1161	6.53E-03	1.34E-15	0.770	9.80E-03
43	1.02E+07	0.377	2.04E-14	3.92E+05	1266	2.32E-02	4.73E-15	0.512	4.19E-03
44	8.76E+06	0.357	1.22E-13	7.26E+04	1207	5.17E-03	2.51E-15	0.693	1.80E-03
45	8.57E+06	0.374	2.96E-13	1.93E+05	1144	1.81E-02	1.30E-14	0.180	7.54E-03
46	9.18E+06	0.645	1.33E-13	2.38E+05	1159	2.85E-02	1.14E-14	0.761	6.94E-03
47	1.15E+07	0.570	1.45E-13	7.12E+05	1321	6.40E-03	1.74E-15	0.351	8.92E-03
48	1.31E+07	0.475	4.28E-14	1.09E+04	1165	1.55E-02	7.68E-14	0.479	5.79E-03
49	1.36E+07	0.533	1.10E-13	1.63E+05	1191	1.42E-02	3.16E-14	0.249	3.96E-03
50	1.19E+07	0.471	4.21E-14	5.09E+05	1217	9.90E-03	2.33E-14	0.169	2.54E-03

3.2 Spherical Geometry Results

The summary of spallings releases using in spherical geometry at 900 seconds is given in Table 3-2. Shown are the uncompacted equivalent spall volume (SPLVOLEQ) defined in Part I, the quantity "tensile radius – cuttings radius" (TENSRAD-DRILLRAD) also defined in Part I, which will be referred to as TENSRAD-DRILLRAD, and the new incremental spall volume (SPLVOL2) that registers all spall failures ahead of the bit even if the bit eventually drills out that volume.

Table 3-2. Summary of key output variables from spherical geometry at 900 seconds. Nonzero values appear in colored font.

Vector	SPLVOLEQ	TENSRAD-DRILLRAD	(Incremental) SPLVOL2	Vector	SPLVOLEQ	TENSRAD-DRILLRAD	(Incremental) SPLVOL2
	m^3	m	m^3		m^3	m	m^3
1	0.000	0.018	0.000	26	0.000	0.000	0.000
2	0.000	0.000	0.000	27	0.000	0.020	0.000
3	0.000	0.000	0.000	28	0.000	0.000	0.000
4	0.000	0.020	0.000	29	0.000	0.000	0.000
5	0.000	0.020	0.000	30	0.000	0.000	0.000
6	0.000	0.018	0.000	31	0.000	0.000	0.027
7	0.000	0.000	0.000	32	0.000	0.000	0.000
8	0.000	0.000	0.000	33	0.000	0.000	0.000
9	0.000	0.000	0.000	34	0.000	0.000	0.000
10	0.000	0.021	0.000	35	0.000	0.000	0.000
11	0.000	0.000	0.000	36	0.000	0.000	0.000
12	0.000	0.000	0.000	37	0.000	0.000	0.000
13	0.000	0.000	0.000	38	0.000	0.000	0.144
14	0.000	0.000	0.000	39	0.000	0.000	0.000
15	0.000	0.000	0.000	40	0.000	0.000	0.181
16	0.000	0.018	0.000	41	0.000	0.000	0.000
17	0.000	0.000	0.000	42	0.000	0.020	0.000
18	0.000	0.000	0.000	43	0.000	0.000	0.000
19	0.000	0.000	0.000	44	0.000	0.000	0.000
20	0.000	0.018	0.000	45	0.000	0.000	0.000
21	0.000	0.000	0.000	46	0.000	0.000	0.000
22	0.000	0.019	0.000	47	0.000	0.000	0.000
23	0.000	0.000	0.000	48	0.000	0.022	0.000
24	0.000	0.000	0.000	49	0.000	0.019	0.310
25	0.000	0.000	0.000	50	0.000	0.000	0.000

According to Table 3-2, the SPLVOLEQ output variable was zero for all vectors. This outcome is similar to the results from Part I in which only one release was observed in the 8-15 MPa runs with SPLVOLEQ = 0.234 m^3 (Table 3-4, Part I). Note that there are two differences between the Part I and Part II analyses. First, the tensile strength sampling range was expanded for Part II. Second, the inner cavity boundary condition was changed during the course of the zone size study. The change was required due to an apparent effect of zone size on the calculation of radial effective stress near the cavity boundary. The cavity radius used to calculate stresses in Part I was at the face of the cavity; in Part II the cavity radius is at the center of a psuedo-cell or the first cell just outside of the repository domain. The cavity radius in the stress calculations is now consistent with how the boundary condition is applied to the numerical solution of the porous flow equation.

The more sensitive output variable, TENSRAD−DRILLRAD, shows 12 nonzero values. Recall that this variable includes the depth of tensile failure beyond the final drilled cavity radius. The presence of 12 (of 50) nonzero values indicates that about 1 in 4 vectors experiences repository material failure due to tensile stresses near the end of drilling. These 12 vectors retain bedded material in the cavity that does not transport to the surface. This "fluidization limiting" phenomenon is discussed again in §3.2.2.3.

Moving to the third output variable given in Table 3-2, the incremental spall volume (SPLVOL2) exhibits 4 nonzero values among the 50 vectors. These 4 vectors do not necessarily coincide with the nonzero vectors flagged in the TENSRAD−DRILLRAD column, and thus show that early failure and fluidization and late failure are not necessarily correlated.

3.2.1 History plots

The history data for tensile radius are shown in Figure 3.2-1. This figure includes all 50 vectors overlaid in a "horsetail" plot. The lower bound for the tensile radius is defined as the cavity radius, so drilling action will increase TENSRAD even if there is no failure ahead of the bit. Data are shown for the entire 900 seconds of simulation time. Repository penetration occurs at about 30 seconds, and drilling ends between 250 and 400 seconds depending on repository height. Recall that repository height is a direct function of sampled porosity, REPIPOR (WIPP PA, 2003), hence the distribution of drilling times and resulting tensile radii. This sensitivity is through the contribution of drilled radius (DRILLRAD), which is a function of the wellbore mapping to the 1D model geometry during the drilling process, which assumes conservation of surface area rather than volume or bit diameter. The sensitivity is removed in subsequent analyses by examining the variable TENSRAD-DRILLRAD. Important to notice here is that tensile failures do not occur before 100 seconds. In fact, most failure occurs after 150 seconds, or about 1/3 of the way through the drilling process. This implies that the early stress state, when the repository is first penetrated and the spherical repository geometry is most valid, is very unlikely to cause tensile failure.

The horsetail plot for CAVRAD is shown in Figure 3.2-2. CAVRAD represents the actual cavity radius and thus requires drilling action or fluidization to remove material for this value to increase. The new incremental spallings volume variable SPLVOL2 corresponds to deviations from the drilled history (DRILLRAD) due to failure and fluidization. These are the small steps in CAVRAD that appear between 150 and 250 seconds. According to Table 3-2, only 4 vectors in 50 exhibited this behavior, and this is also seen in Figure 3.2-2 where most of the CAVRAD histories trace a smooth drilling curve while just a few deviate. The horsetail plot for DRILLRAD is shown in Figure 3.2-3.

The horsetail plot for SPLVOL2, which incrementally sums the equivalent volume corresponding to the deviations from DRILLRAD, is shown in Figure 3.2-4. Note that the curves are monotonically increasing and reflect the equivalent uncompacted volume of waste that was removed strictly due to failure and fluidization. All spalling activity occurs between approximately 150 and 300 seconds.

The horsetail plot for TENSRAD-CAVRAD, which gives the thickness of the bed of failed but non-fluidized material surrounding the cavity, is shown in figure 3.2.5. The bed of failed material is typically formed during drilling (150 to 300 second) except for two of the vectors. The drilling also causes the high frequency noise in the curves. It also appears that at least one vector formed a bed of failed material that was later removed by drilling at around 300 seconds.

The horsetail plot for TENSRAD–DRILLRAD, which includes failed material regardless of whether it fluidized or not is shown in Figure 3.2-6. This combines the results for spalled material and failed but non-fluidized material into a single dependent variable. The curve with the large maximum value at approximately 200 s is for vector 049 which had the largest SPLVOL2. The value of this variable at 900 seconds is used in the sensitivity results presented in subsequent sections.

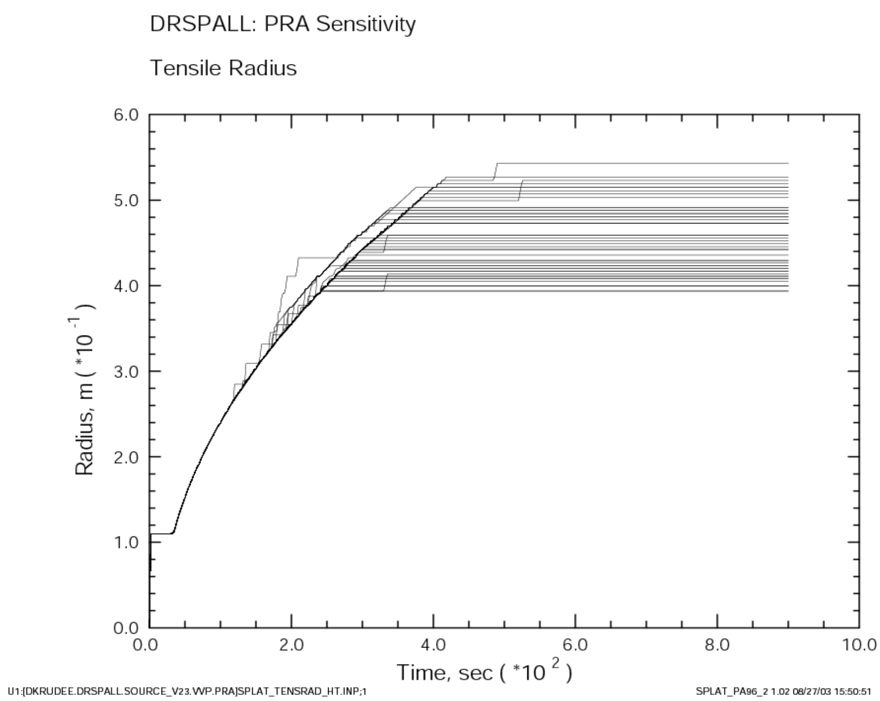

Figure 3.2-1. Horsetail plot of TENSRAD vs. time for all 50 vectors in spherical geometry.

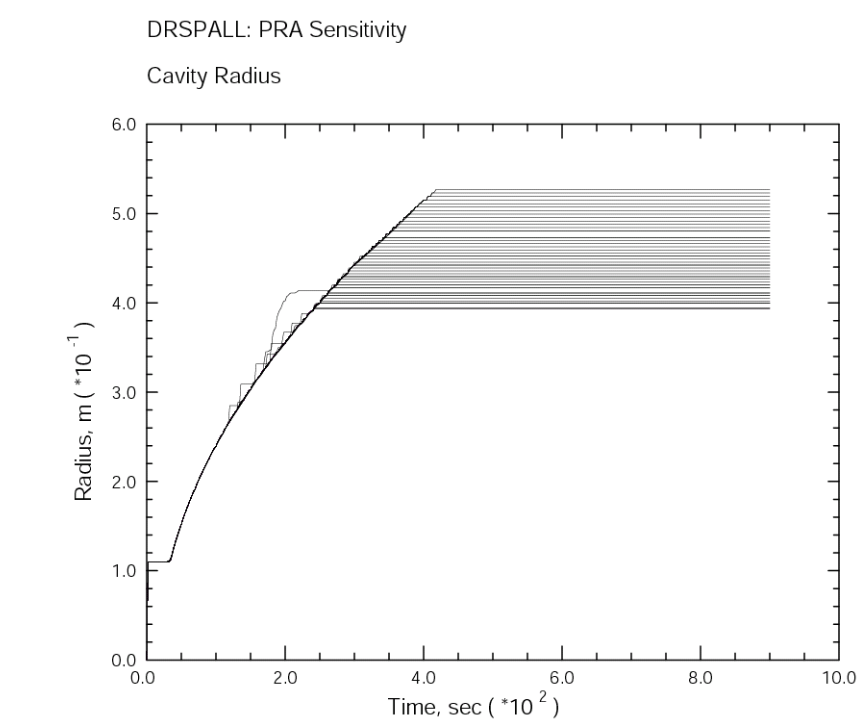

Figure 3.2-2. Horsetail plot of CAVRAD vs. time for all 50 vectors in spherical geometry.

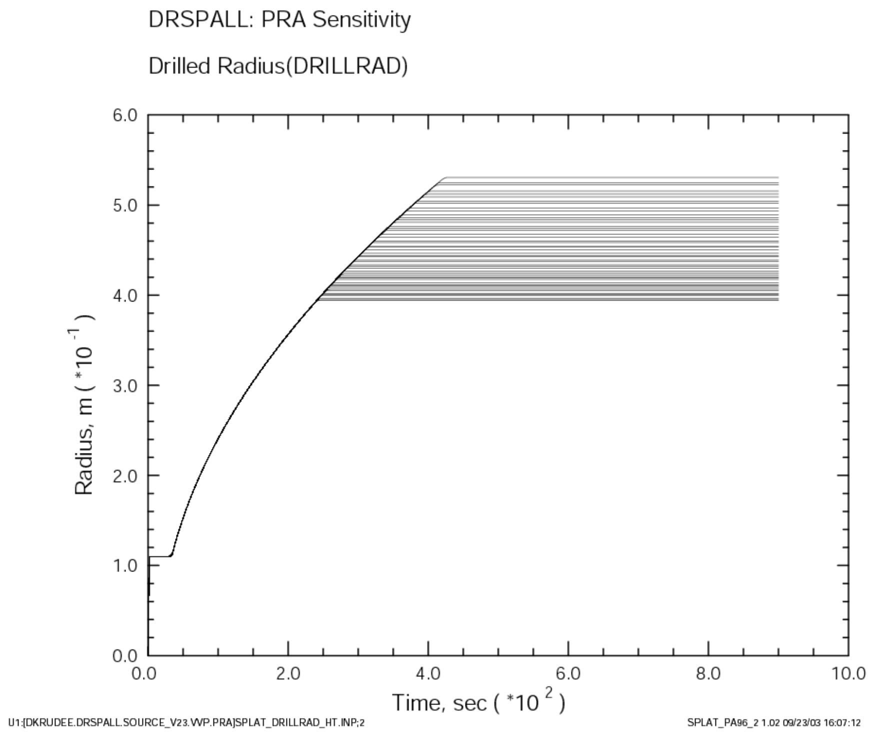

Figure 3.2-3. Horsetail plot of DRILLRAD vs. time for all 50 vectors in spherical geometry.

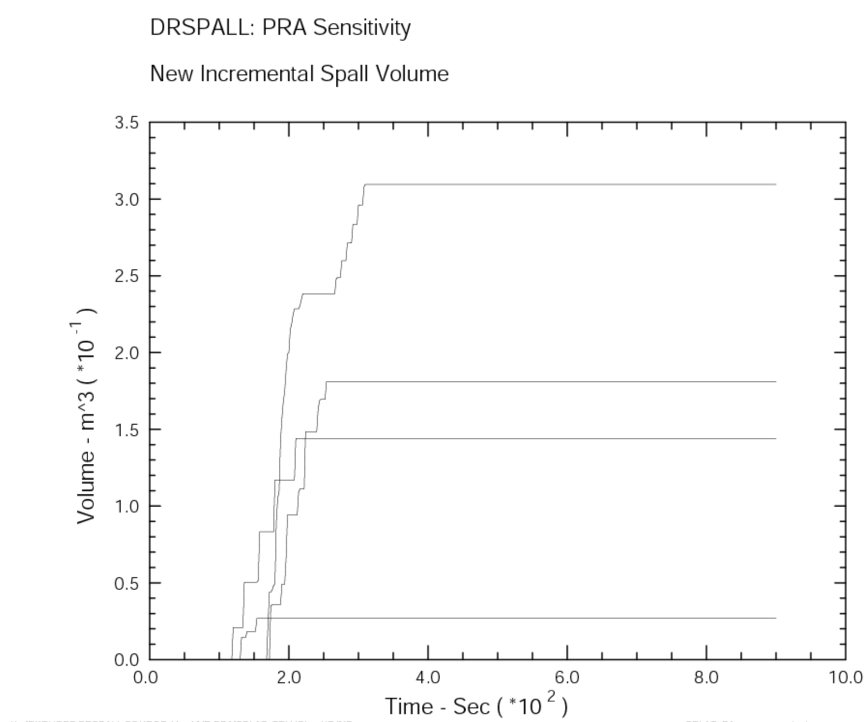

Figure 3.2-4. Horsetail plot of SPLVOL2 vs. time for all 50 vectors in spherical geometry.

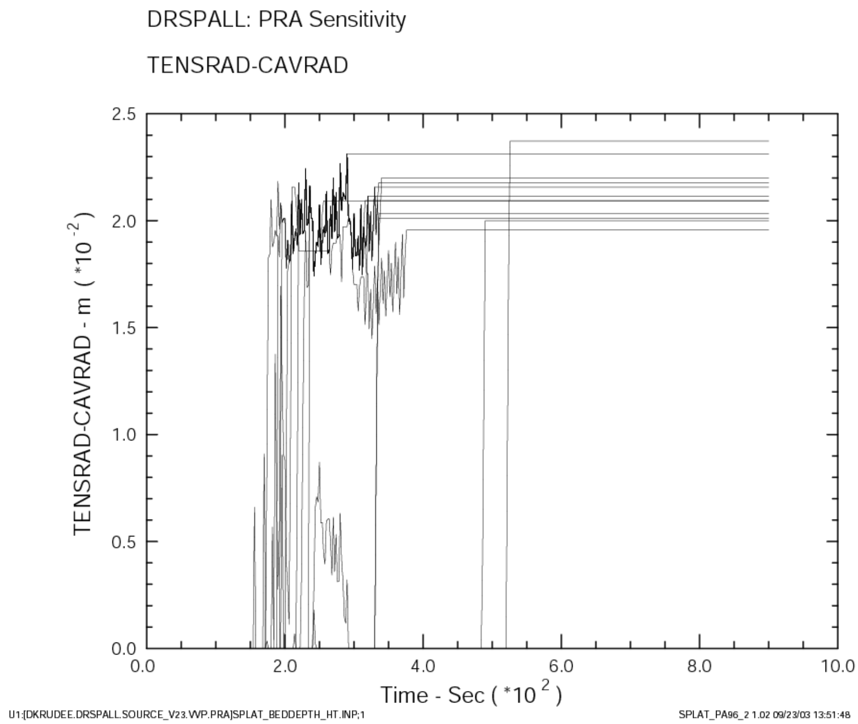

Figure 3.2-5. Horsetail plot of TENSRAD-CAVRAD vs. time for all 50 vectors in spherical geometry.

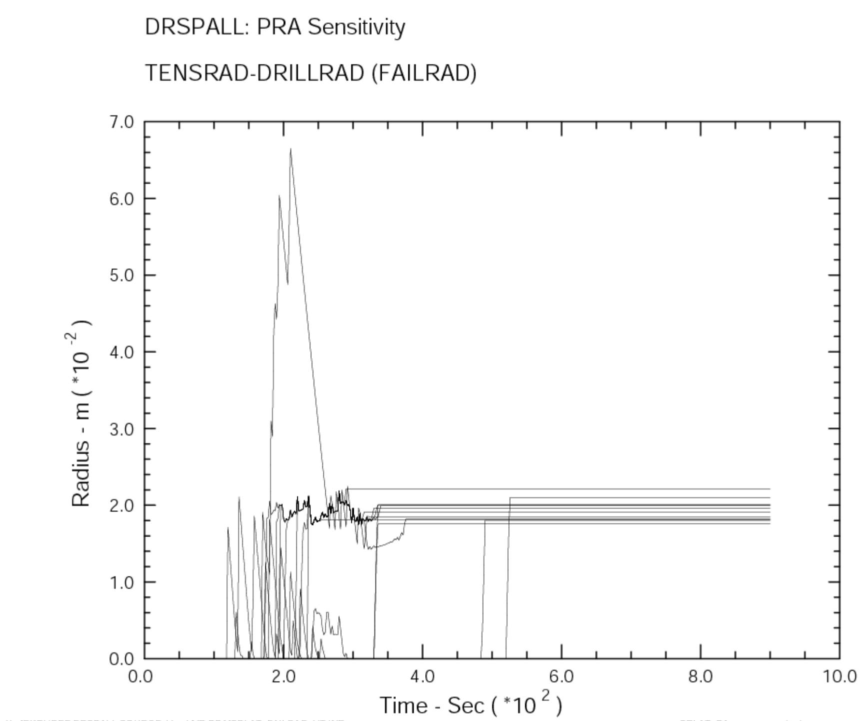

Figure 3.2-6. Horsetail plot of TENSRAD-DRILLRAD vs. time for all 50 vectors in spherical geometry.

3.2.2 Scatter plots

The values of selected output variables at 900 sec, the end of the simulation, are plotted against sampled independent variables in scatter plots below. Each point represents the result from one vector, so every data series contains 50 points. For the data shown here, the following dependent variables were explored:

- tensile radius – cuttings radius
- incremental spall volume
- fluidization velocity
- superficial gas velocity

as a function of the following independent variables:

- repository initial pressure
- repository permeability
- waste tensile strength
- particle diameter × shape factor

According to Table 3-2, the final uncompacted spall volume SPLVOLEQ = 0 m^3 for all 50 vectors examined. While an important output variable to monitor in the overall sensitivity analysis, SPLVOLEQ is not addressed in the scatter plot analysis.

3.2.2.1 Variables controlling TENSRAD−DRILLRAD

Repository initial pressure is a primary variable controlling the spallings process, driving tensile failure and high gas velocities with high pressure gradients near the cavity face. The impact of REPIPRES on TENSRAD-DRILLRAD is shown in Figure 3.2-3. TENSRAD-DRILLRAD appears to be categorically zero at pressure below 10.6 MPa. This is largely because the resulting pressure gradients are not high enough to cause tensile failure. Above 10.6 MPa, failure is observed in some vectors, though not universally because other input variables such as permeability and tensile strength impact failure as well.

Repository permeability is recognized as another variable of primary importance controlling the spallings process. The relationship between permeability and TENSRAD−DRILLRAD is plotted in Figure 3.2-4. Consistent with the findings in Part I, there appears to be a critical permeability, $k \cong 1.1 \times 10^{-13}$ m^2, above which no late-time failure is observed. This does not necessarily imply that tensile failure is limited to low-permeability media, as shown elsewhere (Figure 3.2-7). Rather, failure appears across the permeability spectrum, but tends to occur early at high permeability and late with low permeability.

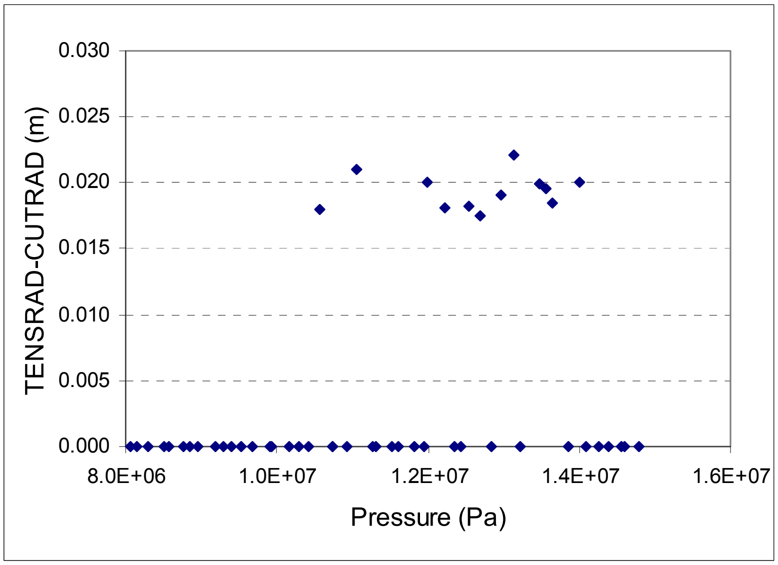

Figure 3.2-3. Scatter plot of TENSRAD-DRILLRAD vs. REPIPRES for spherical geometry.

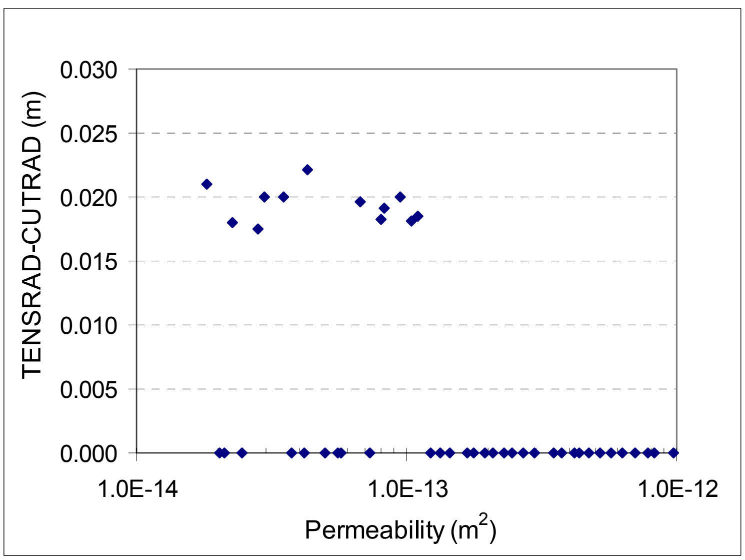

Figure 3.2-4. Scatter plot of TENSRAD-DRILLRAD vs. REPIPERM for spherical geometry

The sensitivity of TENSRAD–DRILLRAD to waste tensile strength is shown in Figure 3.2-5. A distinct cutoff is evident near 0.2 MPa, above which failure beyond the drilled radius is absent. Below this value, some, but not all, vectors fail. Recall that the conceptual model peer review panel requested a sampled range for TENSLSTR from 0.01 to 1.0 MPa for Part II of this study, relative to a range of 0.12 to 0.17 MPa examined in Part I. The new specified range appears to bring two features of DRSPALL to light. First, “runaway” failure and resulting large release volumes are not likely due to low values of tensile strength alone. Second, there appears to be a limit near TENSLSTR = 0.2 MPa above which tensile failure is not observed.

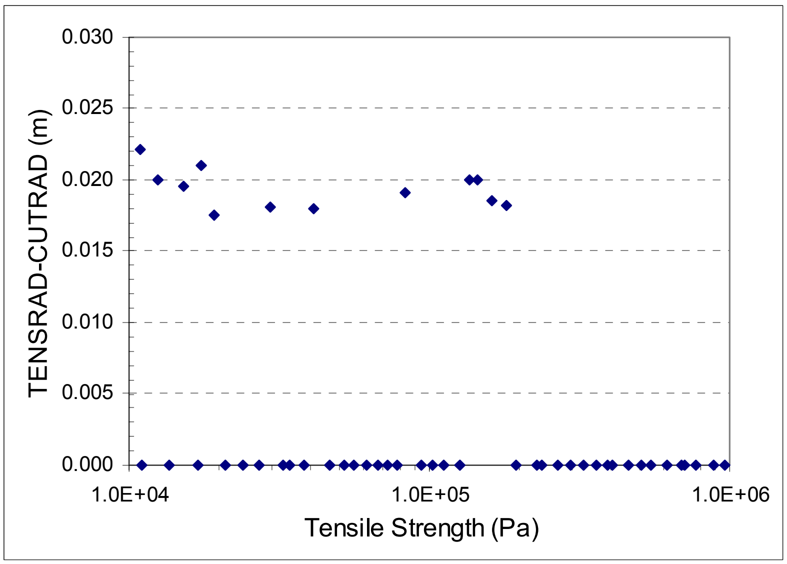

Figure 3.2-5. Scatterplot of TENSRAD-DRILLRAD vs. TENSLSTR for spherical geometry.

3.2.2.2 Variables controlling incremental spall volume (SPLVOL2)

The new incremental spallings volume SPLVOL2 exhibits sensitivity to repository initial pressure as illustrated in Figure 3.2-6. Here the incremental spall releases do not occur at pressures below 13.6 MPa. Though pressure above 10.6 MPa is sufficient to cause tensile failure (see Figure 3.2-3), the fluidization mechanism that moves the failed material into the wellbore requires even higher pressure.

SPLVOL2 is next shown as a function of permeability in Figure 3.2-7. Here it is apparent that some high-permeability vectors lead to incremental spallings. High permeability promotes high gas velocity near the wellbore to drive fluidization of any failed material. Alternatively, low permeability restricts gas flow so that in spite of failure, material may not mobilize. Though certain windows of both REPIPRES and REPPERM appear to lead to incremental spall release, the resulting magnitude of SPLVOL2 does not appear to correlate with either of these variables alone.

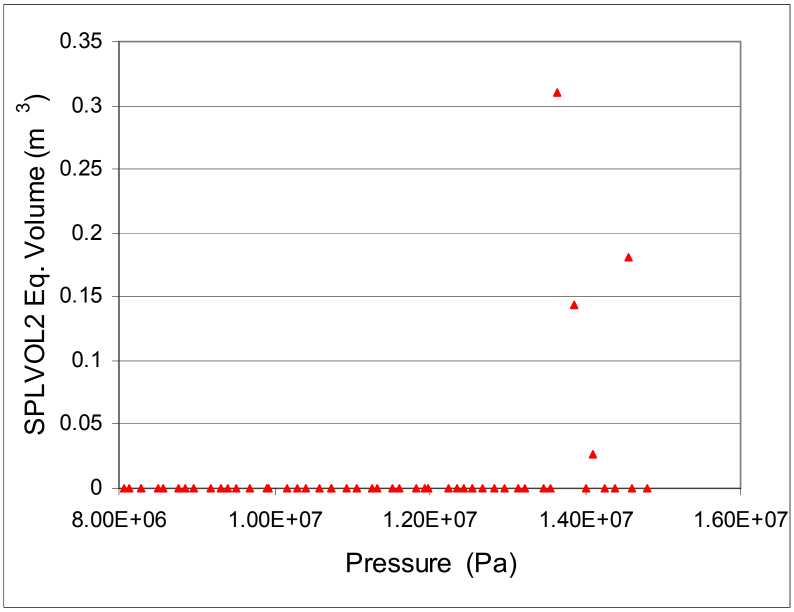

Figure 3.2-6. Scatterplot of SPLVOL2 vs. REPIPRES for spherical geometry.

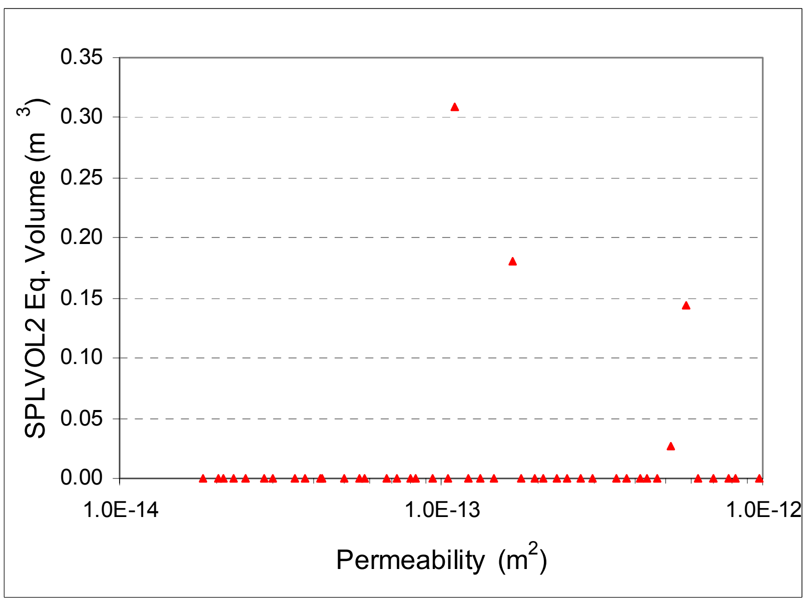

Figure 3.2-7. Scatterplot of SPLVOL2 vs. REPIPERM for spherical geometry.

SPLVOL2 is finally shown as a function of tensile strength in Figure 3.2-8. No particular correlation is evident. Nonzero SPLVOL2 is observed for TENSLSTR ranging from 2E+04 to 3E+05 Pa. Also, the largest SPLVOL2 value was observed at TENSLSTR=1.6 MPa, relatively high in this range.

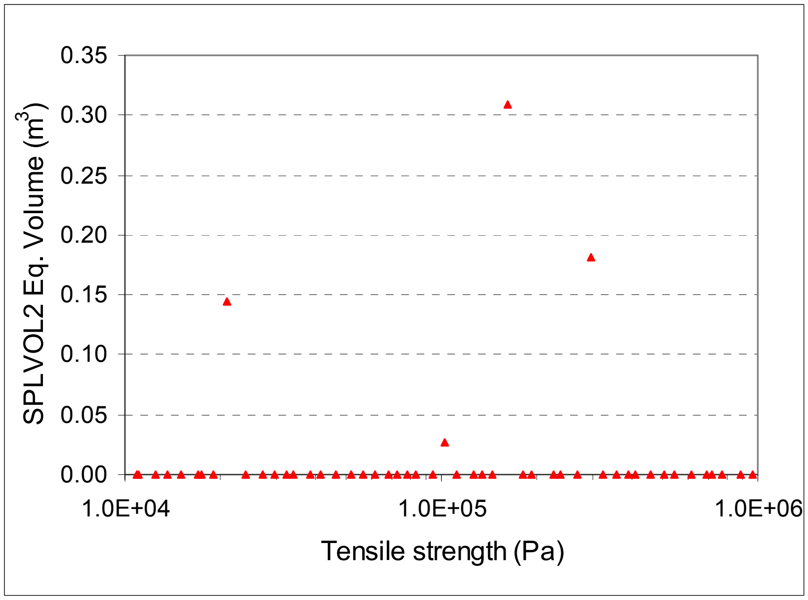

Figure 3.2-8. Scatterplot of SPLVOL2 vs. TENSLSTR for spherical geometry.

3.2.2.3 Role of fluidization

Repository material that is released to the surface may be removed from the repository domain by either drilling or failure and fluidization. Sensitivity analysis on DRSPALL output must include some discussion of the role of fluidization because it is mechanistically important, though potentially overlooked in favor of stress and failure mechanisms. Failed material is not "released" unless it is also fluidized and transported to the land surface. The solution to the Ergun (1952) equation (WIPP PA, 2003) yields a minimum fluidization velocity (FLUIDVEL) that is compared to the superficial gas velocity at the cavity face (WBSUPVEL) to determine if failed material will fluidize. Thus, if WBSUPVEL > FLUIDVEL, then fluidization is active. Otherwise, failed material will remain bedded. To visualize the frequency with which fluidization is active, a scatter plot was created in Figure 3.2-9 in which FLUIDVEL and WBSUPVEL were plotted versus REPIPERM at 450 seconds, a time shortly after the end of drilling in most vectors. The superficial gas velocity correlates strongly with permeability as expected. Where WBSUPVEL exceeds FLUIDVEL for a particular vector, any failed, bedded material will be swept into the wellbore flow stream. Note that the occurrence of WBSUPVEL > FLUIDVEL is non-existent at REPIPERM < 1.0E-13 m^2. Thus, it is unlikely that failed waste will fluidize when permeability is low. The implication of this in incremental spall volumes is apparent in Figure 3.2-7, where SPLVOL2 = 0 m^3 for REPIPERM < 1.0 E-13 m^2. Such vectors that exhibit terminally bedded material are called fluidization-limited.

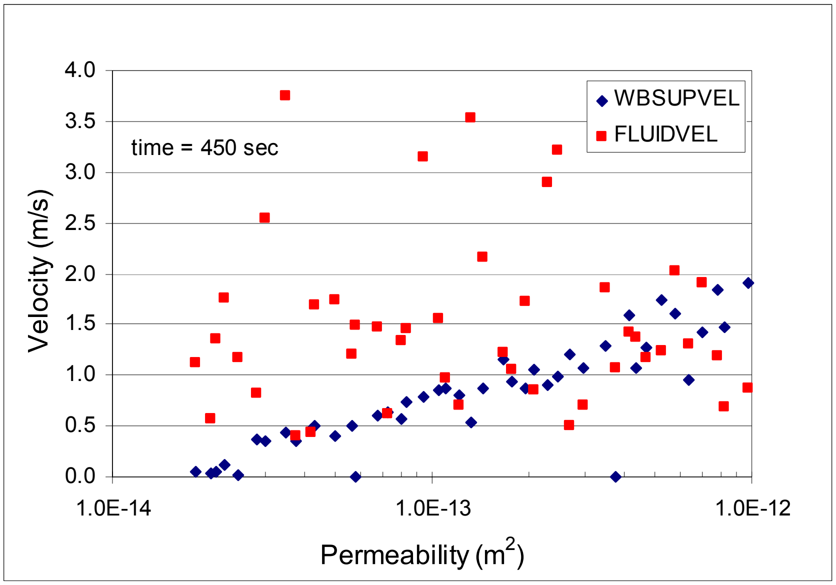

Figure 3.2-9. Scatterplot of Velocity vs. REPIPERM for spherical geometry.

While high superficial gas velocity is one way to promote fluidization, another possibility is low minimum fluidization velocity. The Ergun (1952) equation is quite sensitive to the product of particle shape factor and particle diameter (SHAPEFAC×PARTDIAM). Low values of both of these input variables drive FLUIDVEL similarly low (see Hansen et al, 2003 for more discussion). Their impact on SPLVOL2 is shown in Figure 3.2-10. Here, incremental spall release is observed only when SHAPEFAC×PARTDIAM < 0.004 m. This is a manifestation of the fact that small, tabular particles (PARTDIAM→1mm; SHAPEFAC → 0.1) are easier to fluidize than large, round particles (PARTDIAM→10mm; SHAPEFAC → 1.0) .

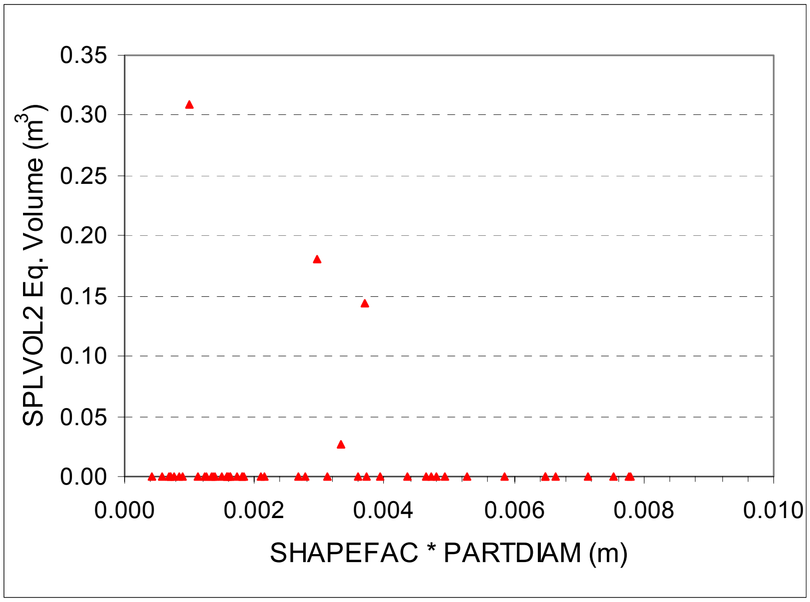

Figure 3.2-10. Scatterplot of SPLVOL2 vs. SHAPEFAC×PARTDIAM for spherical geometry.

3.2.2.4 Other sampled variables

The bulk of the discussion to this point has addressed the sensitivity of DRSPALL output to repository pressure, permeability, tensile strength, particle diameter, and particle shape factor. Of the nine input parameters sampled for this report (Table 2-1), this leaves the sensitivity to four uncertain variables yet unexplored. The remaining variables include repository porosity, initial mud density, initial mud viscosity, and DDZ permeability. In order to test the sensitivity of DRSPALL output to these variables, scatter plots against SPLVOL2 and TENSRAD-DRILLRAD are presented for each.

Shown in Figures 3.2-11 through 3.2-14 are scatter plots for REPIPOR, INITMDEN, MUDVISCO, and DDZPERM respectively. In no case does a clear correlation come to light. For example, nonzero values of TENSRAD-DRILLRAD appear over the entire sampling range for all four variables. There are no distinct clusters or cutoff ranges. From these data, it does not appear that the independent variables REPIPOR, INITMDEN, MUDVISCO, and DDZPERM have a significant effect on incremental spall volume or the formation of failed, bedded material in the cavity.

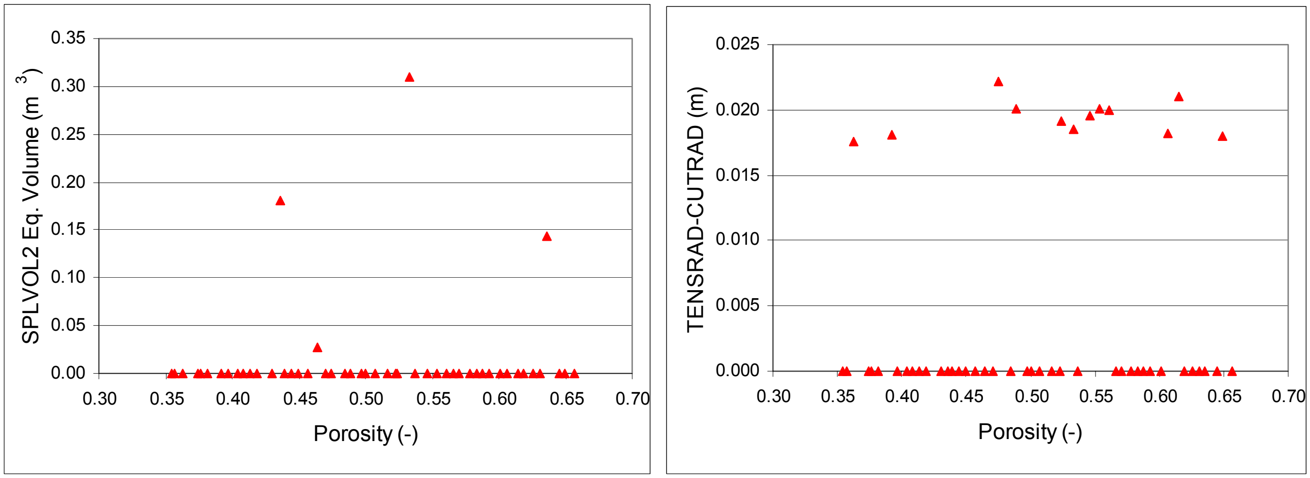

Figure 3.2-11. Scatter plots of SPLVOL2 and TENSRAD-DRILLRAD vs. REPIPOR for spherical geometry.

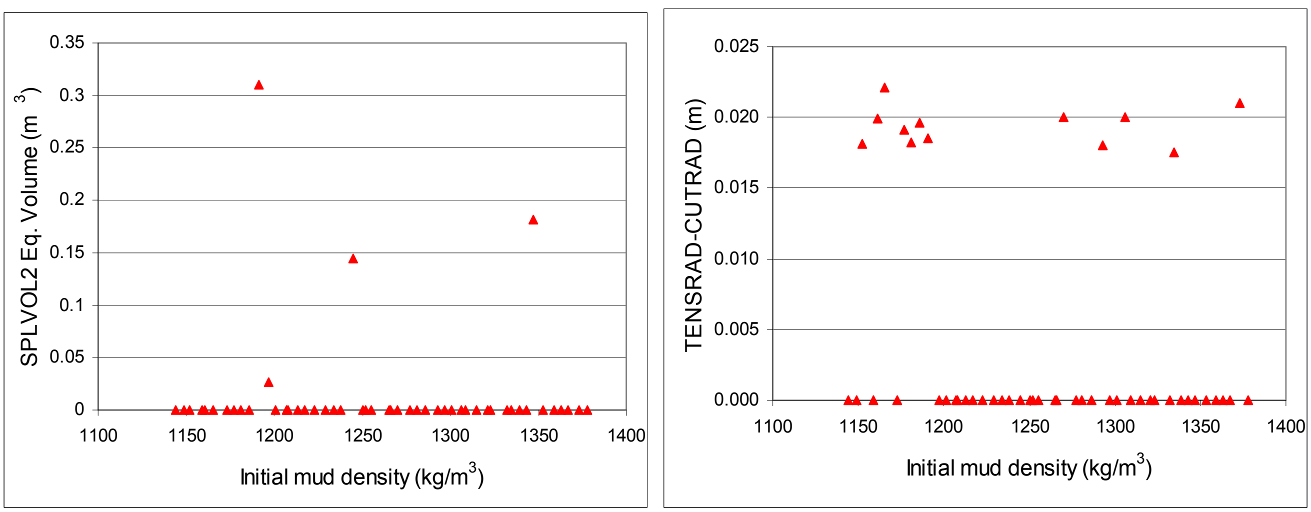

Figure 3.2-12. Scatter plots of SPLVOL2 and TENSRAD-DRILLRAD vs. INITMDEN for spherical geometry.

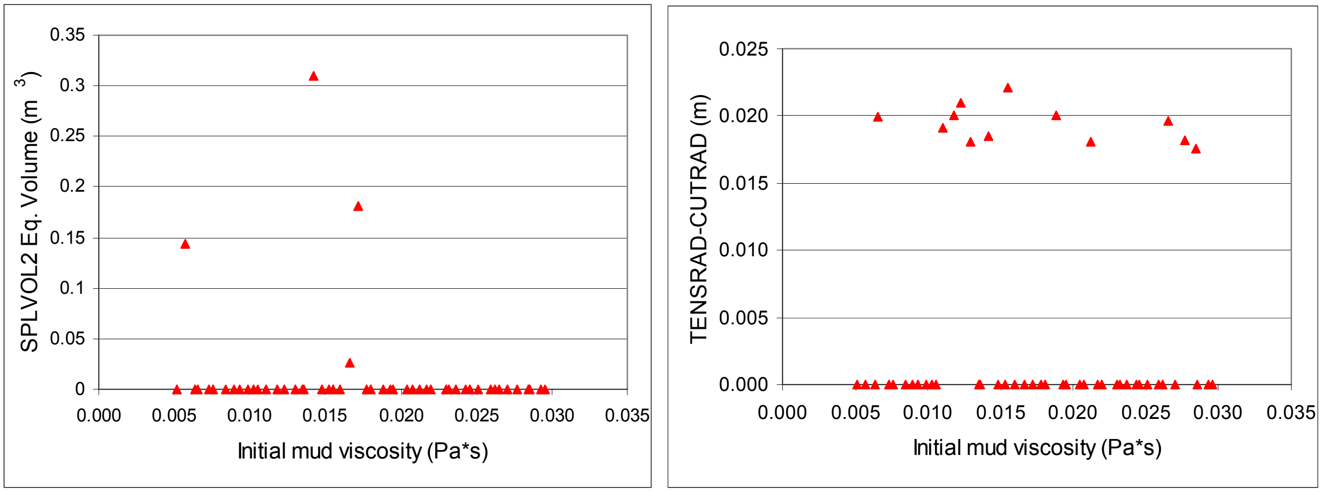

Figure 3.2-13. Scatter plots of SPLVOL2 and TENSRAD-DRILLRAD vs. MUDVISCO for spherical geometry.

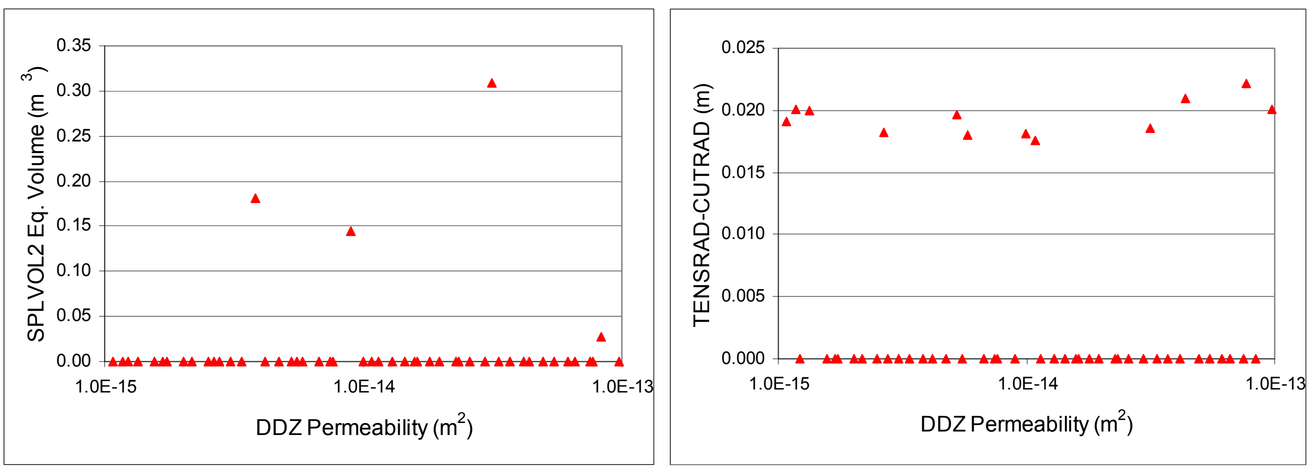

Figure 3.2-14. Scatter plots of SPLVOL2 and TENSRAD-DRILLRAD vs. DDZPERM for spherical geometry.

3.3 Cylindrical Geometry Results

The summary of spallings releases using cylindrical geometry at 900 seconds yields all zeroes for SPLVOLEQ, TENSRAD−DRILLRAD, and SPLVOL2. While this does not imply that failure is precluded in the cylindrical geometry, it does indicate that the likelihood of spallings in this geometry is small enough so that a release does not appear in the current sampling. With the summary data uniformly zero, it will be necessary to explore a sample vector to see why this is so.

3.3.1 Vector 040 volume history

In cylindrical geometry, SPLVOLEQ was zero for all times. The volume history plot for v040 is shown in Figure 3.3-1 for the cylindrical geometry. The results for the same vector assuming spherical geometry were shown previously in Figure 2.3-1. Examination of these figures reveals several differences between the cylindrical and spherical cases. First, all equivalent volumes in the cylindrical geometry are smaller. This results from the DRSPALL convention of conserving the surface area of the cavity when mapping the true drilling geometry to the equivalent 1D cylindrical or spherical model geometry. At any given time, the surface area of the cavity in each geometry is identical. For a given surface area, however, the volume of a cylinder is smaller than the volume of a hemisphere. Thus, the reported volumes (CUTVOLEQ, TOTVOLEQ, etc.) are smaller in the cylindrical geometry. Second, there is no repository tensile failure in the cylindrical run, and therefore the SPLVOLEQ and SPLVOL2 variables never exceed zero.

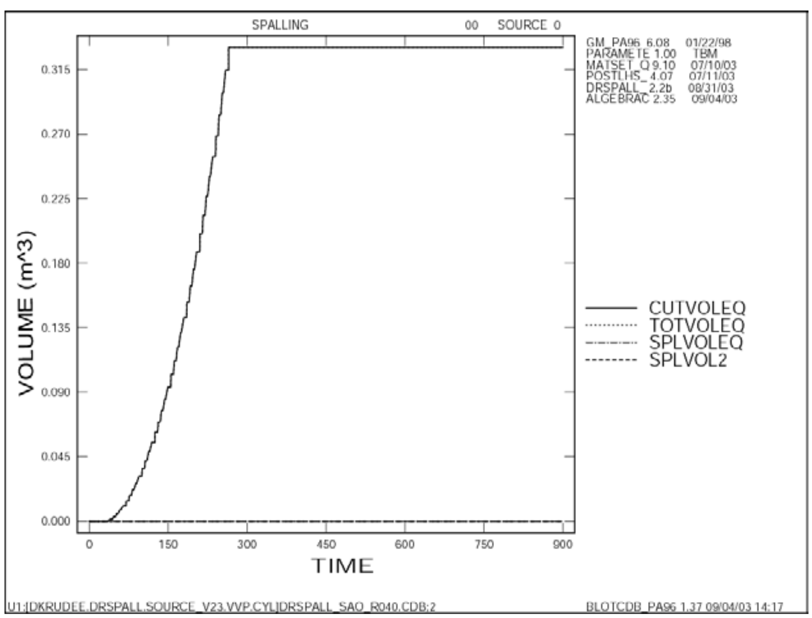

Figure 3.3-1. History plot of radial variables for v040 in cylindrical geometry. No failure is observed.

3.4 Response surface

The effects of three primary independent variables: REPIPRES, REPIPERM, and TENSLSTR, are examined together here in an effort to create a spallings "response surface." While the scatter plots presented earlier in this section analyze model sensitivity to one variable, it is understood that the model is actually sensitive to several variables simultaneously. The figures shown on the following pages attempt to elucidate this more complex relationship by presenting the SPLVOL2 and TENSRAD-DRILLRAD output as a function of two key independent variables. The magnitudes of these dependent variables are expressed in grayscale and symbol size. The legend for grayscale is given at the top of each plot. Zero values are denoted by an "×" symbol.

Starting with Figure 3.4-1, the paired effects of REPIPERM and REPIPRES appear to lead to SPLVOL2 releases primarily at high pressure and low permeability, visible as a concentration of ~0.2 m^3 hits in the lower right corner of the figure. Similar conditions also lead to TENSRAD-DRILLRAD > 0, evidenced by the grouping of hits along the lower REPIPERM axis. Here the pressure need not be as high to fail the waste as opposed to fail and fluidize, so nonzero values for TENSRAD-DRILLRAD are observed down to ~10.5 MPa.

Figure 3.4-2 shows the paired effects of TENSLSTR and REPIPRES. As expected, SPLVOL2 releases are constrained to high pressure, low strength vectors. Similarly, TENSRAD-DRILLRAD nonzero values appear in the same corner, though the high pressure requirement is not as stringent.

Finally, Figure 3.4-3 shows the paired effects of TENSLSTR and REPIPERM. SPLVOL2 releases are more frequent in the low REPIPERM, low TENSLSTR region. The dependence of SPLVOL2 upon REPIPERM is complex, because low permeability tends to promote tensile failure, but high permeability is required to fluidize bedded waste. The requirement for high permeability to fluidize bedded waste is shown clearly in the TENSRAD-DRILLRAD plot where bedded waste appears bunched at REPIPERM < 2E-13 m^2.

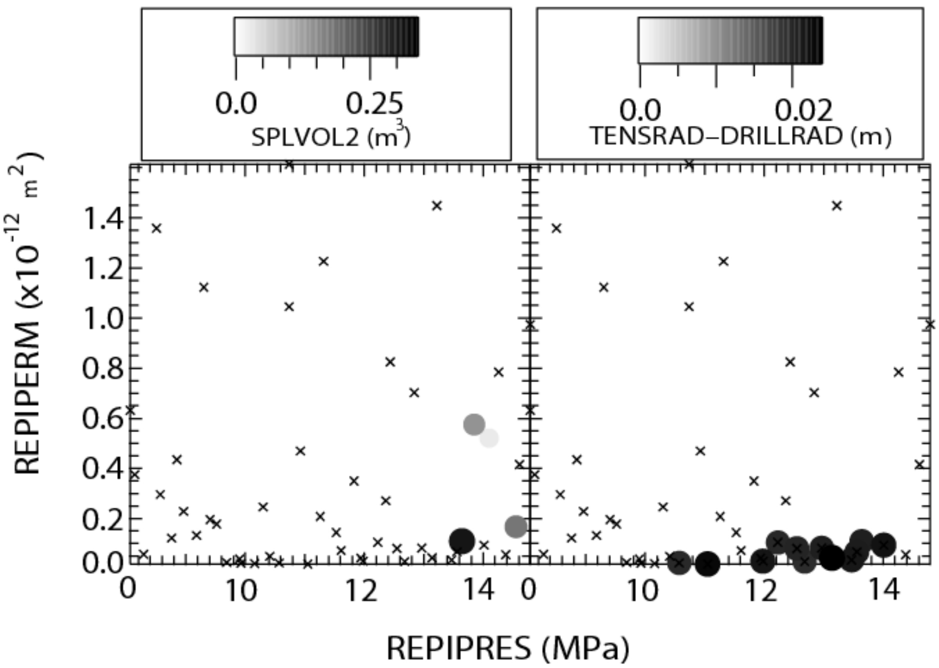

Figure 3.4-1. SPLVOL2 and TENSRAD-DRILLRAD response to REPIPERM and REPIPRES.

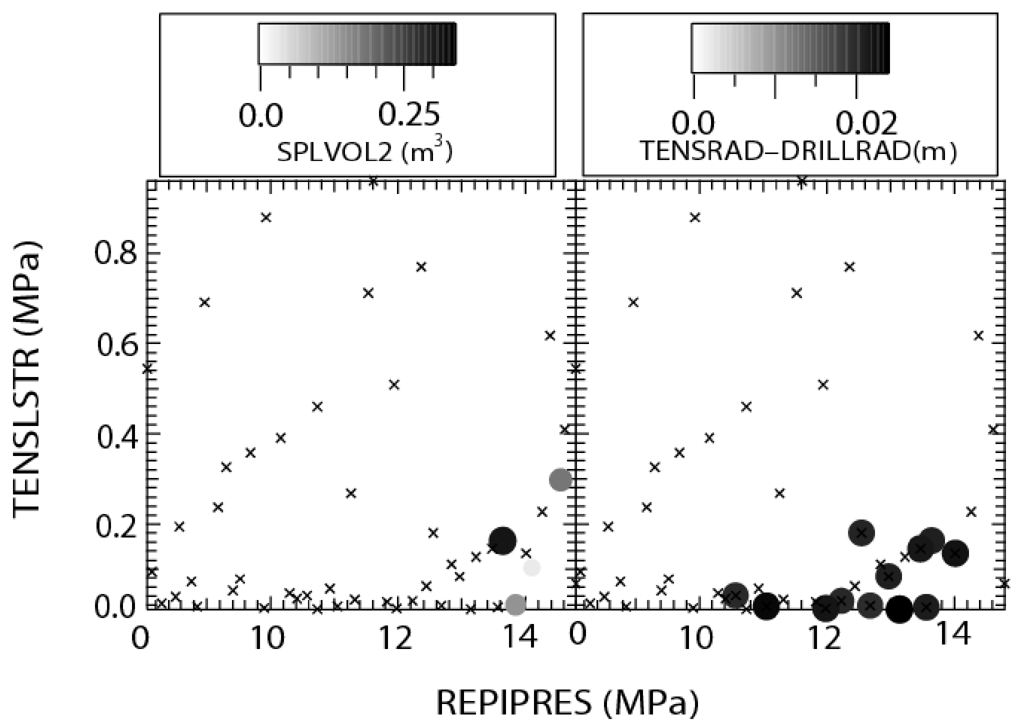

Figure 3.4-2. SPLVOL2 and TENSRAD-DRILLRAD response to TENSLSTR and REPIPRES.

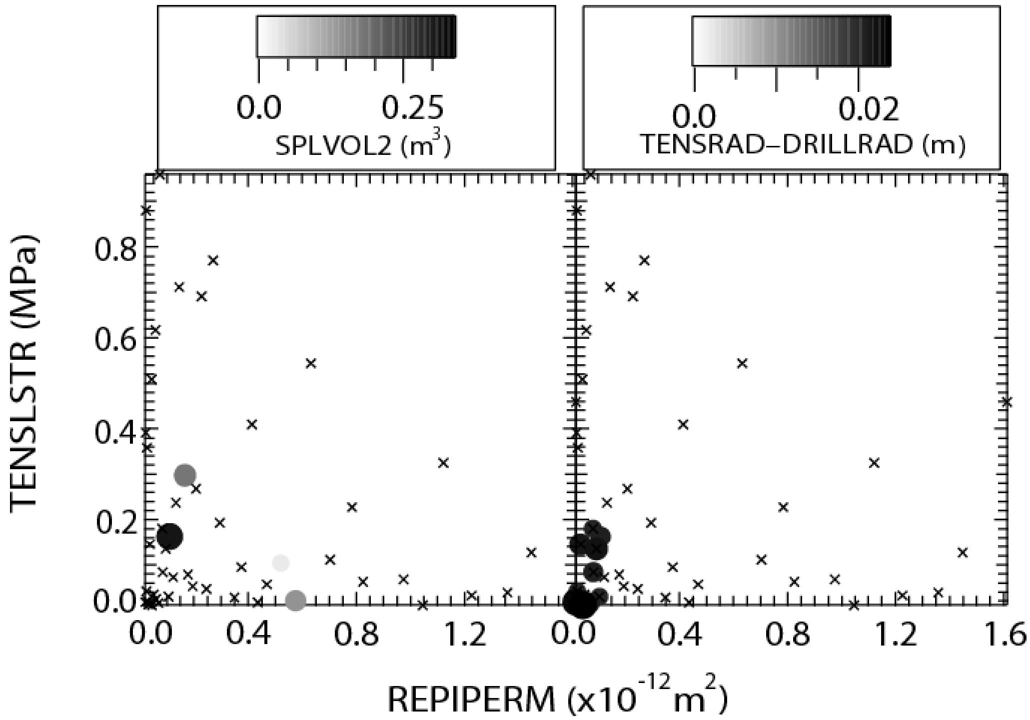

Figure 3.4-3. SPLVOL2 and TENSRAD-DRILLRAD response to TENSLSTR and REPIPERM.

4 SUMMARY

This analysis examines the sensitivity of DRSPALL output variables uncompacted equivalent spall volume (SPLVOLEQ), depth of failed but non-fluidized material (TENSRAD-DRILLRAD) and incremental spall volume (SPLVOL2) to sampled input variables. Input parameters demonstrated to be of primary importance include repository pressure (REPIPRES), repository permeability (REPIPERM), and waste tensile strength (TENSLSTR). Also potentially important due to their influence on the fluidization mechanism are waste porosity (REPIPOR) and particle shape factor × diameter (SHAPEFAC×PARTDIAM). None of the other sampled parameters in Part I or Part II demonstrated any conspicuous influence on the spall output.

Spall release volumes greater than zero were not only low in frequency, but also low in magnitude over the sampling explored here. The maximum SPLVOLEQ for the spherical geometry in Part I for the high pressure runs was 1.2 m^3, while the maximum SPLVOLEQ in Part II was 0.013 m^3. These are small compared to the maximum release of 4.0 m^3 observed in prior WIPP compliance PA runs such as the 1996 CCA and 1997 PAVT. This suggests that the new spall model will result in lower overall frequency and magnitude of spall releases relative to these prior analyses.

The spherical geometry is believed by the authors to best represent early drilling when the bit first penetrates the repository, while the cylindrical geometry best represents the end state of the drilling when the borehole completely penetrates the repository. While some of the spherical runs exhibited small incremental spall releases, the cylindrical geometry did not exhibit spallings in any of the cases examined here. The implication is that spallings in a WIPP scenario with the current conceptual model is both very small, and also very unlikely.

5 REFERENCES

Ergun, S. 1952. "Fluid Flow Through Packed Columns," *Chemical Engineering Progress*, 48:89-94.

Hansen, F.D., Pfeifle, T.W., Lord, D.L. 2003. *Parameter Justification Report for DRSPALL*. ERMS# 531057. Carlsbad, NM: Sandia National Laboratories.

Helton, J. Davis, F.L. 2002. *Latin Hypercube Sampling and the Propagation of Uncertainty in Analyses of Complex Systems.* SAND2001-0417. Albuquerque, NM: Sandia National Laboratories.

Lord, D.L., Rudeen, D.K. 2003. *Sensitivity Analysis Report -- Part I, DRSPALL v1.00.* ERMS#531062. Carlsbad, NM: Sandia National Laboratories.

WIPP PA, 2003. *Design Document for DRSPALL Version 1.00, document version 1.10.* ERMS# 529878. Carlsbad, NM: Sandia National Laboratories.

APPENDIX LHS2_DRSPALL.TRN

The following is a listing of the ASCII output file LHS2_DRSPALL.TRN created by running LHS. Also created are 50 output binary files (1 per vector) that are not listed here. Note that the sampled parameter names, distributions, and ranges are given on the first page of this listing. Below this appears a table of the new parameter values computed by LHS, followed by a similar table showing the rank of a particular value within the distribution of 50 values. Rank = 1 corresponds to the lowest value in the distribution, while rank = 50 corresponds to the highest value. The final collection of tables shows the histograms for each sampled variable.

```
Directory U1:[DKRUDEE.DRSPALL.LHS_PR]LHS2_DRSPALL.TRN;38
11-JUL-2003 09:46:13.67
```

```
    TITLE DRSPALL PEER REVIEW SENSITIVITY SAMPLING

    RANDOM SEED =   585364674

    NUMBER OF VARIABLES =   9

    NUMBER OF OBSERVATIONS =   50
0   THE SAMPLE INPUT VECTORS WILL BE PRINTED ALONG WITH THEIR CORRESPONDING RANKS
0   HISTOGRAMS OF THE ACTUAL SAMPLE WILL BE PLOTTED FOR EACH INPUT VARIABLE
0   THE CORRELATION MATRICES (RAW DATA AND RANK CORRELATIONS) WILL BE PRINTED
1

    TITLE DRSPALL PEER REVIEW SENSITIVITY SAMPLING

    VARIABLE  DISTRIBUTION          RANGE             LABEL
0       1     UNIFORM            8.0000E+06 TO   1.4850E+07  DR_SPALL  REPIPRES
0       2     UNIFORM            0.3500     TO   0.6600      DR_SPALL  REPIPOR
0       3     LOGUNIFORM         1.7000E-14 TO   1.7000E-12  DR_SPALL  REPIPERM
0       4     LOGUNIFORM         1.0000E+04 TO   1.0000E+06  DR_SPALL  TENSLSTR
0       5     UNIFORM             1140.     TO    1380.      DR_SPALL  INITMDEN
0       6     UNIFORM            5.0000E-03 TO   3.0000E-02  DR_SPALL  MUDVISCO
0       7     LOGUNIFORM         1.0000E-15 TO   1.0000E-13  DR_SPALL  DDZPERM
0       8     UNIFORM            0.1000     TO    1.000      DR_SPALL  SHAPEFAC
```

```
0       9     UNIFORM            1.0000E-03 TO   1.0000E-02  DR_SPALL  PARTDIAM
1TITLE DRSPALL PEER REVIEW SENSITIVITY SAMPLING
0LATIN HYPERCUBE SAMPLE INPUT VECTORS
```

RUN NO.		X(1)	X(2)	X(3)	X(4)	X(5)	X(6)	X(7)	X(8)	X(9)
0	1	1.057E+07	6.493E-01	2.257E-14	4.132E+04	1.293E+03	1.298E-02	5.822E-15	2.359E-01	6.828E-03
0	2	1.183E+07	4.497E-01	3.498E-13	2.716E+04	1.265E+03	2.508E-02	2.280E-14	9.073E-01	7.157E-03
0	3	9.301E+06	5.368E-01	1.122E-12	3.253E+05	1.229E+03	1.052E-02	3.362E-14	7.340E-01	4.886E-03
0	4	1.401E+07	5.531E-01	9.415E-14	1.354E+05	1.306E+03	1.179E-02	9.799E-14	9.754E-01	7.963E-03
0	5	1.198E+07	4.886E-01	2.994E-14	1.246E+04	1.270E+03	1.887E-02	1.174E-15	9.359E-01	5.278E-03
0	6	1.223E+07	3.919E-01	1.047E-13	2.971E+04	1.152E+03	2.122E-02	9.956E-15	5.610E-01	8.417E-03
0	7	8.292E+06	6.189E-01	5.753E-14	2.411E+04	1.378E+03	2.703E-02	2.166E-15	4.738E-01	9.829E-03
0	8	9.931E+06	4.078E-01	2.112E-14	8.801E+05	1.213E+03	2.455E-02	4.160E-14	8.195E-01	8.726E-03
0	9	1.322E+07	3.815E-01	1.449E-12	1.269E+05	1.297E+03	1.928E-02	7.428E-15	4.185E-01	8.880E-03
0	10	1.105E+07	6.148E-01	1.822E-14	1.749E+04	1.373E+03	1.227E-02	4.366E-14	7.275E-01	2.057E-03
0	11	8.853E+06	5.660E-01	4.357E-13	1.707E+04	1.238E+03	1.479E-02	5.457E-14	3.537E-01	4.633E-03
0	12	8.139E+06	5.223E-01	3.753E-13	9.434E+04	1.367E+03	8.928E-03	3.711E-14	4.257E-01	9.260E-03
0	13	1.438E+07	6.570E-01	5.596E-14	6.175E+05	1.223E+03	2.045E-02	4.939E-14	6.610E-01	1.142E-03
0	14	8.510E+06	5.835E-01	1.358E-12	3.834E+04	1.323E+03	2.368E-02	3.068E-15	1.470E-01	6.114E-03
0	15	9.408E+06	5.068E-01	1.957E-13	5.218E+04	1.315E+03	1.027E-02	2.595E-14	7.970E-01	3.366E-03
0	16	1.268E+07	3.630E-01	2.826E-14	1.914E+04	1.335E+03	2.846E-02	1.081E-14	2.124E-01	7.692E-03
0	17	1.461E+07	4.042E-01	4.153E-13	4.095E+05	1.363E+03	2.433E-02	1.620E-14	8.807E-01	7.370E-03
0	18	1.074E+07	4.185E-01	1.045E-12	1.102E+04	1.234E+03	2.170E-02	6.164E-14	9.243E-01	6.328E-03
0	19	1.041E+07	5.161E-01	4.969E-14	3.425E+04	1.353E+03	1.953E-02	5.504E-15	5.685E-01	3.673E-03
0	20	1.255E+07	6.063E-01	8.068E-14	1.804E+05	1.181E+03	2.769E-02	2.649E-15	1.337E-01	8.365E-03
0	21	1.479E+07	5.002E-01	9.743E-13	6.773E+04	1.281E+03	2.620E-02	1.562E-15	6.041E-01	3.002E-03
0	22	1.297E+07	5.240E-01	8.282E-14	8.351E+04	1.177E+03	1.108E-02	1.082E-15	6.408E-01	2.827E-03
0	23	1.161E+07	4.568E-01	7.294E-14	9.607E+05	1.309E+03	1.360E-02	1.438E-14	4.500E-01	1.503E-03
0	24	8.964E+06	4.972E-01	2.288E-13	6.914E+05	1.149E+03	1.601E-02	1.960E-14	9.574E-01	8.138E-03
0	25	9.900E+06	3.546E-01	3.771E-14	1.367E+04	1.255E+03	1.346E-02	6.593E-14	2.927E-01	2.403E-03
0	26	9.519E+06	4.387E-01	1.780E-13	7.786E+04	1.286E+03	7.299E-03	1.685E-15	4.025E-01	3.880E-03
0	27	1.356E+07	5.464E-01	6.750E-14	1.513E+04	1.186E+03	2.653E-02	5.241E-15	5.400E-01	3.210E-03
0	28	1.132E+07	3.968E-01	1.226E-12	3.246E+04	1.250E+03	2.954E-02	1.226E-15	6.942E-01	1.199E-03
0	29	9.686E+06	4.847E-01	2.468E-14	3.581E+05	1.339E+03	2.298E-02	1.581E-14	8.636E-01	5.570E-03
0	30	1.074E+07	4.301E-01	1.613E-12	4.596E+05	1.359E+03	8.419E-03	2.780E-15	8.246E-01	1.610E-03
0	31	1.410E+07	4.643E-01	5.210E-13	1.031E+05	1.197E+03	1.663E-02	8.348E-14	5.140E-01	6.487E-03
0	32	1.426E+07	5.873E-01	7.845E-13	2.273E+05	1.208E+03	9.340E-03	7.596E-15	1.938E-01	9.521E-03
0	33	1.284E+07	6.009E-01	7.030E-13	1.111E+05	1.301E+03	2.591E-02	1.801E-14	8.499E-01	5.111E-03
0	34	1.236E+07	4.441E-01	2.709E-13	7.706E+05	1.343E+03	2.201E-02	3.394E-15	2.633E-01	2.658E-03
0	35	1.093E+07	5.785E-01	4.695E-13	5.627E+04	1.201E+03	1.527E-02	6.712E-15	3.051E-01	4.568E-03
0	36	8.065E+06	6.309E-01	6.321E-13	5.438E+05	1.173E+03	2.928E-02	4.166E-15	5.911E-01	2.117E-03
0	37	1.244E+07	6.260E-01	8.244E-13	6.186E+04	1.332E+03	1.774E-02	7.489E-14	1.082E-01	5.396E-03
0	38	1.385E+07	6.357E-01	5.753E-13	2.094E+04	1.245E+03	5.723E-03	8.970E-15	6.221E-01	5.930E-03
0	39	1.126E+07	4.135E-01	2.079E-13	2.679E+05	1.277E+03	2.078E-02	2.953E-14	3.735E-01	4.248E-03
0	40	1.455E+07	4.360E-01	1.671E-13	2.973E+05	1.347E+03	1.719E-02	3.823E-15	3.180E-01	9.355E-03
0	41	1.030E+07	5.929E-01	2.463E-13	4.649E+04	1.252E+03	7.608E-03	2.007E-15	9.892E-01	6.706E-03
0	42	1.347E+07	5.608E-01	3.504E-14	1.449E+05	1.161E+03	6.525E-03	1.342E-15	7.697E-01	9.795E-03

0	43	1.016E+07	3.768E-01	2.039E-14	3.915E+05	1.266E+03	2.319E-02	4.733E-15	5.116E-01	4.188E-03
0	44	8.761E+06	3.569E-01	1.222E-13	7.263E+04	1.207E+03	5.168E-03	2.509E-15	6.926E-01	1.795E-03
0	45	8.572E+06	3.739E-01	2.959E-13	1.934E+05	1.144E+03	1.805E-02	1.300E-14	1.804E-01	7.544E-03
0	46	9.178E+06	6.453E-01	1.325E-13	2.375E+05	1.159E+03	2.852E-02	1.142E-14	7.613E-01	6.942E-03
0	47	1.153E+07	5.701E-01	1.451E-13	7.119E+05	1.321E+03	6.401E-03	1.742E-15	3.507E-01	8.920E-03
0	48	1.314E+07	4.746E-01	4.278E-14	1.092E+04	1.165E+03	1.554E-02	7.675E-14	4.790E-01	5.786E-03
0	49	1.364E+07	5.332E-01	1.099E-13	1.626E+05	1.191E+03	1.420E-02	3.162E-14	2.489E-01	3.955E-03
0	50	1.194E+07	4.705E-01	4.207E-14	5.091E+05	1.217E+03	9.898E-03	2.331E-14	1.693E-01	2.538E-03

1TITLE DRSPALL PEER REVIEW SENSITIVITY SAMPLING

0RANKS OF LATIN HYPERCUBE SAMPLE INPUT VECTORS

	RUN NO.	X(1)	X(2)	X(3)	X(4)	X(5)	X(6)	X(7)	X(8)	X(9)
0	1	19.	49.	4.	16.	32.	16.	20.	8.	33.
0	2	28.	17.	33.	11.	26.	41.	34.	45.	35.
0	3	10.	31.	46.	38.	19.	12.	39.	36.	22.
0	4	44.	33.	19.	29.	35.	14.	50.	49.	39.
0	5	30.	23.	7.	3.	28.	28.	2.	47.	24.
0	6	31.	7.	20.	12.	3.	33.	25.	26.	42.
0	7	3.	44.	14.	10.	50.	45.	9.	21.	50.
0	8	15.	10.	3.	49.	16.	40.	41.	40.	43.
0	9	39.	6.	49.	28.	33.	29.	22.	18.	44.
0	10	23.	43.	1.	7.	49.	15.	42.	35.	6.
0	11	7.	35.	36.	6.	21.	20.	44.	15.	21.
0	12	2.	28.	34.	25.	48.	8.	40.	19.	46.
0	13	47.	50.	13.	45.	18.	31.	43.	32.	1.
0	14	4.	38.	48.	15.	39.	38.	13.	3.	29.
0	15	11.	26.	27.	18.	37.	11.	36.	39.	14.
0	16	35.	3.	6.	8.	41.	47.	26.	7.	38.
0	17	49.	9.	35.	41.	47.	39.	31.	44.	36.
0	18	20.	12.	45.	2.	20.	34.	45.	46.	30.
0	19	18.	27.	12.	14.	45.	30.	19.	27.	15.
0	20	34.	42.	17.	32.	9.	46.	11.	2.	41.
0	21	50.	25.	44.	21.	30.	43.	5.	29.	12.
0	22	37.	29.	18.	24.	8.	13.	1.	31.	11.
0	23	27.	18.	16.	50.	36.	18.	29.	20.	3.
0	24	8.	24.	29.	46.	2.	23.	33.	48.	40.
0	25	14.	1.	9.	4.	25.	17.	46.	11.	8.
0	26	12.	15.	26.	23.	31.	5.	6.	17.	16.
0	27	41.	32.	15.	5.	10.	44.	18.	25.	13.
0	28	25.	8.	47.	13.	23.	50.	3.	34.	2.
0	29	13.	22.	5.	39.	42.	36.	30.	43.	26.
0	30	21.	13.	50.	42.	46.	7.	12.	41.	4.
0	31	45.	19.	38.	26.	12.	24.	49.	24.	31.
0	32	46.	39.	42.	34.	15.	9.	23.	6.	48.
0	33	36.	41.	41.	27.	34.	42.	32.	42.	23.
0	34	32.	16.	31.	48.	43.	35.	14.	10.	10.
0	35	22.	37.	37.	19.	13.	21.	21.	12.	20.

```
0   36        1.        46.        40.        44.         7.        49.        16.        28.         7.
0   37       33.        45.        43.        20.        40.        26.        47.         1.        25.
0   38       43.        47.        39.         9.        22.         2.        24.        30.        28.
0   39       24.        11.        28.        36.        29.        32.        37.        16.        19.
0   40       48.        14.        25.        37.        44.        25.        15.        13.        47.
0   41       17.        40.        30.        17.        24.         6.         8.        50.        32.
0   42       40.        34.         8.        30.         5.         4.         4.        38.        49.
0   43       16.         5.         2.        40.        27.        37.        17.        23.        18.
0   44        6.         2.        22.        22.        14.         1.        10.        33.         5.
0   45        5.         4.        32.        33.         1.        27.        28.         5.        37.
0   46        9.        48.        23.        35.         4.        48.        27.        37.        34.
0   47       26.        36.        24.        47.        38.         3.         7.        14.        45.
0   48       38.        21.        11.         1.         6.        22.        48.        22.        27.
0   49       42.        30.        21.        31.        11.        19.        38.         9.        17.
0   50       29.        20.        10.        43.        17.        10.        35.         4.         9.
1   TITLE DRSPALL PEER REVIEW SENSITIVITY SAMPLING
0  HISTOGRAM FOR VARIABLE NO.  1     UNIFORM         DISTRIBUTION

     MIDPOINT          FREQ.

    7990000.             2    XX
    8330000.             1    X
    8669999.             3    XXX
    9009999.             3    XXX
    9349999.             3    XXX
    9689999.             1    X
   0.1003000E+08         3    XXX
   0.1037000E+08         2    XX
   0.1071000E+08         3    XXX
   0.1105000E+08         2    XX
   0.1139000E+08         3    XXX
   0.1173000E+08         2    XX
   0.1207000E+08         3    XXX
   0.1241000E+08         3    XXX
   0.1275000E+08         2    XX
   0.1309000E+08         3    XXX
   0.1343000E+08         2    XX
   0.1377000E+08         2    XX
   0.1411000E+08         3    XXX
   0.1445000E+08         3    XXX
   0.1479000E+08         1    X
0                       50


      MIN            MAX            RANGE           MEAN           MEDIAN         VARIANCE

    8064610.      0.1479040E+08   6725794.      0.1142181E+08  0.1142440E+08  0.3944230E+13
```

```
1   TITLE DRSPALL PEER REVIEW SENSITIVITY SAMPLING
0  HISTOGRAM FOR VARIABLE NO.  2     UNIFORM         DISTRIBUTION

     MIDPOINT          FREQ.

   0.3525000             2    XX
   0.3675000             2    XX
   0.3825001             2    XX
   0.3975001             3    XXX
   0.4125001             3    XXX
   0.4275001             1    X
   0.4425001             4    XXXX
   0.4575001             2    XX
   0.4725001             2    XX
   0.4875002             2    XX
   0.5025002             3    XXX
   0.5175002             3    XXX
   0.5325001             2    XX
   0.5475001             2    XX
   0.5625001             2    XX
   0.5775001             3    XXX
   0.5925001             2    XX
   0.6075001             3    XXX
   0.6225001             2    XX
   0.6375000             2    XX
   0.6525000             3    XXX
0                       50

      MIN            MAX           RANGE           MEAN          MEDIAN        VARIANCE

   0.3545705      0.6569982      0.3024277      0.5047517      0.5035076      0.8028069E-02

1   TITLE DRSPALL PEER REVIEW SENSITIVITY SAMPLING
0  HISTOGRAM FOR VARIABLE NO.  3     LOGUNIFORM      DISTRIBUTION

     MIDPOINT          FREQ.

   0.3999998E-13        16    XXXXXXXXXXXXXXXX
   0.1199999E-12         8    XXXXXXXX
   0.1999999E-12         5    XXXXX
   0.2799998E-12         3    XXX
   0.3599998E-12         2    XX
   0.4399997E-12         3    XXX
   0.5199997E-12         1    X
   0.5999997E-12         2    XX
```

```
   0.6799996E-12         1    X
   0.7599996E-12         1    X
   0.8399996E-12         1    X
   0.9199995E-12         0
   0.9999995E-12         1    X
   0.1079999E-11         1    X
   0.1159999E-11         1    X
   0.1239999E-11         1    X
   0.1319999E-11         1    X
   0.1399999E-11         0
   0.1479999E-11         1    X
   0.1559999E-11         0
   0.1639999E-11         1    X
0                       50

      MIN             MAX           RANGE           MEAN          MEDIAN        VARIANCE

   0.1822097E-13  0.1613045E-11  0.1594824E-11  0.3632711E-12  0.1725522E-12  0.1786772E-24

1   TITLE DRSPALL PEER REVIEW SENSITIVITY SAMPLING
0  HISTOGRAM FOR VARIABLE NO.  4     LOGUNIFORM      DISTRIBUTION

     MIDPOINT          FREQ.

    23499.99            17    XXXXXXXXXXXXXXXXX
    70499.98             7    XXXXXXX
    117500.0             5    XXXXX
    164500.0             3    XXX
    211499.9             2    XX
    258499.9             2    XX
    305499.9             2    XX
    352499.9             1    X
    399499.9             2    XX
    446499.9             1    X
    493499.9             1    X
    540499.9             1    X
    587499.9             0
    634499.9             1    X
    681499.9             1    X
    728499.9             1    X
    775499.9             1    X
    822499.9             0
    869499.9             1    X
    916499.9             0
    963499.9             1    X
0                       50
```

```
     MIN           MAX           RANGE          MEAN          MEDIAN        VARIANCE

   10924.72      960705.3      949780.6      215899.8      98705.41      0.6289259E+11

1   TITLE DRSPALL PEER REVIEW SENSITIVITY SAMPLING
0  HISTOGRAM FOR VARIABLE NO.  5     UNIFORM         DISTRIBUTION

     MIDPOINT          FREQ.

    1146.000             3    XXX
    1158.000             2    XX
    1170.000             2    XX
    1182.000             3    XXX
    1194.000             2    XX
    1206.000             3    XXX
    1218.000             3    XXX
    1230.000             2    XX
    1242.000             2    XX
    1254.000             3    XXX
    1266.000             3    XXX
    1278.000             2    XX
    1290.000             2    XX
    1302.000             3    XXX
    1314.000             2    XX
    1326.000             3    XXX
    1338.000             3    XXX
    1350.000             2    XX
    1362.000             3    XXX
    1374.000             2    XX
0                       50

     MIN           MAX           RANGE          MEAN          MEDIAN        VARIANCE

   1143.778      1378.341      234.5627      1260.126      1260.037      4768.640

1   TITLE DRSPALL PEER REVIEW SENSITIVITY SAMPLING
0  HISTOGRAM FOR VARIABLE NO.  6     UNIFORM         DISTRIBUTION

     MIDPOINT          FREQ.

   0.5399999E-02         2    XX
   0.6599999E-02         2    XX
   0.7799999E-02         2    XX
   0.8999999E-02         3    XXX
```

```
   0.1020000E-01         3    XXX
   0.1140000E-01         2    XX
   0.1260000E-01         2    XX
   0.1380000E-01         3    XXX
   0.1500000E-01         3    XXX
   0.1620000E-01         2    XX
   0.1740000E-01         2    XX
   0.1860000E-01         2    XX
   0.1980000E-01         2    XX
   0.2100000E-01         3    XXX
   0.2220000E-01         2    XX
   0.2340000E-01         3    XXX
   0.2460000E-01         3    XXX
   0.2580000E-01         2    XX
   0.2700000E-01         2    XX
   0.2820000E-01         3    XXX
   0.2940000E-01         2    XX
0                       50


      MIN            MAX           RANGE           MEAN          MEDIAN        VARIANCE

   0.5167625E-02  0.2953797E-01  0.2437034E-01  0.1747031E-01  0.1746353E-01  0.5168220E-04

1   TITLE DRSPALL PEER REVIEW SENSITIVITY SAMPLING
0  HISTOGRAM FOR VARIABLE NO.  7     LOGUNIFORM      DISTRIBUTION

     MIDPOINT          FREQ.

   0.2399999E-14        17    XXXXXXXXXXXXXXXXX
   0.7199998E-14         7    XXXXXXX
   0.1200000E-13         5    XXXXX
   0.1680000E-13         3    XXX
   0.2159999E-13         3    XXX
   0.2639999E-13         1    X
   0.3119999E-13         2    XX
   0.3599999E-13         2    XX
   0.4079999E-13         1    X
   0.4559999E-13         1    X
   0.5039999E-13         1    X
   0.5519999E-13         1    X
   0.5999999E-13         1    X
   0.6479999E-13         1    X
   0.6959999E-13         0
   0.7439999E-13         2    XX
   0.7919999E-13         0
   0.8399999E-13         1    X
```

```
   0.8879999E-13         0
   0.9359999E-13         0
   0.9839999E-13         1    X
0                       50

      MIN            MAX           RANGE           MEAN          MEDIAN        VARIANCE

   0.1082278E-14  0.9798927E-13  0.9690699E-13  0.2142826E-13  0.1038332E-13  0.6164347E-27

1   TITLE DRSPALL PEER REVIEW SENSITIVITY SAMPLING
0  HISTOGRAM FOR VARIABLE NO.  8     UNIFORM         DISTRIBUTION

     MIDPOINT          FREQ.

   0.1100000             1    X
   0.1540000             3    XXX
   0.1979999             3    XXX
   0.2419999             3    XXX
   0.2859999             2    XX
   0.3299999             2    XX
   0.3739999             2    XX
   0.4179999             3    XXX
   0.4619999             3    XXX
   0.5059999             2    XX
   0.5499999             3    XXX
   0.5939999             2    XX
   0.6379998             2    XX
   0.6819998             3    XXX
   0.7259998             2    XX
   0.7699997             2    XX
   0.8139997             3    XXX
   0.8579997             2    XX
   0.9019997             2    XX
   0.9459996             3    XXX
   0.9899996             2    XX
0                       50

      MIN            MAX           RANGE           MEAN          MEDIAN        VARIANCE

   0.1082363      0.9891761      0.8809398      0.5490831      0.5505027      0.6771753E-01

1   TITLE DRSPALL PEER REVIEW SENSITIVITY SAMPLING
0  HISTOGRAM FOR VARIABLE NO.  9     UNIFORM         DISTRIBUTION

     MIDPOINT          FREQ.
```

```
   0.1075000E-02         2    XX
   0.1505000E-02         2    XX
   0.1935000E-02         3    XXX
   0.2365000E-02         2    XX
   0.2795000E-02         3    XXX
   0.3225000E-02         2    XX
   0.3655000E-02         1    X
   0.4085000E-02         4    XXXX
   0.4515000E-02         2    XX
   0.4945000E-02         2    XX
   0.5375000E-02         3    XXX
   0.5805000E-02         2    XX
   0.6235000E-02         2    XX
   0.6665000E-02         3    XXX
   0.7095000E-02         2    XX
   0.7525000E-02         3    XXX
   0.7955000E-02         2    XX
   0.8385000E-02         2    XX
   0.8815000E-02         3    XXX
   0.9245000E-02         2    XX
   0.9675000E-02         3    XXX
0                       50


      MIN            MAX           RANGE           MEAN          MEDIAN        VARIANCE

   0.1142324E-02  0.9828614E-02  0.8686290E-02  0.5497297E-02  0.5482946E-02  0.6750899E-05

1TITLE DRSPALL PEER REVIEW SENSITIVITY SAMPLING
0CORRELATIONS AMONG INPUT VARIABLES CREATED BY THE LATIN HYPERCUBE SAMPLE FOR RAW DATA                              PAGE   1
0    1  1.0000
0    2  0.0205  1.0000
0    3 -0.0033 -0.0354  1.0000
0    4 -0.0343 -0.0861 -0.1053  1.0000
0    5 -0.0309 -0.0266  0.1369  0.0068  1.0000
0    6  0.0210 -0.0737  0.0758  0.0166  0.0000  1.0000
0    7  0.1247  0.0083 -0.0484 -0.0939 -0.0403 -0.1079  1.0000
0    8 -0.0328 -0.0212  0.0225  0.0369 -0.0142  0.0110  0.0666  1.0000
0    9  0.0734  0.0696 -0.0760 -0.0923 -0.0224  0.0260 -0.0027 -0.0416  1.0000
0            1       2       3       4       5       6       7       8       9
0VARIABLES
0THE VARIANCE INFLATION FACTOR FOR THIS MATRIX IS  1.05
1TITLE DRSPALL PEER REVIEW SENSITIVITY SAMPLING
0CORRELATIONS AMONG INPUT VARIABLES CREATED BY THE LATIN HYPERCUBE SAMPLE FOR RANK DATA                              PAGE   1
0    1  1.0000
0    2  0.0212  1.0000
```

```
0    3  0.0051  0.0342  1.0000
0    4  0.0209 -0.0343  0.0385  1.0000
0    5 -0.0257 -0.0300  0.0210 -0.0239  1.0000
0    6  0.0213 -0.0735  0.0138 -0.0388 -0.0096  1.0000
0    7  0.0267 -0.0185 -0.0257 -0.0286 -0.0302 -0.0360  1.0000
0    8 -0.0252 -0.0193  0.0044 -0.0139 -0.0175  0.0133  0.0233  1.0000
0    9  0.0726  0.0677  0.0014  0.0083 -0.0226  0.0323  0.0177 -0.0473  1.0000
0            1       2       3       4       5       6       7       8       9
0VARIABLES
0THE VARIANCE INFLATION FACTOR FOR THIS MATRIX IS  1.02
```

APPENDIX VARIABLE GLOSSARY

Glossary of DRSPALL variable names

Spallings Model Peer Review

July 7-11, 2003

Table VG-1. Property Names

Property Name	Drspall input parameter
SURFELEV	Land elevation
REPOSTOP	Repository top
REPOSTCK	Total thickness
DRZTCK	DRZ(disturbed Rock Zone) thickness
DRZPERM	DRZ permeability
REPOTRAD	Outer radius
REPIPRES	Initial gas pressure
FFPORPRS	Far-field Pore Pressure and Initial repository pressure
FFSTRESS	Far-field In-Situ Stress
REPIPOR	Repository initial porosity
REPIPERM	Repository initial permeability
BIOTBETA	Biot beta
PIOSRAT	Poisson's ratio
COHESION	Cohesion
FRICTANG	Friction angle
TENSLSTR	Tensile strength
PARTDIAM	Particle diameter
GASBSDEN	Gas base density
GASVISCO	Gas viscosity
INITMDEN	Initial mud density
MUDVISCO	Mud viscosity
WALLROUG	Wall roughness
MUDSOLMX	Max mud solids volume fraction
MUDSOLVE	Mud solids viscosity exponent
BITDIAM	Bit diameter
PIPEDIAM	Pipe diameter

COLRDIAM	Collar diameter
PIPEID	Pipe inside diameter
COLRLNGT	Collar length
EXITLEN	Exit pipe length
EXITDIA	Exit pipe diameter
DRILRATE	Drilling rate
INITBAR	Initial bit distance above repository
MUDPRATE	Mud pump rate
MAXPUMPP	Maximum allowed mud pump pressure
DDZTHICK	DDZ (Drill Damage Zone) thickness
DDZPERM	DDZ permeability
SDEVR	Stop drilling exit volume rate
SPEVR	Stop pumping exit volume rate
SDTIME	Stop drilling time
MAXTIME	Max run time
PI	Pi
REFPRES	Atmospheric pressure
GRAVACC	Gravity
RGAS	Gas constant
TREP0	Repository temperature
GASDENS0	Gas base density
COMPRES	Water compressibility
RHOS	Waste density
SALTDENS	Salt density
SHAPFAC	Shape factor
TENSVEL	Tensile velocity
BITNZNO	Bit nozzle number
BITNZDIA	Bit nozzle diameter
CHOKEFF	Choke efficiency
CAVRAD0	Initial cavity radius

Table VG-2. History Variables
(at a location or spatial integrated value)

History Variable Name	Description
PUMPRS	Pump pressure
BOTPRS	Well bottomhole pressure
CAVPRS	Cavity pressure
DRILLRAD	Drilled Radius (Geometry dependent Equivalent)
CAVRAD	Cavity Radius (Geometry dependent Equivalent)
TENSRAD	Tensile Radius (Geometry dependent Equivalent)
CUTRAD	Maximum Cuttings Radius (Geometry dependent Equivalent)
WBSUPVEL	Waste boundary superficial (Darcy) pore velocity
FLUIDVEL	Critical fluidization velocity
MUDEJVEL	Mud ejection velocity
WASWELL	Mass of Waste in Well
WASEJCT	Mass of Waste Ejected
CUTMASMX	Maximum possible Cuttings Mass
GASINJ	Mass of Gas Injected
WELLGAS	Mass of Gas in Well
GASEJCT	Mass of Gas Ejected
GASPOSN	Gas Position in Well
WASPOSN	Waste Position in Well
CPUTIME	CPU time
RUNSTEP	Run step Index
VOLSTORE	Volume of Waste in Storage (failed and fluidized but waiting release to wellbore)
GASTORE	Mass of Gas in Storage
WASTORE	Mass of Waste in Storage
WASINJ	Waste Injected into wellbore
GASCAV	Mass of gas in psuedo-cavity prior to penetration
SWELLGAS	Sum gas mass in each wellbore computational cell
SREPOGAS	Sum gas mass in each repository cell
GASTOTAL	Total gas in system
GASFROMW	Total gas from waste
CUTMASS	Mass of cuttings
SPLMASS	Mass of spalled material
TOTMASS	Mass of spalled and drilled waste
CUTVOLEQ	Cutting volume assuming uncompacted waste porosity=0.85
SPLVOLEQ	Spall volume assuming uncompacted waste porosity=0.85

TOTVOLEQ	Spall and drilled volume assuming uncompacted waste porosity=0.85
CUTRUVOL	True cuttings volume assuming uncompacted waste porosity=0.85 (no geometric equivalence)
CUTRUMAS	True cuttings mass (no geometric equivalence)
PUMPRATE	Mud pump rate
SHEARRAD	Maximum radius at which shear stress exceeded maximum
NOZLVEL	Bit nozzle (Choke) fluid velocity
WBUPVEL	Wellbore velocity at well bottom
FLUIDTIM	Fluidization time for first Intact cell
SWELLGAS	Summation of gas mass in each cell
WASFROMR	Mass of waste lost from repository due to drilling and spall
WASTOTAL	Total spalled and drilled waste in system
PITGAIN	Pit gain
MUDEJCT	Mass of mud ejected

TableVG- 3. Element Variables (space and time dependent)

Element Variable Name	Where Variable Defined	Description
POREPRS	Repository	Repository pressure
RADEFSTR	Repository	Radial effective stress
TANEFSTR	Repository	Tangential effective stress
POREVEL	Repository	Pore velocity
RADELSTR	Repository	Radial elastic stress
TANELSTR	Repository	Tangential elastic stress
RADSPSTR	Repository	Radial seepage stress
TANSPSTR	Repository	Tangential seepage stress
FLUDSTRT	Repository	Fluidization start time
FLUDSTOP	Repository	Fluidization stop time
FAILSTRT	Repository	Failure start time
SUPRVEL	Repository	Superficial fluid velocity
FORCHRAT	Repository	Monitoring variable for Forchheimer assumption
WELLPRS	Wellbore	Well pressure
WELLVEL	Wellbore	Well velocity
WELLGSMS	Wellbore	Well gas Mass
WELLWSMS	Wellbore	Well waste Mass
WELLRHO	Wellbore	Well fluid density
WELLWSVF	Wellbore	Well waste volume fraction
WELLGSVF	Wellbore	Well gas volume fraction
WELLSAVF	Wellbore	Well salt volume fraction
WELLWSMF	Wellbore	Well waste mass fraction
WELLGSMF	Wellbore	Well gas mass fraction
WELLMDMF	Wellbore	Well mud mass fraction
WELLVOL	Wellbore	Well cell volume
COORD	Wellbore	Well cell center coordinate

APPENDIX INPUT

Listing of the "properties" specified in the template CAMDAT file MS_DRSPALL.CDB showing values for all the input parameters to DRSPALL prior to running LHS. Variables not sampled in LHS assume the values shown in this file. Sampled variables are overwritten. This file was generated using the WIPP PA utility GROPECDB.

Directory U1:[DLLORD.DRSPALL.MS_PR] INPUT.LIS;1

31-JUL-2003 07:50:00.53

```
                                  GROPECDB_PA96

  GGGGG  RRRRRR   OOOOO  PPPPPP  EEEEEEE  CCCCC  DDDDDD  BBBBBB          PPPPPP
 GG   GG RR   RR OO   OO PP   PP EE      CC   CC DD   DD BB   BB         PP   PP
 GG      RR   RR OO   OO PP   PP EE      CC      DD   DD BB   BB         PP   PP
 GG      RRRRRR  OO   OO PPPPPP  EEEEE   CC      DD   DD BBBBBB          PPPPPP
 GG  GGG RRRRR   OO   OO PP      EE      CC      DD   DD BB   BB         PP
 GG   GG RR  RR  OO   OO PP      EE      CC   CC DD   DD BB   BB         PP
  GGGGG  RR   RR  OOOOO  PP      EEEEEEE  CCCCC  DDDDDD  BBBBBB  _______ PP

                            GROPECDB_PA96 Version 2.12
                             PROD PA96 Built 06/27/96
                             Sponsored by Amy Gilkey

                            Run on 07/31/03 at 07:49:36
                        Run on ALPHA AXP CCR OpenVMS V7.3-1

 Database:  U1:[DLLORD.DRSPALL.MS_PR]MS_DRSPALL.CDB;13
 Written on:  07/10/03 16:32:34

 CAMDAT Version:   1        (EXODUS Version:   1)

 PROPERTIES

 Element Block 1)    "GLOBAL  "     1=ID     1 elements (1..1)
       8-node     5 attributes     0 properties

 Element Block 2)    "DR_SPALL"     2=ID     0 elements
       0-node     0 attributes    44 properties
    SURFELEV     REPOSTOP     REPOSTCK     DRZTCK       DRZPERM      REPOTRAD
    REPIPRES     FFPORPRS     FFSTRESS     REPIPOR      REPIPERM     BIOTBETA
    POISRAT      COHESION     FRICTANG     TENSLSTR     PARTDIAM     GASBSDEN
    GASVISCO     INITMDEN     MUDVISCO     WALLROUG     MUDSOLMX     MUDSOLVE
    BITDIAM      PIPEDIAM     COLRDIAM     PIPEID       COLRLNGT     DRILRATE
    INITBAR      MUDPRATE     DDZTHICK     DDZPERM      SDEVR        SPEVR
    SDTIME       MAXTIME      INITRZS      INITWZS      MAXPR        MINPS
    MAXPS        SHAPEFAC
   1.03730E+03  3.85310E+02  0.00000E+00  8.50000E-01  1.00000E-19  1.92000E+01
   1.45000E+07  1.45000E+07  1.49000E+07  5.05000E-01  1.70000E-13  1.00000E+00
   3.80000E-01  1.30000E+05  4.58000E+01  1.00000E+05  5.50000E-03  8.20000E-02
   8.93389E-06  1.21000E+03  1.10000E-02  5.00000E-05  6.15000E-01 -1.50000E+00
   3.11200E-01  1.14300E-01  2.03200E-01  9.71800E-02  1.82900E+02  4.44500E-03
   1.50000E-01  2.01810E-02  1.56000E-01  1.00000E-14  1.00000E+03  1.00000E+03
   1.00000E+03  1.00000E+03  1.00000E-02  1.00000E+00  1.00000E+01 -2.00000E+06
   8.00000E+06  5.50000E-01

 Element Block 3)    "REFCON  "     3=ID     0 elements
       0-node     0 attributes     2 properties
```

```
   PI            GRAVACC
  3.14159E+00  9.80665E+00

Element Block 4)    "BLOWOUT "     4=ID     0 elements
      0-node     0 attributes     3 properties
   RGAS         TREPO        RHOS
  4.11600E+03  3.00000E+02  2.65000E+03

Element Block 5)    "BRINESAL"     5=ID     0 elements
      0-node     0 attributes     1 properties
   COMPRES
  3.10000E-10
```